MAX-PLANCK-INSTITUT FÜR PLASMAPHYSIK

GARCHING BEI MÜNCHEN

PROCEEDINGS
of the Second Topical Conference
on Pulsed High-Beta Plasmas
3-6 July 1972

W. Lotz, Editor

IPP 1/127 July 1972

Contents:

Die nachstehende Arbeit wurde im Rahmen des Vertrages zwischen dem Max-Planck-Institut für Plasmaphysik und der Europäischen Atomgemeinschaft über die Zusammenarbeit auf dem Gebiete der Plasmaphysik durchgeführt.

Acknowledgements

The Second Topical Conference on Pulsed High-Beta Plasmas was held on 3 - 6 July 1972, in Garching bei München with about 143 conferees in attendance. It was jointly sponsored by the Max-Planck-Institut für Plasmaphysik, the American Physical Society, and the German Physical Society. The first topical conference (on high-density plasmas) was held on 19 - 22 September 1967 in Los Alamos. +)

The organizing committee consisted of the following persons: J.P. Freidberg (Los Alamos), E. Fünfer, W. Grossmann, H. Herold, M. Kaufmann, M. Keilhacker, W. Lotz (Chairman), J. Neuhauser, and F.L. Ribe (Los Alamos). Local arrangements were made primarily by W. Lotz and Mrs. Daniela Pohl. Particular thanks are due the following IPP secretaries for their invaluable aid during the conference: Margaretha Butera, Eleonore Lüddecke, Irmhild Richter and Ute Zannoni.

On the afternoon of 5 July, the conferees enjoyed an excursion on Lake Starnberg with M/S Bayern.

Papers G4 and G9 were read by title only.

The abstracts (page 5 to 15) have been submitted to the American Physical Society for publication in the APS Bulletin.

W. Lotz

+) Bull.Am.Phys.Soc. 12, 1153 (1967)
and Los Alamos Report LA-3770 (1967).

SECOND TOPICAL CONFERENCE ON PULSED HIGH-BETA PLASMAS

Program (6 July 1972)

Monday, 3 July, 09.00 - PINCHES I, Chairman: H. Zwicker

A1 PLASMA EXPERIMENTS ON $\ell = 1,0$ HELICAL EQUILIBRIA IN THE SCYLLAC 5-METER, THETA-PINCH TOROIDAL SECTOR. W.R.Ellis, C.F.Hammer, F.C.Jahoda, W.E.Quinn, F.L.Ribe, and R.E.Siemon, Los Alamos Scientific Lab.

A2 TOROIDAL HIGH-BETA STELLARATOR EXPERIMENTS ON ISAR T1. E.Fünfer, M.Kaufmann, W.Lotz, M.Münich, J.Neuhauser, G.Schramm, and U.Seidel, Max-Planck-Institut für Plasmaphysik, Garching, Germany.

A3 HIGH-BETA REVERSED FIELD DISCHARGES WITH EXTENDED LIFETIMES. C.W. Gowers, G.F.Nalesso, A.A.Newton, D.C.Robinson, A.Verhage, and H.A.B.Bodin, Culham Laboratory, England.

A4 THEORETICAL AND EXPERIMENTAL STUDY OF HEATING AND ENERGY LOSSES IN PINCH DISCHARGES. C.W.Gowers, G.F.Nalesso, A.A.Newton, D.C.Robinson, A.Verhage, A.Wootton, and H.A.B.Bodin, Culham Laboratory.

A5 RECENT RESULTS FROM THE SHOCK-HEATED TOROIDAL Z-PINCH EXPERIMENT ZT-1. L.C.Burkhardt, J.N.di Marco, P.R.Forman, A.Haberstich, H.J.Karr, and J.A.Phillips, Los Alamos Scientific Laboratory.

A6 OBSERVATIONS OF M.H.D. INSTABILITIES NEAR THE KRUSKAL-SHAFRANOV LIMIT IN LINEAR AND TOROIDAL HIGH-BETA PINCHES. I.K.Pasco, D.C.Robinson, and P.P.L.A.Smeulders, Culham Laboratory.

A7* EXPERIMENTAL RESULTS ON THE HIGH-BETA COMPACT TORUS EXPERIMENT TEE. P.Noll, H.J.Belitz, E.Kugler, F. Sand, G. Waidmann, F. Waelbroeck,Institut für Plasmaphysik der Kernforschungsanlage Jülich,Germany.

14.00 - THEORY OF STABILITY AND EQUILIBRIUM, Chairman: D. Pfirsch

B1 A VLASOV-FLUID MODEL FOR STUDYING GROSS STABILITY OF HIGH-BETA PLASMAS. J.P.Freidberg, and H.R.Lewis, Los Alamos Scientific Laboratory.

B2 EXPANSION OF TOROIDAL EQUILIBRIUM WITH FINITE PERIODICITY LENGTH AND $\ell = 0,1$ FIELDS IN LEADING ORDER. F. Herrnegger and J. Nührenberg, Max-Planck-Institut für Plasmaphysik, Garching.

B3 A CLASS OF HELICALLY SYMMETRIC MHD EQUILIBRIA. D.Correa and D.Lortz, MPI für Plasmaphysik, Garching.

B4 SPECIFIC MAGNETIC INDUCTANCE IN TOROIDAL SYSTEMS. G.Bateman, Courant Institute, New York University.

B5 ON THE SPECTRUM OF IDEAL MHD. J.A.Tataronis and W.Grossmann, Max-Planck-Institut für Plasmaphysik.

B6 THE EXCITATION OF WAVES AND RESONANCES IN HIGH-BETA PLASMAS. W. Grossmann and J.A.Tataronis, Max-Planck-Institut für Plasmaphysik, Garching.

B7 MHD STABILITY STUDIES OF NUMERICALLY OBTAINED TOROIDAL EQUILIBRIA. D.A.Baker and L.W.Mann, Los Alamos Scientific Laboratory.

B8 STABILITY OF TWO-DIMENSIONAL MAGNETOHYDRODYNAMIC EQUILIBRIA.J.P.Freidberg and B.M.Marder,Los Alamos.

B9 STABILITY OF A FINITE BETA, $\ell = 2$ STELLARATOR. J.P.Freidberg, Los Alamos Scientific Laboratory.

B10* TOROIDAL HIGH-BETA EQUILIBRIUM. H.Weitzner, Courant Institute, New York University.

Tuesday, 4 July, 09.00 - PINCHES II, Chairman: H.A.B. Bodin

C1 COMPUTATION OF GROWTH RATES OF INSTABILITIES FOR A GENERAL PINCH CONFIGURATION. J.E.Crow and D.C.Robinson, Culham Laboratory.

C2 THE PADOVA HIGH-BETA PROGRAM. G.Malesani, Università di Padova.

C3 PLASMA EXPERIMENTS IN THE SCYLLAC 5-METER, LINEAR THETA-PINCH. K.S.Thomas, H.W.Harris, F.C.Jahoda, G.A.Sawyer, and R.E.Siemon, Los Alamos Scientific Laboratory.

C4 THE PROPAGATION OF m = 1 ALFVÈN WAVES IN A HIGH-BETA PLASMA COLUMN. A.Wootton, G.F.Nalesso, and A.A.Newton, Culham Laboratory.

C5 NEGATIVE THETA-PINCH. I.Kawakami, K.Sato, R.Akiyama, and T.Uchida, Institute of Plasma Physics, Nagoya University, Japan.

C6 INITIAL PHASE OF THETA PINCH WITH MULTIPOLE CUSP FIELD. T.Miyamoto, Y.Nogi, H.Yoshimura, and K.Hayase, Nihon University, Tokyo, Japan.

C7 ANALYSIS OF THE ENERGY BALANCE IN THE ISAR II LINEAR THETA-PINCH BY EXPERIMENTAL AND COMPUTATIONAL INVESTIGATIONS. W.Engelhardt, W.Köppendörfer, W.Schneider, and J.Sommer, MPI für Plasmaphysik,Garching.

C8 TWO-DIMENSIONAL HARD CORE THETA-PINCH OBSERVATIONS OF SPIRAL STRUCTURE ASSOCIATED WITH INITIAL BREAKDOWN. D.Düchs, R.H.Dixon, and R.C.Elton, Naval Research Laboratory, Washington.

C9* MODELING OF LONG STRAIGHT THETA-PINCHES. W.P.Gula and R.L.Morse, Los Alamos Scientific Laboratory.

14.00 - SHOCK WAVES, Chairman: R.L. Morse

D1 SHOCK HEATING OF LOW DENSITY PLASMAS IN A FAST THETA-PINCH. K.J.Dietz and K.Höthker, Institut für Plasmaphysik der Kernforschungsanlage Jülich, Germany.

D2 PROPERTIES OF A LARGE DIAMETER, FAST THETA-PINCH OPERATED AT LOW DENSITIES. K.J.Dietz, K.H.Dippel, and E.Hintz, Institut für Plasmaphysik der Kernforschungsanlage Jülich, Germany.

D3 SHEATH FORMATION AND ION HEATING IN LOW DENSITY HIGH-VOLTAGE THETA-PINCHES. M.Keilhacker, M.Kornherr, F.Lindenberger, G.Maret, H.Niedermeyer, K.-H.Steuer, Max-Planck-Institut für Plasmaphysik, Garching.

D4 ELECTROSTATIC INSTABILITIES IN A COLLISIONLESS PLASMA DRIVEN BY AN ELECTRIC CURRENT PERPENDICULAR TO THE MAGNETIC FIELD. C.N.Lashmore-Davies and T.J.Martin, Culham Laboratory.

D5 ION THERMALIZATION IN STRONG, HIGH-BETA SHOCKS. D.L.Morse, P.L.Auer, and W.W.Destler, Cornell University, Ithaca,N.Y., USA.

D6 TWO STAGE HEATING OF THETA-PINCHES. J.P.Freidberg and R.L.Morse, Los Alamos Scientific Laboratory.

D7 ASYMPTOTIC BEHAVIOUR OF THE ELECTROSTATIC CURRENT-DRIVEN CROSSFIELD INSTABILITY. D. Biskamp and R.Chodura, Max-Planck-Institut für Plasmaphysik, Garching.

Wednesday, 5 July, 09.00 - PLASMA FOCUS, Chairman: A.A. Coudeville

E1 NEUTRON MEASUREMENTS, THOMSON SCATTERING AND HOLOGRAPHIC INTERFEROMETRY ON THE FOCUS EXPERIMENT. A.Bernard, A.Coudeville, J.Durantet, A.Jolas, J.Launspach, J.de Mascureau, and J.P.Watteau, Centre d'Etudes de Limeil, Villeneuve-Saint-Georges, France.

E2 A CRITICAL COMPARISON OF A TWO-DIMENSIONAL MHD CODE AND A FOCUS EXPERIMENT. G.Basque, C.Patou, and R.Vezin, Centre d'Etudes de Limeil.

E3 X-RAY FINE STRUCTURE OF THE DENSE PLASMA FOCUS. W.H.Bostick, V.Nardi, and W.Prior, F.Rodriguez-Trelles, Stevens Institute of Technology, Hoboken, N.J., USA.

E4 THEORY OF THE VORTEX BREAKDOWN IN THE PLASMA FOCUS. F.Gratton, Universidad de Buenos Aires, Argentine.

E5 TOROIDAL VORTICES IN PULSED PLASMAS. V.Nardi, Stevens Institute of Technology, Hoboken, N.J., USA.

E6 THEORY OF THE ADIABATIC CONTRACTION OF THE "Z-PINCH". P.Gratreau, Laboratori Gas Ionizzati, Frascati.

E7 A MODEL FOR THE DENSE PLASMA FOCUS. Ch.Maisonnier, F.Pecorella, J.P.Rager, and M.Samuelli, Laboratori Gas Ionizzati, Frascati, Italy.

E8 PROJECT OF A MEGAJOULE PLASMA FOCUS EXPERIMENT. C.Gourlan, Ch.Maisonnier, F.Pecorella, B.Robouch, and M.Samuelli, Laboratori Gas Ionizzati, Frascati.

E9* MEASUREMENT OF BETA IN A PLASMA FOCUS. P.D. Morgan and N.J. Peacock, Culham Laboratory.

E10* FILAMENTS IN A SMALL 1 KJ PLASMA-FOCUS EXPERIMENT. W. Braun, Heinz Fischer, and L. Michel, Technische Hochschule Darmstadt, Germany.

E11* CHARACTERISTIC PROPERTIES OF A PLASMA FLOW IN A PULSED MAGNETIC COMPRESSOR. I.N.Aretov, J.Burdonsky, Yu.A.Valkov, V.I.Vasiljev, A.P.Lototsky, Yu.V.Skvortsov, V.Solovjova, Yu.F.Suslov, I.V.Kurchatov Institute, Moscow.

E12* SOME RESULTS OF THE INVESTIGATION OF HIGH ENERGY DEUTERONS IN THE PLASMA FOCUS DEVICE. I.F.Belyaeva and N.V.Filippov, I.V.Kurchatov Institute, Moscow.

Thursday, 6 July, 09.00 - PINCHES III, Chairman: R.W. Gould

F1 PLASMA CONFINEMENT IN THE TOROIDAL BELT PINCH. W.Grossmann, H.Krause, R.Wilhelm, and H.Zwicker, Max-Planck-Institut für Plasmaphysik, Garching.

F2 BELT PINCH EQUILIBRIA WITH SMOOTH CURRENT DISTRIBUTION. F.Herrnegger, MPI für Plasmaphysik, Garching.

F3 THE INFLUENCE OF THE EXTERNAL CIRCUIT ON THE DECAY OF THE INDUCED PLASMA CURRENT. A.A.M.Oomens and B.J.H.Meddens, FOM-Instituut voor Plasmafysica, Rijnhuizen, Jutphaas, The Netherlands.

F4 NON-CYLINDRICAL Z-PINCH DENSITY PROFILES FROM HOLOGRAPHIC INTERFEROMETRY. A.Bernard, A.Jolas, J.Launspach, and J.P.Watteau, Centre d'Etudes de Limeil, Villeneuve-Saint-Georges, France.

F5 LOW PRESSURE OPERATION OF A FAST TOROIDAL PINCH. K.Hirano, M.Ohi, S.Kitagawa, and Y.Hamada, Nagoya University, Japan.

F6 THETA-PINCH PLASMA CONFINED IN A CAULKED-CUSP TORUS FIELD. T.Uchida, K.Sato, R.Akiyama, N.Noda, and N.Inoue, Nagoya University, Japan.

F7 PRELIMINARY STUDY OF THE HIGH PRESSURE CONFINEMENT OF A Z-PINCH, THEORY AND SOME EXPERIMENTAL RESULTS. D.Y.Cheng, Mechanical Engineering Department, University of Santa Clara, Cal., USA.

F8* MHD-STABILITY CONSIDERATIONS OF THE BELT-PINCH. W.Grossmann, MPI für Plasmaphysik, Garching.

F9* PULSED HIGH-BETA TOKAMAC-LIKE SYSTEM WITH RECTANGULAR CHAMBER CROSS-SECTION. V.M.Atamanov, G.B.Levadnyi, Yu.F.Nasedkin, N.I.Shchedrin, I.V.Kurchatov Institute, Moscow.

14.00 - MISCELLANEOUS TOPICS, Chairman: F. Waelbroek

G1 FEEDBACK STABILIZATION ON AN $\ell = 1$ THETA-PINCH PLASMA COLUMN. R.F.Gribble, S.C.Burnett, and C.R.Harder, Los Alamos Scientific Laboratory.

G2 DYNAMIC STABILIZATION EXPERIMENTS WITH STANDING WAVE MAGNETIC FIELDS. G.Becker, O.Gruber, and H.Herold, Max-Planck-Institut für Plasmaphysik, Garching.

G3 SOLUTION TO IMAGE CURRENT PROBLEMS IN HELICAL EQUILIBRIUM TOROIDAL THETA-PINCH EXPERIMENTS. E.L.Cantrell, O.M.Friedrich, Jr., and A.A.Dougal, The University of Texas, Austin.

G4 CO_2 LASER HEATING OF A SMALL THETA-PINCH. N.A.Amherd and G.C.Vlases, University of Washington.

G5 FORMATION OF HIGH-BETA FUSION PLASMAS WITH INTENSE RELATIVISTIC ELECTRON BEAMS. S.D.Putnam and C.H.Stallings, Physics International Company, San Leandro, USA.

G6 INTERACTION OF INTENSE RELATIVISTIC ELECTRON BEAMS WITH LINEAR PINCHES. J.Benford, B.Ecker, and S.Putnam, Physics International Company, San Leandro, USA.

G7 NON-THERMAL PROCESS IN A LINEAR PINCH DEVICE. T.N.Lee, US Naval Research Laboratory, Washington.

G8 THE PROPERTIES OF A COAXIAL DEFLAGRATION PLASMA GUN. D.Y.Cheng and P.Wang, University of Santa Clara, USA.

G9* SIMULATION AND OPTIMIZATION OF THETA-PINCH IMPULSING CIRCUIT PARAMETERS, WORKING FROM CUMULATIVE GENERATOR WITH CURRENT INTERRUPTER. V.M.Aleksandrov, A.P.Baikov, V.A.Ivanov, A.M.Iskoldski, L.S.Krotman, Y.E.Nesterikhin, and A.A.Nesterov, Institute of Automation and Electrometry, Siberian Academy of Sciences, Novosibirsk, USSR.

G10 PARAMETRIC STUDIES OF LINUS, AN ULTRA-HIGH MAGNETIC FIELD THETA-PINCH. J.P.Boris and R.A.Shanny, U.S. Naval Research Laboratory, Washington.

G11* A PULSED HIGH-BETA FUSION REACTOR BASED ON THE THETA-PINCH. S.C.Burnett, W.R.Ellis, T.Oliphant, and F.L.Ribe, Los Alamos Scientific Laboratory.

* Post deadline papers

A 1 Plasma Experiments on ℓ = 1,0 Helical Equilibria in the Scyllac 5-Meter, θ-Pinch Toroidal Sector.* W. R. ELLIS, C. F. HAMMER, F. C. JAHODA, W. E. QUINN, F. L. RIBE, and R. E. SIEMON, Los Alamos Scientific Laboratory, Los Alamos, N. Mex.--We report experiments on a sector comprising one third of the 4.8-m diameter Scyllac torus.[1] The toroidal force and outward plasma drift are compensated by an interference force produced by a combination of ℓ = 1 helical fields and ℓ = 0 bumpy fields. We observe the toroidal equilibrium, followed by an m = 1 (sideward) motion of the plasma column, which is nearly the same all along the torus, independent of the ℓ = 0 periodicity, with plasma containment times as large as 11 μsec, comparable to times for plasma end loss. The m = 1 motions, which occur predominantly in the horizontal plane of the torus, suggest either an imbalance between the ℓ = 1,0 and toroidal forces at later times or a long wavelength m = 1 instability. Measurements of the applied magnetic fields show that the product of ℓ = 1 and ℓ = 0 fields for plasma equilibrium agrees with sharp-boundary MHD theory. Time resolved measurements of the plasma diamagnetism, electron density distribution, neutron emission, and beta are reported.

* Work performed under the auspices of the U. S. Atomic Energy Commission.

1. S. C. Burnett, et al., Plasma Phys. and Controlled Nuclear Fusion Research 3, 201 (1971).

A 2 Toroidal High-Beta Stellarator Experiments on ISAR T 1. E.FÜNFER, M.KAUFMANN, W.LOTZ, M.MÜNICH, J.NEUHAUSER, G.SCHRAMM, U.SEIDEL, MPI für Plasmaphysik, Euratom Association, Garching, Germany.--First experiments on the toroidal theta-pinch ISAR T 1 (R = 135 cm, r_t = 4.5 cm, B_{max} = 34 kG, T/4 = 7.5 μs) were performed at 1/5 of the bank energy, using different combinations of ℓ = 1, ℓ = 2 and very small ℓ = 0 fields. Plasma parameters (p_o = 20 μ, 15% preionization, t = 5 μs) were $T_i = T_e$ = 70 eV, n = 10^{16}cm^{-3}, β = 0.4. M&S like combinations of ℓ = 1 and ℓ = 2 fields only moderately reduced the toroidal drift. The addition of only small ℓ = 0 fields ($\Delta r/r_p$ = 3%) led to a stronger reduction of the drift or even to an inward motion. End effects were now observed in keeping with the fact that only a sector had ℓ = 2/ℓ = 0 fields. The formation time of the helical equilibria is of the same order as the toroidal drift time. Therefore the forces of the ℓ = 1/ℓ = 2/ℓ = 0 fields on initially cylindrical plasma were calculated. The toroidal drift force should be balanced already during the formation of the helical distrotions.

A 3 High-Beta Reversed Field Discharges with Extended Lifetimes.* C.W. GOWERS, G.F. NALESSO, A.A. NEWTON, D.C. ROBINSON, A.J.L. VERHAGE, H.A.B. BODIN, U.K.A.E.A., Culham Laboratory, Abingdon, Berkshire, England. - Criteria for setting up stable distributions are discussed. In particular, the growth of instabilities in the outer regions of the stabilised pinch prior to field reversal, wall contact, a negative pressure gradient near the axis and over-compression (which can violate wall stabilization) must be avoided. Experiments are described in which these criteria are fulfilled and distributions have been set with neither instability nor wall contact which have β ∿ 0.8 and lifetimes, when crowbarred, of 30-40 microseconds, which is about the classical resistive decay time for the longitudinal current and reversed field outside the plasma. It is to be compared with 3 milliseconds on Zeta, where the plasma radius was larger by a factor approaching 10. Measurements at 40 mtorr using magnetic probes and Thomson scattering (mainly without crowbar) showed hollow pressure and density distributions and temperatures up to 20 eV. Estimates of the conductivities, $\sigma_{\parallel}$ and $\sigma_{\perp}$, indicated approximately classical values. *Submitted by R.S. PEASE.

A 4 Theoretical and Experimental Study of Heating and Energy Losses in Pinch Discharges. C.W. GOWERS, G.F. NALESSO, A.A. NEWTON, D.C. ROBINSON, A.J.L. VERHAGE, A. WOOTTON and H.A.B. BODIN, UKAEA Culham Laboratory, Abingdon, Berkshire, England. - In HBTX Z-pinches, screw-pinches and reversed field-pinches have been investigated with probes, Thomson scattering and spectrally resolved photography. The measured electron temperature and density distributions have been compared with predictions from an MHD code using a circuit. Agreement within experimental error is obtained in all cases for the compressed regions of the column starting with partially ionised initial conditions corresponding to the pre-ionization plasma. For example, for stabilized pinches both computation and experiment show that the temperature increases as I_z^2 with $\beta_\theta \sim 0.5$; the peak temperature obtained at 30 mTorr with a current of 90 kA is about 30 eV.

The effect of partial ionization in B_z compression heated systems has been studied in positive and negative bias field in order to investigate ways of controlling beta. Experimentally and theoretically the rate of temperature becomes sensitive to the degree of ionization when the electric field is reduced.

A 5 Recent Results from the Shock-Heated Toroidal Z-Pinch Experiment ZT-1. L. BURKHARDT, J. DI MARCO, P. FORMAN, A. HABERSTICH, H. KARR, J. PHILLIPS, Los Alamos Sci. Lab., Los Alamos, New Mexico* - Preionization in this stabilized toroidal z-pinch experiment is by a longitudinal current < 20 kA and period 40 μsec. The radial distribution of current density and degree of ionization are functions of the filling pressure and the preionization current. When a main pinch current which rises to 140 kA in 10 μsec is applied to the preionized plasma, pressure profiles derived from measured radial distributions of magnetic fields show: 1) a pressure peak on axis and a second peak near the wall if preionization is < 50% and; 2) a single pressure peak on axis at 100% ionization. In the shock heating mode, with initial $\dot{B}_\theta$'s of < 40 kG/μsec, plasma pressure profiles show a positive pressure gradient on axis, as required for MHD stability, for times of at least 8 μsec (current zero at 10 μsec). The plasma β_θ is < 0.4 at 5 mTorr filling pressure increasing with filling pressure. Plasma temperatures ($T_i + T_e$) of 1-4 keV are inferred from the pressure profiles and initial gas filling densities. Work is in progress to reverse the toroidal magnetic field outside the pinch column for MHD stability.

*Work performed under the auspices of the U.S. A.E.C.

A 6 Observations of MHD Instabilities Near the Kruskal-Shafranov Limit in Linear and Toroidal High Beta Pinches. I.K. PASCO, D.C. ROBINSON and P.P.L.A. SMEULDERS, UKAEA Culham Laboratory, Abingdon, Berkshire, England. - The growth rate and wavelength of MHD instabilities have been measured in the High Beta Toroidal Experiment and its linear 2 metre counterpart over a wide range of pitch lengths ($2\pi r B_z/B_\theta$). Optical and electrical measuring techniques are used. The wavelength of the Kruskal-Shafranov m = 1 instability varies in accordance with q(= rB_z/RB_θ, toroidal, = $\pi rB_z/LB_\theta$ linear). The growth rate of the instability is found to be approximately proportional to the axial current in the straight system, and this agrees with theory for small plasma displacements. The m = 1 instability disappears in both cases at the Kruskal-Shafranov limiting value of $q(r_m) = 1$ where r_m is the radius at which q is a minimum. This lies near the plasma boundary in the linear case and further out in the torus. Values of q up to 3 were studied and in the toroidal experiment evidence of an m = 2 instability was obtained when q ∿ 2.5 . The field configuration was varied by altering the preionisation current induced in the plasma, and configurations were usually of the screwpinch type, with the current flowing principally in the outer regions. In the linear device measurements below 12kA were made with the current flowing principally in the plasma column.

A 7 Experimental Results on the High-ß Compact Torus Experiment TEE. P. NOLL, H.J. BELITZ, E. KUGLER, F. SAND, G. WAIDMANN, F. WAELBROECK, Institut für Plasmaphysik der Kernforschungsanlage Jülich GmbH, Association Euratom-KFA.-- A plasma is produced by fast simultaneously rising toroidal and poloidal magnetic fields ($\tau/4$ = 1.6/usec) in a Tokamak-like configuration to study its equilibrium and stability behaviour for the case $1 < \beta_J \leq R/a$ and $q = 2\pi/\iota \geq 1$ (β_J = poloidal beta, R/a = major/minor plasma radius, ι = rotational transform). The glass torus has an inner wall radius of 9.5 cm and a major radius of 25 cm, its outer periphery is covered by a copper shell. With B_{max} = 4.3 kG and a filling pressure of 1 mtorr D_2, initial plasmas with $R \approx 28$ cm, $a \approx 6$ cm, total $\bar{\beta} \approx 0.1$, temperature $\bar{T} \approx 150$ eV and $q(a) \approx 0.8$ were obtained. After crowbar, the plasma current decreases at first quickly until $q(a) \approx 1$, thereafter smoothly with a characteristic time of ≈ 50/usec. With auxiliary resistive toroidal rings, placed near the inner periphery of the torus, the current was maintained near the Kruskal-Shafranov limit $q(a) = 1$ for ~ 50/usec. No major instabilities were observed when $q(a) \gtrsim 1$.

B 1 A Vlasov-fluid Model for Studying Gross Stability of High-Beta Plasmas.* J. P. FREIDBERG and H. R. LEWIS, Los Alamos Scientific Laboratory.--A formulation of the linearized Vlasov-fluid model[1] in a way suitable for numerical computation is described, and application to equilibria with axial and translational symmetry discussed. The formulation has two very important practical features which make the study of exponential stability feasible. Firstly, although equilibrium particle trajectories do enter, they enter more simply than in the usual procedure in which integrations along equilibrium trajectories must be carried out. Secondly, the truncated algebraic equations that result from the formulation and which must be solved numerically are in a form that is convenient for computation, even when the dimension of the algebraic problem is very large. The new formulation can be derived in part from a treatment of linearized Vlasov plasmas that is based on Hamilton's variational principle.[2] The first application of the method will be to the sharp boundary screw pinch.

*Work was performed under the auspices of the U.S. AEC.

[1] J. P. Freidberg, to be published in Phys. Fluids.
[2] H. R. Lewis, Phys. Fluids 15, 103 (1972).

B 2 Expansion of Toroidal Equilibrium with Finite Periodicity Length and ℓ=0,1 Fields in Leading Order. F. HERRNEGGER and J. NÜHRENBERG, Max-Planck-Institut für Plasmaphysik, Euratom Association, Garching, Germany.--The existence of a class of expandable toroidal MHD equilibria without longitudinal current is investigated. The expansion parameter is $R \kappa \sim \varepsilon$, R plasma or wall radius, κ lowest order curvature of the magnetic axis, plasma β, periodicity length L, and torsion τ of the magnetic axis in lowest order are scaled as $\beta \sim 1$, $2\pi R/L \sim 1$, $R\tau \sim 1$. The equilibrium is an $l=0,1$ high-β stellarator with additional $l = 2,3,\ldots$ corrugations in first order and has a rotational transform of order one; therefore in general, the Pfirsch-Schlüter (PS) effect occurs. It is shown that the necessary condition in order to eliminate the PS-effect over the entire cross section, is an $l=0$(M&S) corrugation of definite size which is determined by the form of the magnetic axis. This condition is however not sufficient, therefore equilibria of the type characterized above do not exist.

B 3 A class of helically symmetric equilibria. D. CORREA, D.LORTZ, Max-Planck-Institut für Plasma Physik, Garching b. München, West Germany.-- For MHD-equilibrium a class of solutions (with helical symmetry) satisfying the following conditions was investigated:

1) There is a helical magnetic axis such that in its neighborhood the cross sections of the magnetic surfaces are closed lines.
2) The pressure decreases continuously outward from the magnetic axis and the plasma is surrounded by vacuum.
3) The current density vanishes on the magnetic axis.
4) For finite ß some of these solutions are stable with respect to all disturbances, i.e. the sufficient criteria derived in [1] can be satisfied.

[1] D.Lortz, E.Rebhan and G. Spies, Nuclear Fusion 11 (1971), 583

B 4 Specific magnetic Inductance in Toroidal Systems. G.BATEMAN, Max-Planck Institut für Plasmaphysik, Euratom Association, Garching, Germany.-- The magnetic inductance matrix, which depends upon geometry alone, has been generalized to toroidal systems with distributed current[1]. This generalization can be made after the magnetic energy is minimized on each flux surface, holding the surface shapes and flux profiles fixed ($\Rightarrow \mathbf{j} \cdot \nabla \Psi = 0$). It then follows that the flux between differentially close surfaces equals the total current within the surface times the specific inductance (the matrix relates longitudinal and azimuthal components). A special coordinate system appears naturally in the derivation and provides a useful alternative to Hamada coordinates. The coordinate system depends upon geometry alone, but, in it, the magnetic field lines are straight. The general formalism is being applied to the approximation of flux surface shapes for plasma systems with a given topology. The specific inductance can be explicitly calculated for systems with an ignorable coordinate.

[1] The formalism was suggested by H.Grad and developed at the N.Y.U.Courant Inst. The derivation may be found in report NYO-1480-182.

B 5 On the Spectrum of Ideal MHD. J. TATARONIS and W.GROSSMANN, Max-Planck-Institut für Plasmaphysik, Euratom Association, Garching bei München, Germany. -- The assumption of $e^{i\omega t}$ in the linearized equations of ideal MHD, leads to an eigenvalue problem, whose solutions may possess singularities in space. The question arises as to whether or not the singular eigenfunctions are physical. To answer this we leave the time dependence of the variables arbitrary and solve the equations as an initial value problem. This process leads to a Green's function of the MHD operator which can be singular in the complex frequency plane. The singularities can be divided into two groups: (1) simple poles corresponding to a discrete spectrum and (2) branch points corresponding to a continuous spectrum. The branch points result from the singularities in space of the MHD operator, and lead to modes which have a time dependence other than exponential. The Green's function has been derived for several configurations in plane and cylindrical geometry. Depending on the configuration, modes are found which decay as $1/t^{\alpha}$ where $\alpha > 0$, or increase either linearly with time or with some other complicated dependence on time.

B 6 The Excitation of Waves and Resonances in High-Beta Plasmas. W. GROSSMANN and J.A. TATARONIS, Max-Planck-Institut für Plasmaphysik, Euratom Association, Garching bei München, Germany. -- The problem of the excitation of the natural modes of any physical system can be reduced to the problem of the coupling of a source to the system. Use is made of the results of a previous paper (B5) reported at this conference applied to high-β cylindrical plasmas (θ-pinch, screw-pinch) showing that under stable conditions the natural modes form a continuous spectrum of singular Alfvén waves if the density and magnetic field profiles are diffuse. We show here that the continuous spectrum implies (1) the excitation of Alfvén waves only if the source spectrum is sharply peaked somewhere within the continuous spectrum of the plasma and (2) the decay of the excited signal, due to phase mixing, at all points in the plasma except at the point where the applied frequency equals the local Alfvén frequency. This result would tend to explain the failure in several experiments to observe propagating Alfvén waves at appreciable distances away from the imposed disturbance.

B 7 MHD Stability Studies of Numerically Obtained Toroidal Equilibria. D.A.BAKER,L.W.MANN, University of California,Los Alamos Scientific Laboratory,Los Alamos,New Mexico.--This work pertains to axisymmetric toroidal MHD equilibria and their stability. Of particular interest are high β equilibria with hollow pressure profiles as observed experimentally in the Los Alamos toroidal z-pinch.
This study includes an examination of toroidal curvature effects and a determination of MHD stable toroidal z-pinch configurations. Diffuse profile toroidal equilibria free from limitations on aspect ratio, were obtained numerically. These solutions are analyzed for MHD stability by means of a double Fourier expansion of δW in the poloidal and toroidal variables and finite differencing the remaining variable. The resulting large, quadratic form is then tested for positive definiteness corresponding to stability.

B 8 Stability of Two-Dimensional Magnetohydrodynamic Equilibria.* J. P. FREIDBERG and B. M. MARDER, Los Alamos Scientific Laboratory.--A method is developed to study the stability properties of general two-dimensional magnetohydrodynamic equilibria. With the equilibrium given either analytically or on a numerical grid, the perturbation functions are expanded in a truncated Fourier series of admissible functions. A variational approach is used in which the quotient δW/K is minimized over the coefficients of the expansion. Numerically, this means computing the eigenvalues and eigenvectors of a symmetric matrix. The stability of the bumpy pinch is investigated as a trial problem. It was found that if the expansion functions are carefully chosen, very few are actually needed for convergence.

*Work was performed under the auspices of the U.S. AEC.

B 9 Stability of a Finite β, ℓ=2 Stellerator.* J. P. FREIDBERG, Los Alamos Scientific Laboratory.--The stability of an infinitely long, high β, ℓ=2 stellerator is investigated. The calculation is carried out by using the new scyllac expansion in the sharp boundary ideal magnetohydrodynamic model. It is found that for any given size ℓ=2 field and mode number m, an infinite but discrete set of wave numbers k exist for which the plasma is unstable to all β; that is the critical β equals zero. These modes can be described as long wavelength interchanges. Thus, with regard to sharp boundary stability, neither ℓ=0 nor ℓ=2 offer any particular advantage over the other as a sideband field required to produce toroidal equilibrium in the ℓ=1 scyllac configuration.

*Work was performed under the auspices of the U.S. AEC.

B 10 Toroidal High Beta Equilibrium. H.WEITZNER. Courant Inst. Math.Sci.,N.Y.U.-
Most toroidal high beta equilibrium studies have been based on the piecewise constant pressure, sharp boundary model. Here, equilibrium is obtained by formal expansion for the case of a continuous pressure profile in ideal magnetohydrodynamics. The small parameter on which the expansion is based is the approximate helical wave number times plasma radius;hence the equilibrium is assumed to vary slowly the long way around the torus. With the assumption that there be no net current flowing the long way around the torus on any flux surface, or with any other constraint on this current, the equilibrium is essentially uniquely determined for any value of beta. Numerical work indicates that the expansion breaks down at low beta and that the distortions of the flux surfaces from cylinders are not small. Numerical results of the approximate equilibrium equations are given and the pressure profiles appear to be quite reasonable. Preliminary comparisons with the Scyllac experiment indicate that the distributed pressure equilibrium condition is a closer approximation to the experiment than the sharp boundary model. Some comments on the stability of such configurations will be included.

C 1 Computation of Growth Rates of Instabilities for a General Pinch Configuration. J.E. CROW and D.C. ROBINSON, U.K.A.E.A., Culham Laboratory, Abingdon, Berksh., England. -- A comprehensive 1D computer code has been written to calculate growth rates of instabilities in both experimental and theoretical situations, and their associated eigenfunctions. Completely general field and density profiles are used, including cases in which a true vacuum exists between the conducting and the insulating wall. Both incompressible motions and compressible have been considered. The results for growth rates, wavelengths and eigenfunctions show good agreement with experiment. The computed stability of theoretical field configurations has been compared with that obtained using an existing code based on Newcomb's analysis, and the correlation between growth rate and stability established. The program uses a matrix method to obtain eigenvalues of the second-order ordinary differential equation. The dependent variable may be chosen as either the radial displacement ξ_r or the radial magnetic field b_r. The computation includes a full treatment of the vacuum region.

C 2
The Padova High Beta Program. G.MALESANI, Centro di studio sui Gas Ionizzati, CNR - Università di Padova, via Gradenigo, 6a - Padova - A short account is given of the work in progress concerning the study of the early stages, and expecially the plasma heating in detail, in various toroidal configurations. The works described are:

a) Experimental observations of the ionization growth and efforts to improve density distribution, gas purity and ionization degree, in a low energy toroidal device.
b) Numerical computations on the heating of a pinched column, to investigate mainly the effect of a reversed bias field. Heating and diffusion and their dependence on the plasma behaviour and on the circuit configurations will be investigated in a new toroidal experiment.
c) The construction of a very flexible axisymmetric toroidal device; main parameters of the new machine are:
$W_c = 120$ kJ ; $R = 40$ cm ; $r_{coil} = 6$ cm ;
$I_z \simeq 200$ kA ; $B_z \leq 25$ kG ; $T/4 = 1.5 \div 50$ μs.

C 3 Plasma Experiments in the Scyllac 5-Meter, Linear θ Pinch.* K. S. THOMAS, H. W. HARRIS, F. C. JAHODA, G. A. SAWYER, R. E. SIEMON, Los Alamos Scientific Laboratory, Los Alamos, New Mexico--Experiments are reported on the behavior of the plasma column in a straight high-voltage θ pinch which may be operated both with and without strong magnetic mirrors. Operation without mirror fields produced a high temperature (2 - 3 keV) plasma column which lasted about 15 μsec, showed considerable "wobble," and also showed effects due to plasma contamination of the discharge tube by material "boiled" off the quartz discharge tube by the previous discharge. Enlarging the discharge tube outside the coils reduced this problem. In the data so far, when mirror fields which give a mirror ratio of 2 - 3 are applied at the same time as the main field the plasma column shows evidence of a m = 1 instability.

* Work performed under the auspices of the U. S. Atomic Energy Commission.

C 4 The Propagation of m = 1 Alfvèn Waves in a High Beta Plasma Column. A. WOOTTON , G F NALESSO and A A NEWTON , UKAEA, Culham Laboratory, Abingdon, Berkshire, UK.--Observations have been made of the displacements of a plasma column by the magnetic field of a small nearby coil. The column is generated by a theta pinch (peak field 18 kG, rise time 9 μsec) in preionised deuterium and has a maximum electron temperature and density on axis of 60 eV and 10^{16} cm^{-3}. With an overall length of 350 cm end effects can be neglected for at least 10 μsec and both high and low beta plasma were obtained.

The perturbing field was produced by 20 kA in a three turn sector coil (16 cm^2 area) placed outside the discharge tube at the mid plane of the pinch driven by a small capacitor ($c = 0.4$ μF, $V = 40$ kV and $\omega = 1.35 \times 10^6$ rad sec^{-1}). Gross displacements of several millimeters were observed which propagated away from the sector coil region at about 10-20 cm/μs with a damping length of 10 to 20 cm.

This propagation is expected from ideal hydromagnetic theory and is included in a simple model based on the equation for m = 1 waves with a spatially distributed forcing term.

C5 Negative Theta-Pinch. I. KAWAKAMI*, K. SATO, R. AKIYAMA and T. UCHIDA, Institute of Plasma Physics, Nagoya University, Nagoya, Japan--Numerical computations on a negative theta-pinch process are carried out. An artificial resistivity often serves to suppress the onset of some numerical instabilities in the computation, and is chosen relating to the anomalous resistivities which are studied theoretically. Several types of artificial resistivity are examined in the computation and it is found that one which is one-hundredth of the Sagdeev resistivity seems to be most plausible, even in the case of the negative theta-pinch. Using this resistivity, numerical calculations are made on both negative and ordinary theta-pinch processes. Compared with the ordinary pinch, the negative theta-pinch builds a higher temperature region near the wall and a lower one near the center of the plasma column, at the maximum contraction. Stored energy per unit length in the negative theta-pinch plasma is comparable with that of the ordinary pinch plasma.

* On leave from Nihon University, Tokyo.

C6 Initial Phase of Theta Pinch with Multipole Cusp Field. T. MIYAMOTO, Y. NOGI, H. YOSHIMURA and K. HAYASE*, Department of Physics, College of Science and Engineering, Nihon University, Tokyo, Japan--The theta pinch experiment with the sixteen-pole cusp field, which could produce the circular isobar in the vicinity of the discharge tube, was carried out. The plasma was strongly affected by the multipole cusp field at the initial phase of pinch. The main part of the plasma current was separated from the tube wall and was on the cylindrical surface with small ripples. The cusp losses existed and the plasma contacted with the tube wall through the line cusps. The trapped reverse field increased by the superimposing of the multipole cusp field at the start of the second half cycle. The results suggest that the multipole cusp field makes the preheating effective or that it permits the powerful preheating. For the rotating plasma the average radius and the ripples of the column were calculated. The cusp losses and the ripples of the plasma column corresponding to the cusps vanished after the pinch. The instabilities were observed. It is, however, presumed that they do not directly relate with the multipole cusp field.

* Present address: Nagoya University, Nagoya, Japan

C 7 Analysis of the Energy Balance in the ISAR II Linear Theta-Pinch by Experimental and Computational Investigations. W.ENGELHARDT, W. KÖPPENDÖRFER, W.SCHNEIDER, J.SOMMER, Max-Planck-Institut für Plasmaphysik, Euratom Association, Garching bei München, Germany.--For a fast Theta-Pinch discharge (coil length 1m, energy 300 kJ) a detailed energy balance was obtained by comparison of measured quantities with results of a two dimensional (r,z) MHD-code. The measurements were carried out at filling pressures from 10 to 80 mTorr deuterium. They encompassed the electron density, the electron temperature by laser scattering, the ion temperature from neutron fluxes, diamagnetic fluxes and the line radiation of impurities in the x-ray region, in the vacuum ultra violet and in the visible. In addition the radial and axial velocities of impurity ions could be determined from side on and end on measured Doppler profiles. Plasma heating, mass-and energy losses in regimes of isotropic and anisotropic plasma pressures are discussed. The distribution of energy losses into kinetic energy, convection, thermal conduction and radiation losses is analysed.

C 8 Two-Dimensional Hard Core Theta-Pinch Observations of Spiral Structure Associated With Initial Breakdown. D. DÜCHS,* R. H. DIXON, and R. C. ELTON, Naval Research Laboratory, Washington, D.C.--The luminous plasma structure in a theta-pinch has been studied in two dimensions (r,z) in both the conventional configuration and the hard-core configuration (with spiral field lines). Parallel, antiparallel, and zero bias field conditions were analyzed. At the time of initial gas breakdown by θ-currents, a distinct axial structure is formed. In the conventional theta-pinch case, segmentation is axial and the "wavelength" of the structure increases with decreasing pressure, i.e., the structure is a plasma effect. In the antiparallel field case, locally-closing field lines accent the structure. In the hard-core case the initial axial plasma segmentation from the θ-preheater changes to a spiral-sheath, and coalesces into a few distinct spirals with antiparallel bias. The pitch of the spiral increases with axial compression, creating the illusion of rotating flutes when viewed through radial coil slots. Further observations through the current-feed slot with a solid rather than a perforated coil confirm these results.

*Present address: Institut für Plasmaphysik, Garching

C 9 Modeling of long straight Theta-Pinches. W.P.GULA and R.L.MORSE, University of California, Los Alamos Scientific Laboratory, Los Alamos, New Mexico.--Theoretical models of straight θ-pinches, including a two-dimensional (r&Z) transport code, have been constructed.
Ions and electrons are treated separately and electron thermal conduction is included. Preliminary results agree well with previous θ-pinch experiments. The results of these models will be compared with recent experimental measurements on the five meter Los Alamos θ-pinch at the time of the meeting.

D 1 Shock Heating of Low Density Plasmas in a Fast Theta Pinch. K.J. DIETZ and K. HÖTHKER, Institut für Plasmaphysik der Kernforschungsanlage Jülich GmbH, Assoziation EURATOM/KFA, Germany. -- Investigations are made during the implosion phase of a large diameter 120 kV theta-pinch at low initial densities. The ion energy, the compression ratio, and the magnetic field diffusion rates are measured as a function of the initial electron density and the coil voltage. In the parameter range investigated ($10^{12} \leq n_1 \leq 10^{13}cm^{-3}$, 60 kV ≤ U ≤ 120 kV) mean ion energies between 5 and 15 keV are found. The volume compression ratio is 10 and is independent on initial voltage and density. Measured values of piston velocity, compression ratio and ion energy agree well with those obtained from the "free particle" model. The width of the current sheath is time dependent during the implosion. A diffusion profile is formed. The observed effective collision frequency scales $\sim\sqrt{n_1}$ and is two orders of magnitude larger than the classical collision frequency in the initial plasma.

D 2 Properties of a Large Diameter, Fast Theta Pinch operated at Low Densities. K.J.DIETZ, K.H. DIPPEL, and E. HINTZ, Institut für Plasmaphysik der Kernforschungsanlage Jülich, Assoziation EURATOM/KFA, Germany. -- Studies of the dynamic phase of a high voltage theta pinch, /1/, are extended to times where pressure equilibrium exists. At current maximum mean ion energies are derived from neutron yield and from pressure balance equation (electron temperatures are negligible, ion temperature is constant across the radius). Comparison shows good agreement. Ion energies E vary between 3 and 20 keV, depending on density and coil voltage ($E \sim n_1^{-3/4}$). The width of the plasma boundary is about c/ω_{pi}, the peak β varies between 1 and 0.6, decreasing rapidly for densities below $N_c=\pi(c/\omega_{pi})^2 n_1$, $N_c = 3\cdot10^{15}cm^{-1}$. There is no indication that the insertion of probes does change the plasma properties. Observations show that the plasma is rapidly lost near current maximum caused by end losses.

/1/ K.J. Dietz, and K. Höthker, Proc. 2nd Conf. High-Beta, Garching, 1972

D 3 Sheath Formation and Ion Heating in Low Density High-Voltage Theta Pinches. M. KEILHACKER, M.KORNHERR, F.LINDENBERGER, G.MARET, H. NIEDERMEYER, and K.-H. STEUER, Max-Planck-Institut für Plasmaphysik, Euratom Association, Garching bei München, Germany. -- Fast magnetic compression of a low density (3×10^{10}-$3\times10^{12}cm^{-3}$) magnetic field free deuterium plasma in a large diameter ($2R_o$ = 40cm) high-voltage (U_o = 500 kV) theta pinch is investigated. In the whole range of densities effective piston heating is observed resulting in ion energies of a few 10keV. For an initial deuteron density of $2.5\times10^{12}cm^{-3}$ (U_o = 420 kV) the sheath thickness during implosion is 8 c/ω_{peo} or 3 c/ω_{ce}. At maximum compression the mean ion energy is 15 to 20 keV, the deuteron density $4\times10^{13}cm^{-3}$ and the plasma radius 6 cm. After expansion to an equilibrium radius the plasma β is about 0.5. From a model of anomalous sheath broadening a scaling law for the low density limit $n_{o,c}$ of shock compression is derived:

$$n_{o,c}\pi R_o^2 \sim R_o^4 \dot{B}_o^2.$$

D 4 Electrostatic Instabilities in a Collisionless Plasma driven by an Electric Current Perpendicular to the Magnetic Field. C.N. LASHMORE-DAVIES, and T.J. MARTIN, Culham Laboratory - The growth rates and frequencies of fast growing instabilities, $\gamma > \omega_{ci}$, are computed for a wide range of parameters (γ is the growth rate and ω_{ci} the ion cyclotron frequency). The many instabilities which can occur are related to each other and compared in an attempt to decide under what conditions a given instability will dominate.

D 5 Ion Thermalization in Strong, High-Beta Shocks.* D. L. MORSE, P. L. AUER, and W. W. DESTLER, Laboratory of Plasma Studies, Cornell University, Ithaca, N.Y.-- Strong, high-beta collisionless shocks are generated by the interaction of a flowing plasma with a magnetic obstacle in a plasma wind tunnel device. The shock waves thus formed are grossly stationary in the laboratory reference frame, and simulate in many respects the earth's bow shock. The upstream plasma flow is characterized by beta $\simeq 3$ and magnetosonic Mach number $M \simeq 7$, and the duration of the experiment is greater than one-half millisecond, or 10 ion gyro-periods. The shock waves are observed to be nonstationary on a time scale comparable with the upstream ion gyro-period. The electrons are heated only moderately, and the bulk of the upstream flow energy appears as thermal energy of the ions. In this paper we report measurements of the ion energy distribution function as the shock wave is traversed, and space-resolved density measurements of the shock transition using guided microwaves. The results will be discussed in the context of current theories of particle thermalization in the bow shock.

*Work supported by National Science Foundation under Grant GA 31175.

D 6 Two Stage Heating of Theta-Pinches.* J.P. FREIDBERG and R.L.MORSE, Los Alamos Scientific Laboratory, Los Alamos, N.M. -- The heating of θ-Pinches by fast implosion, followed by slow adiabatic compression will be discussed. Numerical simulations of the initial fast implosion will be shown, which indicate the technological requirements for this stage of the heating, and a scheme will be shown by which the efficiency of this stage can be improved. From estimates of the effects of the thermalization on the subsequent slow compression, the fractional filling of the pinch tube can then be estimated.

* Work was performed under the auspices of the United States Atomic Energy Commission.

D 7 Asymptotic Behaviour of the Electrostatic Current-Driven Cross Field Instability. D.BISKAMP and R.CHODURA, Max-Planck-Institut für Plasmaphysik, Euratom Association, Garching bei München, Germany. -- Onset, evolution, and final state of the instability driven by a current perpendicular to a magnetic field are investigated in one- and two-dimensional computer simulation experiments. Though the influence of the magnetic field is quite different in one- and two-dimensional plasmas the final state is characterized by $U \sim c_s$ (U drift-, c_s ion-acoustic velocity) where the instability switches off. Peak values of the effective collision frequency during the heating period are $\sim 5 \cdot 10^{-3} \omega_{Pe}$ independent of ion mass in two-dimensional calculations.

E 1 Neutron measurements, Thomson Scattering and Holographic Interferometry on the Focus experiment. A. BERNARD, A. COUDEVILLE, J. DURANTET, A. JOLAS, J. LAUNSPACH, J. de MASCUREAU and J.P. WATTEAU, Centre d'Etudes de Limeil, B.P. 27 - 94. Villeneuve-Saint-Georges, France.-- Neutron measurements have been made on a newer apparatus (100 kJ - 40 kV) designed mechanically to prevent scattering so that fluences can be measured in three directions : at 0°, 90° and 180° with respect to the axis directed from the center electrode outwards. Also the energy spectrum at 0° is obtained by time of flight at 120 meters. It is confirmed that the Focus machine can be operated at different regimes. At high enough filling pressures there are discharges with neutron fluence isotropy, mean energy of 2.5 MeV ± 0.1 MeV and broadening in agreement with a 2 keV or less deuteron temperature, which is evidence for a thermonuclear origin of the neutrons. At lower filling pressures the neutron emission exhibits essentially the same lack of isotropy as was found in other laboratories. On smaller devices (15 kJ - 18 kV - 0.5 MA) the ion temperature and the electron density are measured by forward Thomson scattering and holographic interferometry, respectively.

E 2 A Critical Comparison of Two-Dimensional MHD Code and a Focus Experiment . C. BASQUE, C. PATOU and R. VEZIN, Centre d'Etudes de Limeil, 94 - VILLENEUVE-ST-GEORGES, France. -- We have run the POTTER MHD code[1] adapted to the geometry of the first FOCUS experiment used in Limeil[2] to make a direct comparison between computational results and experimental measurements. First runs with a gross scale mesh (LAX-WENDROFF double step $\sim$0.3 cm) gave a dynamics a little slower than in the experiment, same maximum densities, but maximum temperatures (500 eV) much lower than the several keV estimated by the X-ray absorbing foil technique. After correction of several transport coefficients we obtained an enhancement of the maximum temperature of less than 20 %. To increase the precision of the computation, as a first step, we have divided the linear mesh size by two (0.15 cm, 5 hours run). This middle scale mesh run gave us a good dynamics and maximum temperatures of the order of one keV. Then the computation is much more sensitive to the choice of the transport coefficients and artificial viscosity.

1. POTTER D.E., Phys. Fluids 14, 9 sept. 1971, p. 1911
2. PATOU C. Journal de Physique, 31, avril 1970, p. 339

E 3 X-ray Fine Structure of the Dense Plasma Focus W. H. BOSTICK, V. NARDI, W. PRIOR, F. RODRIGUEZ-TRELLES, Stevens Inst. of Tech-X-ray photos with 0.075 mm dia. pinholes and Be screens of 0.018 mm and 0.050 mm in front of the film show finer detail than has hitherto been reported in plasma focus measurements. Several small intense x-ray (> 2Kev) sources ∿ 0.1 mm in dia. and ∿ 0.3 mm long in the general axial region can be resolved in each shot. From densitometry of the film and an estimate of an x-ray emission time of ∿ 10 n sec from each source a peak electron density in the source is estimated at $n_e \simeq 10^{20}/cm^3$. Sometimes these sources appear also off axis in the halo. In the general background of softer x-rays (> 1Kev) in the axial region a distinct porosity in the image can be observed. The authors believe that both the small intense sources and the porosity can be explained by the existence of many small toroidal or Hill shaped vortices which are the debris left behind after the decay of the longer filamentary vortices in the current sheath. The authors suggest that the toroidal vortices are basically similar to those observed by Komelkov et al. in the fountain pinch. The toroidal vortices provide a suitable "model" to explain the "doppler shifted" neutron energy.

Work supported by the Air Force OSR.

E 4 Theory of the Vortex Breakdown in the Plasma Focus FAUSTO GRATTON* Departamento de Fisica, Facultad de Ciencias Exactas y Naturales, Buenos Aires--A simple MHD model is given for the breakdown of a plasma vortex with axial flow. The phenomenon of the disruption of vortices in plasma have been observed in a plasma focus device by 5 n sec image-converter pictures[1]. An interpretation as vortex breakdown, akin to similar processes in neutral fluids, has been given recently[2]. Our theoretical model gives the criterion for the appearence of breakdown, the ratio of the radii of the vortex in the transition, and the energy released. Explosive and weak breakdown have been found depending upon a physical parameter which involves axial, rotational and Alfven velocities. Several features observed in the current sheath vortices of the Plasma Focus can be explained within the present model.

*Member of the Argentine CNICT. Work supported in part by a grant from Argentine Comision Nacional de Estudios Geo-Helio-Fisicos

1. W.Bostik et al.,Proc.IUTAM Dyn.Ionized Gases,Tokyo,1971.
2. W.Bostik et al.,Bull.APS II,17,494 (1972).

E 5 Toroidal Vortices in Pulsed Plasmas, V. NARDI, Stevens Inst. of Tech-A theory of plasma vortices with a toroidal configuration similar to the plasmoids produced by Komelkov et al. (Proc. 5th I. Conf. Ionized Gases, Munich 1961, p. 2191) is derived by solving the equations for self-consistent fields and phase-space density f_+ for ions and electrons. The f_+ -equations contain source terms which account for radiative processes, ionization and recombination reactions and other collision phenomena. The method of solution of the equations (not involving perturbative expansions) is based on the same procedure that was used in a theory of magnetic bundles in dense plasma (Phys. Rev. L., 25, 718, 1970). The time of trapping of high-energy electrons and ions is related to the parameters describing the plasmoid geometry. Boundary conditions and symmetry properties of the solutions for fields and particle flows fit experimental observations from coaxial accelerator discharges, at a specific time after the maximum-compression stage of the discharge.

Work supported in part by U.S. A.F.O.S.R.

E 6 Theory of the adiabatic contraction of the z-pinch. P.GRATREAU,Laboratori Gas Ionizzati, Associazzione Euratom/CNEN/Frascati,Italy.--The theory of the collisionless "z-pinch" transient equilibrium is developed in the hypothesis of a radial adiabatic contraction. A detailed collisionless solution is established in the particular case of no space-charge field, where an axial electron beam is supposed to generate the radial electrostatic field. As in the Bennett static equilibrium, there is no radial variation of temperatures; the density, the magnetic field, and the macroscopic axial velocities are increasing towards the axis; at the time of the transient equilibrium, when the total intensity reaches a maximum, the net radial force begins to be defocusing. In a numerical example, chosen in relation with typical values of P.F. experiments, the axial drift velocities are shown to be two orders of magnitude less that the ionic thermal one in the range of validity of the model.

E 7 A Model for the Dense Plasma Focus. Ch. MAISONNIER, F. PECORELLA, J.P. RAGER, M.SAMUELLI, Laboratori Gas Ionizzati, Frascati , Italy. -- A model is proposed in order to explain the second neutron pulse observed in DPF devices. The plasma column ($3\ 10^{19}$ ions/cm^3, 1.6 keV, $\emptyset$ = 4 mm, agreement with the neutron yield of the first pulse) is disrupted by macroscopic instabilities. The radial extension of the plasma increases and the magnetic field gets mixed with plasma which stores internally the magnetic energy (dark pause). At some radius of expansion the conditions for the onset of microturbulence (ion acoustic, electron cyclotron drift instabilities) are satisfied, turbulent heating occurs, transforming the stored magnetic energy into thermal energy (second burst of neutrons). The plasma parameters calculated at this time on the basis of the model (10^{18} ions/cm^3), 7 keV, $\emptyset$ = 15 mm) agree with the neutron yield. Experimental abservations seem to check well with the model.

E 8 Project of a Megajoule Plasma Focus Experiment. C. GOURLAN, CH. MAISONNIER, B.ROBOUCH, M.SAMUELLI, Laboratorio Gas Ionizzati (Associazione EURATOM-CNEN, Frascati, Rome, Italy, and A. BENUZZI and P.FASOLI, CETIS, C.C.R.-EURATOM, Ispra, Italy. -- The scaling laws of the plasma focus devices of the Filippov type are established theoretically, and shown to compare satisfactorily with the available experimental scaling laws. The main parameters of the Megajoule experiment to be built in Frascati within the framework of a joint European programme are deduced. Two dimensional M.H.D. numerical calculations confirm the theoretical expectations.

E 9 Measurement of Beta in a Plasma Focus. P.D. MORGAN*, and N.J. PEACOCK, U.K.A.E.A., Culham Laboratory, Abingdon, Berks., England. - The electron and ion line-densities obtained by interferometry during the collapse, dense-pinch and break-up stages of a Plasma Focus discharge are reported. Using these values, together with previously reported values of the average temperatures of the particles, the Bennett relation, $I^2\ \beta_\theta = 2\ k\ _e\Sigma_i\ NT$, is satisfied in the dense pinch for a value of β_θ (beta) ~ 0.6. This is consistent with a fluid model in which plasma is transiently in equilibrium with the self-magnetic field of the current in the pinch.

* Royal Holloway College, Englefield Green, Surrey, England.

E 10 Filaments in a Small 1 KJ Plasma-Focus Experiment. W. BRAUN, Heinz FISCHER and L. MICHEL, Applied Physics, Technische Hochschule, Darmstadt, Germany. -- The influence of spoke type filaments upon the field structure of the focus was studied by means of two 10 ns image converters, end- and side-on - with a) a flat insulator ring at the bottom between the inner and outer electrode (5 and 8 cm) and b) an insulator along the inner electrode (1.2 cm long) - voltage 15 kV, current max approx. 120 kA. Energy 0.75 kJ, Hydrogen 1 mm Hg - focus after 1400 ns (a) and 900 ns (b). a) spokes across the insulator surface flow through the acceleration into the focus, sharpening and gaining strongly in intensity before focus formation. b) filaments along the surface of the pyrex sleeve flow radially into the cavity without indication of a z-axis acceleration. Optical flux densities are 5-10 times stronger than in case a). Intensity pikes demonstrate strong directed fields. They seem to originate from early filament structures.

E11 Characteristic Properties of a Plasma Flow in a Pulsed Magnetic Compressor. I.N.ARETOV, J. N.BURDONSKY, YU.A.VALKOV, V.I.VASILJEV, A.P. LOTOTSKY, YU.V.SKVORTSOV, V.SOLOVJOVA, YU.F. SUSLOV; I.V.Kurchatov Institute of Atomic Energy, Moscow, USSR.-- The results obtained from the studies of a hydrogen plasma accelerated in the plasma focus device are presented. Hydrogen was introduced into the interelectrode gap by a pulsed injector containing 20 cm^{-3} of gas at 100 atm. The capacitor bank parameters were as follows: C = 510 µF, L_o = 35 nH, $U_o \leq 30$ kV, $I_{max} \leq 1{,}5$ MA, $T/2 \sim 20$ µs. It is shown that as the current sheet moves in the interelectrode gap the current loops are formed and the magnetic field energy of the loops is transferred to the plasma flow. Plasma focus life time, the length and diameter are (5-6)µs (3-4)cm, (1.5-2)cm correspondingly. The plasma density at the boundary of the focus is equal to 3×10^{18} cm^{-3}. For U_o = 20 kV the plasma velocity at the output is equal to 8×10^6 cm/s, the kinetic energy of the flow is about 25 kJ.

E12 Some Results of the Investigation of High Energy Deuterons in the Plasma Focus Device. I.F.BELYAEVA and N.V.FILIPPOV, I.V. Kurchatov Institute of Atomic Energy, Moscow, USSR.-- Some results obtained in the study of high energy deuterons generated in the plasma focus device are presented. The pinhole cameras with the chosen types of emulsions were used to detect the high energy deuterons, the d-d reaction protons and soft x-ray emission. It was observed the existence of the different regimes of the discharge processes with unchanged initial conditions. The regimes with hard x-ray emission were accompanied by high energy deuterons. The energy spectrum and spatial distribution of such deuterons are presented. The contribution of deuterons with energies $E_d \geq 300$ keV to the neutron yield does exceed 1 per cent.

F 1 Plasma Confinement in the Toroidal Belt-Pinch. W.GROSSMANN, H.KRAUSE, R.WILHELM and H. ZWICKER, Max-Planck-Institut für Plasmaphysik, Euratom Association, Garching, Germany.-- A plasma belt with 80 cm initial height, approximately 45 cm diameter and 3 cm thickness was produced with the help of a special coil system. Streak and framing pictures taken side-and end-on showed an axial contraction of the belt by a factor of 2 within about 20 µsec. This configuration was grossly stable for the whole observation time of 100 µsec. In particular, the upper and lower edges of the belt showed no decisive deformation. The measurements indicated that the plasma life-time is limited by diffusion to about 90 - 100 µsec (filling pressure 50 mTorr D_2). Direct probe measurements gave a β-value of ~70-80% during the heating stage of a few microseconds. Flux and field measurements showed further that the toroidal plasma current had a decay time of about 70 µsec. Assuming classical resistivity this gives 40-50 eV temperatures which is in agreement with other calculations.

F 2 Belt Pinch Equilibria with Smooth Current Distribution. F.HERRNEGGER, Max-Planck-Institut für Plasmaphysik, Euratom Association, Garching, Germany.-- Exact toroidal MHD equilibria have been investigated which are characterized as follows: the half-axis ratio of the plasma cross section is large (typical values 15-20), the ratio of the large torus diameter to the axial extension of the plasma is of order one. The toroidal current density depends linearly on the flux function. This configuration with an elongated plasma cross section has the advantage that the poloidal magnetic field can be increased considerably while the toroidal current remains below the Kruskal-Shafranov limit. The general solution for the plasma region is given in terms of the Coulomb wave functions F_o and G_o which depend on a single parameter determined by the torus diameter, the half-axis ratio of the plasma cross section and the plasma β. It is shown numerically, that the Mercier criterion necessary for local stability, is satisfied in certain parameter ranges.

F 3

The Influence of the External Circuit on the Decay of the Induced Plasma Current. A.A.M. Oomens and B.J.H. Meddens. FOM-Instituut voor Plasmafysica, Jutphaas, The Netherlands.

In pulsed toroidal devices the toroidal plasma current is produced by means of an inductive coupling with the external circuit. The effect of this coupling on the decay of the plasma current is considered. The equivalent Z-circuit, after crowbarring, consists in general of three parallel branches, containing (a) the external impedance, (b) the mutual inductance, and (c) the stray inductance of the plasma in series with its resistance.
The differential equations describing this circuit have two independent solutions; the plasma current is given by a combination of two exponentials. This may give rise to a rapid decrease or a reversal of the current. If one more parallel branch is added, the behaviour of the plasma current is governed by three characteristic times. With a proper choice of the circuit parameters, it is possible to generate a temporarily rising plasma current (pseudo-power crowbar). The above-mentioned circuits have been studied on an analog computer. The results are compared with experiments done in screw-pinch device SP III.

F 4 Non-Cylindrical Z-Pinch Density Profiles from Holographic Interferometry, A. BERNARD, A. JOLAS, J. LAUNSPACH, J.P. WATTEAU, Centre d'Etudes de Limeil, B.P. 27 - 94. Villeneuve-Saint-Georges, France.-- A 16 kJ 98 kV Z-pinch is produced in a 60 cm long, 18 cm diameter pyrex chamber with an 8 cm diameter center narrowing and filled with 1 torr deuterium. The current rises to its 300 kA maximum in 900 nsec and typical values of the focused plasma density and temperature are 10^{18} cm^{-3} and 30 eV. The chamber optical quality is very poor, so that double exposure holographic interferometry was compulsory.

Density profiles in the median plane obtained after Abel inversion are compared with the results of a MHD code. The shock dynamics are in good agreement. From the linear density variations one deduces a 200 nsec formation time of the magnetic piston and axial leaks at the end of the compression. Density maps give the shock curvature dynamics close to the one computed from a two-dimensional snowplough model and reveal the plasma flow inside the shock away from each side of the median plane. From the wavelength measurement of a Rayleigh-Taylor instability a 30 eV electron temperature is evaluated at 650 nsec.

F 5 Low Pressure Operation of a Fast Toroidal Pinch. K. HIRANO, M. OHI, S. KITAGAWA, and Y. HAMADA, Institute of Plasma Physics, Nagoya University, Nagoya, Japan-- Electron beam injection made it possible to operate the fast toroidal pinch down to 2 mtorr, which is sufficiently lower than the critical line density 10^{16}/cm. The minor and major radius of the glass torus are 3 cm and 12 cm, respectively. The maximum toroidal field B_t is 1.5 T and the plasma current of 150 kA can be induced. The magnetic field and the plasma current rise in 2.5 μsec. In standard screw pinch operation, it was not successful to suppress the violent toroidal drift appears in low pressure regime of around 10 mtorr. Increasing the filling pressure to 40 mtorr, however, the plasma begins to oscillate around the equilibrium position. The laser scattering measurement shows that when the density is 2×10^{15}cm^3, the electron temperature becomes 25 eV. The peculiar screw pinch mode is also studied here, in which the toroidal electric field is so programed not to reverse its sign to prevent the current reversal in the outer sheath of the plasma. This kind of operation was possible under the filling pressure of 2 to 16 mtorr. Stable discharge is found to be realized when q is larger than 1.5.

F 6 Theta-Pinch Plasma Confined in a Caulked-Cusp Torus Field. T. UCHIDA, K. SATO, R. AKIYAMA, N. NODA and N. INOUE*, Institute of Plasma Physics, Nagoya University Nagoya, Japan--A toroidal theta-pinch plasma is stably confined in a periodic caulked-cusp torus (abbreviated to C.C.T.) field which is formed by superposition of the field generated with the current induced inside the buried rings on the theta-pinch field. The toroidal drift of a theta-pinch plasma is suppressed and no macroscopical instabilities are observed[1]. A relatively rapid decrease of the plasma pressure seems to be unavoidable, because it may result from the expansion of the cylindrical plasma pinched near the minor axis into the confining region of the C.C.T. field. The particle confinement may be limited by the plasma contacting on the inside of the ring, owing to the approach of the stagnation point. The approach is caused by the differences between the decay time of the coil current and that of the induced ring current, which originates in a proximity effect between both currents.

* Present address: University of Tokyo, Tokyo

1 T. Uchida et al, Proc. Madison Conf. IAEA CN-28/J-1 (1971).

F 7 Preliminary Study of the High Pressure Confinement of a Z-Pinch--Theory and Some Experimental Results D.Y.Cheng Univ. of Santa Clara ----The high temperature plasma in an arc channel surrounded by a munch higher density, low temperature or neutral gas can be heated preferentially to even higher temperatures. This is because the electrical conductivity increases with temperature as $T^{3/2}$ and the ohmic heating rate is inversely proportional to the conduc-tivity. Ordinarily, the heat losses from Bremsstra-hlung radiation and heat conduction from concentric cylinders increase with temperature as $T^{1/2}$ only. However, the shrinking of the heated area will be slowed down by the cyclotron radiation as it loses heat as T^2. Experimentally, such an arc channel can be created by the explosion of a deuterium-filled metal tube, As a result, pure deuterium plasma can be produced which is surrounded and confined by a high dnesity mass. Neutron signals will be presented together with the current trace to indicate the time of neutron production. Plasma density in the channel is estimated to be 7×10^{17}/c.c. and n is about 6×10^{12}. This work is partially supported by NASA Grant NGR 05-017-019.

F 8 MHD-Stability Considerations of the Belt-Pinch.W.GROSSMANN, Max-Planck-Institut für Plasmaphysik,Garching,Germany.-- An infinitely long approximation of the belt-pinch is made and the MHD stability of this configuration is examined. The usual role of the fourier variables "m" and "k" are switched in this approximation and "m" now refers to perturbations in the toroidal direction and "k" refers to the corresponding perturbations in the poloidal direction. Some interesting comparisons of the belt-pinch are made with the usual screw and theta pinches. Both diffuse and sharp boundary calculations are presented. Tearing modes are examined by including resistivity and it is found that the same mechanism for the m = 0 mode in a reversed field θ-pinch occurs in the belt-pinch plasma. Comparisons are made with the experimental results obtained with the Garching ISAR IV belt-pinch.

F 9 Pulsed High-β Tokamac-Like Sistem with Rectangular Chamber Cross-Section.V.M.ATAMANOV, G.B.LEVADNYI,YU.F.NASEDKIN,N.I.SHCHEDRIN, I.V. Kurchatov Institute of Atomic Energy,Moscow, USSR.--Magnetic sistem for producing closed, equilibrium and stable configuration of high-β plasma in a toroidal chamber with rectangular cross-section is described. Closed configuration is formed owing to non-uniform inducing field. Magnetic field distribution obtained with a model and measures eliminating the asymmetry are considered.

G 1 Feedback Stabilization on an $\ell = 1$ Theta-Pinch Plasma Column.* R. F. GRIBBLE, S. C. BURNETT, C. R. HARDER, Los Alamos Scientific Laboratory, Los Alamos New Mexico--An $\ell = 0$ MHD feedback experiment to control the m = 1 instability on a plasma column subject to ℓ = 1 helical fields is described. The feedback system has three basic components: a position detector, a signal processor, and a power amplifier. Feedback stabilization is being tried first on a linear θ pinch (Scylla IV-3). Horizontal and vertical motions of the plasma column are optically sensed with fast-rise-time silicon bi-cell detectors. The signal processor provides amplitude and derivative control and normalization of the detector signals. Ten power-amplifier modules in push-pull configurations are used to drive the $\ell = 0$ windings. The $\ell = 1$ coils which drive the instability are driven by a crowbarred capacitor bank. The module output power of 30 MW rises in 1.3 μsec and may be sustained for as much as 20 μsec. From detector output to power-module output the power gain of the feedback system is 7×10^{14}.

* Work performed under the auspices of the U. S. Atomic Energy Commission

G 2 Dynamic Stabilization Experiments with Standing Wave Magnetic Fields. G. BECKER, O. GRUBER, H.HEROLD, Max-Planck-Institut für Plasmaphysik, Euratom Association, Garching bei München, Germany. -- The magnetic field configuration of a standing wave is applied to a linear screw pinch ($T_e+T_i \approx 120$ eV; $\beta \approx .3$; $n \approx 10^{16}cm^{-3}$ B_z = 18 kG) for dynamic stabilization of the helical m=1 mode. The HF fields (amplitude : $\tilde{B}_z$) are produced by loops spaced equidistantly ($\lambda_B/2$ = 14.5cm) in the θ-coil and fed in counter-phase by a high Q, high voltage capacitor bank. The stabilizing frequency is about $5.10^6 s^{-1}$ and the ratio $\epsilon = \tilde{B}_z/B_z$ is up to .26. Stabilization experiments were carried out for a wide variation range of relevant parameters (ϵ; m=1 growth rate 3.10^5 to $10^6 s^{-1}$ and wavelength λ of 200 to 460cm). A stabilizing effect on the m=1 mode by the standing wave fields is not observed in any of these cases although the stability condition of sharp boundary, linearized MHD theory /1/ ($\epsilon > C\,\lambda_B/\lambda$; C between 1 and 2) is well fulfilled.

/1/ G.Berge and J.P.Freidberg, Phys.Fluids 14, 1035 (1971)

G 3 Solution to Image Current Problems in Helical Equilibrium Toroidal Theta Pinch Experiments, E. L. CANTRELL, O.M. FRIEDRICH, JR. and ARWIN A. DOUGAL, U. Texas at Austin -- An equilibrium condition is derived where the axial, spatial period of the $\ell = 0$ field is twice that of the $\ell = 1$ field. This eliminates an undesirable vertical force which results from wall image currents without reducing the $\ell = 0$ field. The analysis treats the spatial dependence of the inductive coupling between the plasma and the theta pinch coil. For Scyllac[1] an equilibrium condition is obtained and agrees with previously reported analyses[2]. Inclusion of image currents results in an asymmetry in the vertical plane and thus in a vertical force. Calculated wall collision times agree with those reported in initial Scyllac experiments[3]. An experiment with $\ell = 0, 1$ fields in a 30 Kj toroidal sector of an aspect ratio comparable to Scyllac is described which demonstrates equilibrium.

1. F. L. Ribe, et al LASL Report LA-4597-MS (1971).
2. Morse, R. L., W. B. Riesenfeld, and J. L. Johnson, Plasma Physics 10, 543 (1968).
3. F. L. Ribe, LASL Status Report LA-4888-PR, 3 (1972).

G 4 CO_2 Laser Heating of a Small Θ Pinch.* N. A. AMHERD, G. C. VLASES, U. of Washington.--It has recently been suggested that pulsed, CO_2 lasers can be used effectively to heat Θ and stabilized z pinches.[1,2] In such laser augmented pinches it is in principle possible to independently adjust the final plasma density, temperature, and pinch ratio. Implications of these techniques for the CTR program have been previously discussed.[1] In the present work a small experiment involving a Θ pinch 19 cm x 3.5 cm, irradiated axially by a 3-5 joule TEA laser, has been used to study refraction and absorption. The results indicate that the beam is trapped and absorbed during periods in which the density profile is favorable.

*Work supported by the National Science Foundation and NASA

[1]J. M. Dawson et al., Proc. Esfahan Symposium of Fundamental and Applied Laser Physics, Esfahan, Aug. 1971 (to be published by John Wiley and Sons).
[2]G. C. Vlases, Physics of Fluids 14, 1287 (1971).

G 5 Formation of High β Fusion Plasmas with Intense Relativistic Electron Beams.* S.D. PUTNAM and C.H. STALLINGS. Physics International Company, San Leandro, CA.--The availability of intense relativistic electron beams with a wide range of parameters (energies up to megajoules, power levels up to 10^{13}-10^{14} watts) and the continuing downward trend in the cost of electron beam power systems make these beams interesting energy sources for generating high β, high temperature plasmas. We consider various beam plasma energy transfer mechanisms in the context of existing beam parameters: (1) collisional, (2) excitation of turbulent fields, and (3) energy transfer via zero-order fields. (Zero-order fields refer to beam-induced space charge and B_θ fields and dia- or paramagnetic changes in an externally applied longitudinal field.) We also show that electron-beam-accelerated ions can be used as energy supplements for high density plasmas as, e.g., the dense plasma focus.

*This work supported in part by the Defense Nuclear Agency.

G 6 Interaction of Intense Relativistic Electron Beams with Linear Pinches.* JAMES BENFORD, BRUCE ECKER and SIDNEY PUTNAM. Physics International Company, San Leandro, CA.--Intense relativistic electron beams (0.5-1 MeV, 100-400 kA) propagate in linear pinches with high efficiency. The beam-pinch interaction can be modeled as a single particle orbit motion of beam electrons in the pinch field unless beam transverse pressure is comparable to unbalanced pinch pressure and $\beta \equiv [(nkT)_p + nW_{\perp b}]/B_\theta^2/8\pi > 1$, where $(nW_\perp)_b$ is the beam transverse energy density. A model of pinch field distortion due to transverse pressure imbalance is presented and applied to experimental data, and the results of a tapered pinch experiment to generate a local increase in β are described. Implications of the models to turbulent beam heating of pinch plasmas are briefly discussed.

* Work supported in part by Defense Nuclear Agency.

G 7 Non-Thermal Process in a Linear Pinch Device. T. N. LEE, Naval Research Laboratory, Washington, D.C.-- A low pressure, linear discharge initiated by focusing a pulsed laser beam between two electrodes produces a concentrated thermal plasma of $T_e \approx 8$ keV and $N_e \approx 10^{21}$ cm^{-3}. This plasma emits x-ray line radiation arising from highly stripped atoms such as hydrogen and helium-like iron ions. The temperature of the Fe XXV-ion estimated from Doppler line broadening is higher than the electron temperature, in agreement with the results obtained by Peacock, et al[1] The heating mechanism for attaining such high temperatures during the very short periods of interest is considered, and some experimental results supporting the contribution to the plasma heating by a non-thermal process are presented.

[1]N. J. Peacock, M. G. Hobby and P. D. Morgan, 4th Conf. Proc. Plasma Physics and Controlled Nuclear Fusion Research, 2 537 IAEA, Vienna, 1971.

G 8 The Properties of a Coaxial Deflagration Plasma Gun D.Y.Cheng and P. Wang, Univ. of Santa Clara----- Theories show that deflagration and detonation(snow-plough) discharge modes are two branches of the possible solutions of the conservation equations with energy addition. Deflagration is on the expansion branch of a MHD Hugoniot Curve and detonation is on the compression branch. The ionization wave propagates along the particle path for the detonation and in opposite direction for deflagration. In deflagration, the high-density ionization wave is held by the on-coming neutrals injected through a coaxial gun breech. The plasma is expanded downstream until the Larmor radius and the mean free path are longer than the electrode spacing, following the direction of the Poynting vector formed by the electrode configuration and the self magnetic field. The results of the deflagration theory were confirmed by the image converter pictures of the discharge and by the magnetic field structure inside the gun barrel. Plasma density and other measurements will also be presented.
This work is supported by NASA Univ. Grant NGR-05-017 -019.

G 9 Simulation and Optimization of Theta-Pinch Impulsing Circuit Parameters, Working from Cumulative Generator with Current Interrupter. Aleksandrov V.M., Baikov A.P., Ivanov V.A., Iskoldski A.M., Krotman L.S.,Nesterikhin Yu.E., Nesterov A.A. Institute of Automation and Electrometry of the USSR Ac.Sci. Novosibirsk. - To determine the efficiency of the method the simulation and optimization of Theta-pinch impulsing circuit acting from a cumulative generator with a current interrupter was performed with an analog computer. The circuit inductance, initial resistance and mass of the interrupter were optimized. As a result it is stated, that with the generator inductance $Ig = 1.2 \cdot 10^{-8}$ H at the end of the collapse cycle and the same circuit inductance, the optimal interrupter makes it possible to obtain the rate of rising current in Theta-pinch impulsing circuit of 10^{13} A/sec at the circuit e.m.f. of 200 kv and maximum current amplitude of 3 MA. The Battery giving initial current has the following parameters:
$C = 1.8 \cdot 10^{-3}$ F, $U_{charge} = 4$ kv.

G 10 Parametric Studies of LINUS, An Ultra-High Magnetic Field Theta-Pinch. J.P.BORIS and R.A.SHANNY, Naval Research Laboratory, Washington.--Numerical investigations describing the gross behavior of a theta-pinch in which a large magnetic field is produced by imploding a rotating liquid lithium liner (as suggested by Velikov) will be reported. A regime of magnetic field strengths from 1 to 10 megagauss, plasma temperatures from 1 to 20 keV and number densities up to few times 10^{19} have been investigated and radial confinement of the order of a few microseconds has been predicted. The results of these studies indicate that the LINUS concept is a feasible thermonuclear reactor. Curves indicating optimized design parameters will be presented and the technological and scientific difficulties will be discussed.

G 11 A Pulsed High-Beta Fusion Reactor Based on the Theta Pinch.* S.C. BURNETT, W.R. ELLIS, T. OLIPHANT, F.L. RIBE, University of California, Los Alamos Scientific Laboratory, Los Alamos, New Mexico. -- A design study of a pulsed high-beta θ-pinch reactor is presented. In the case chosen the reactor is designed to generate 1750 MWe with a duty factor chosen to limit the first wall nuclear power loading to 3.5 MW/m^2. The question of energy balance is discussed and it is shown that the reactor system described has a total circulating power of less than 10%. Some advantages of a pulsed system with respect to a steady state system are outlined.

* Work performed under the auspices of the U.S. Atomic Energy Commission.

PLASMA EXPERIMENTS ON ℓ = 1,0 HELICAL EQUILIBRIA IN THE SCYLLAC 5-METER, θ-PINCH TOROIDAL SECTOR

W. R. Ellis, C. F. Hammer, F. C. Jahoda, W. E. Quinn,
F. L. Ribe and R. E. Siemon
Los Alamos Scientific Laboratory, University of California, Los Alamos, New Mexico U.S.A.

ABSTRACT

We report experiments on a sector comprising one third of the 4.8-m diameter Scyllac torus. The toroidal force and outward plasma drift are compensated by an interference force produced by a combination of ℓ = 1 helical fields and ℓ = 0 bumpy fields. We observe the toroidal equilibrium, followed by an m = 1 (sideward) motion of the plasma column, which is nearly the same all along the torus, independent of the ℓ = 0 periodicity, with plasma containment times as large as 11 μsec, comparable to times for plasma end loss. The m = 1 motions, which occur predominantly in the horizontal plane of the torus, suggest either an imbalance between the ℓ = 1,0 and toroidal forces at later times or a long wavelength m = 1 instability. Measurements of the applied magnetic fields show that the product of ℓ = 1 and ℓ = 0 fields for plasma equilibrium agrees with sharp-boundary MHD theory. Time resolved measurements of the plasma diamagnetism, electron density distribution, neutron emission, and beta are reported.

I. INTRODUCTION

When a straight theta pinch is bent into a torus the combination of plasma pressure and the gradient of the toroidal longitudinal compression field B_o forces the plasma toward the outside of the torus. For a plasma of major radius R and minor radius a the force per unit length is $F_R = \beta B_o^2 a^2/4R$, where β is the ratio of plasma pressure to the external magnetic pressure $B_o^2/8\pi$. In the Scyllac experiment [1] the force F_R is opposed by a combination of ℓ = 1 helical transverse fields and ℓ = 0 bumpy fields. The toroidal equilibrium [2,3] of this system and the stability [4,5,6,7] of a straight ℓ = 1 or ℓ = 0 plasma column have been treated in the MHD approximation. In the experiments reported here on the Scyllac toroidal-sector the ℓ = 1 helical field is chosen because theory[4,5,6,7]predicts a growth rate for the dominant k ≈ 0, m = 1 mode which vanishes in leading order. The smaller ℓ = 0 fields produce the asymmetry in the overall plasma excursions $\delta_1 + \delta_o$ which is necessary to produce the equilibrating force,

$$F_{1,0} = [\beta(3-2\beta)/8]\ B_o^2 h^2 a^3 \delta_1 \delta_o \quad (ha<<1), \quad (1)$$

where $2\pi/h$ is the wavelength of the ℓ = 1,0 fields. Initial experiments demonstrating the ℓ = 1,0 toroidal equilibrium were presented at the 1971 IAEA Conference in Madison. [1]

II. EXPERIMENTAL ARRANGEMENT

The Scyllac toroidal sector [1] has a major radius of 237.5 cm, extends through an angle of 120° and has a coil arc length of 5 m. Each meter section of the compression coil is driven by a 700-kJ capacitor bank of 210 1.85-μF, 60 kV capacitors. The experiments reported here were performed with one-half the bank charged to 45 and 50 kV to produce peak magnetic compression fields of 40 to 50 kG with rise times of ~ 4μsec, followed by crowbarred waveforms with L/R times of 250 μsec.

Figure 1 shows the arrangement for applying ℓ = 1 and ℓ = 0 fields to the Scyllac plasma. The ℓ = 1 fields were applied by means of bifilar helical windings, divided into one-period (λ = 33.2 cm) lengths with 5.75-cm radius. The ℓ = 1 coils' current, driven by a capacitor bank, rose to its maximum value in ~ 3 μsec followed by a crowbarred L/R decay of 95 μsec. The ℓ = 0 fields were generated by annular grooves in the inner surface of the compression coil (Fig. 1). In some experiments the onset of the ℓ = 0 fields were delayed a few tenths

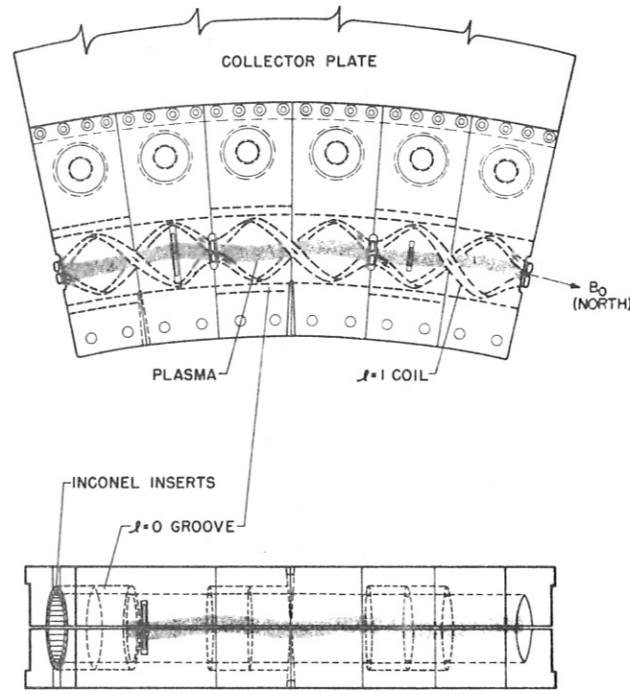

Fig. 1. Arrangement of ℓ = 1 coils and ℓ = 0 grooves (with time-delay inserts) to give a toroidal equilibrium in the Scyllac 5-m toroidal sector.

of microseconds by annular sets of stainless-steel trapezoidal sections (stuffers). In other experiments split copper cylinders(shells) were installed over the ℓ = 0 grooves, with appropriate flux gaps at the edges, to provide an effectively uniform wall for the ℓ = 1 image currents. These shells were also used to reduce the effective depth of the ℓ = 0 grooves.

The following measurements were made of the plasma properties: (1) Three high-speed streak cameras, viewing the plasma column side-on were used to record the transverse motions of the plasma column; (2) A coupled-cavity He-Ne laser interferometer was used to measure the time history of plasma electron density integrated along a chord of the plasma cross section; (3) A magnetic loop and probe arrangement was used to measure the magnetic flux exclud-

ed by the plasma. Combined with density profiles from the luminosity, the excluded flux can be expressed in terms of the plasma β; (4) A ten-channel, side-on luminosity experiment was used to obtain the intensity profiles of the plasma column. These luminosity profiles, in conjunction with the coupled cavity interferometer data, gave absolute density profiles; and (5) Scintillation and silver-foil activation counters were used to measure the neutron emission.

III. RESULTS

The experimental procedure was to vary the ℓ = 1,0 equilibrium configuration by changing the conditions of the ℓ = 0 grooves, which include their depth, whether they are stuffed or unstuffed, and the presence or absence of shells. For each of these ℓ = 0 geometries, the ℓ = 1 fields were varied to optimize the plasma containment time τ_{Plasma}. Table I lists the ℓ = 0 geometries and experiments performed in the various equilibrium configurations, where B_o is the average toroidal field, b_L is the radius of the coil bore in the land regions, δ_o is determined from luminosity profiles, and δ_1 is derived from the measured magnetic fields and β through the relation $\delta_1 = B_{\ell=1}/B_o ha(1-\beta/2)$. [2]

Control experiments [1] in a smooth-bore coil (14.4-cm diam) with a pure toroidal field (no helical or bumpy fields) showed that: (1) The plasma heating processes are unaffected by the toroidal curvature; and (2) The plasma column drifts to the discharge tube wall (inside radius = 4.3 cm) in 2.2 (P_{D_2} = 10 mTorr) to 2.7 μsec (20 mTorr filling) because of the toroidal force. The peak plasma β was ~ 0.8, the ion temperature ~ 1 keV, and the density on axis 2 to 3 x 10^{16} cm^{-3} with a 10-mTorr deuterium filling pressure. Similar plasma parameters are measured in the experiments described below.

A. Transverse Motions of the Plasma Column With the 1.8-cm ℓ = 0 grooves (Exp. B, Table I), the

TABLE I

SCYLLAC TOROIDAL SECTOR EXPERIMENTS

EXPERIMENT	ℓ = 0 GROOVE DEPTH (cm)	GROOVE CONDITION	b_L (cm)	B_o (kG)	$\frac{B_{\ell=0}}{B_o}$	$\frac{B_{\ell=1}}{B_o}$	δ_o	δ_1	τ_{PLASMA} (μsec)
A	0	-	7.21	50	0	0	0	0	2.5
B	1.8	STUFFED	7.21	42.6	0.220		0.3	-	4-6
C	0.9	UNSTUFFED	8.12	40.0	0.105	0.080	0.2	0.68	6-9
D	0.9	STUFFED	8.12	40.0	0.105	0.086	0.2	0.73	5-7
E	0.75	UNSTUFFED W/SHELLS (1.5 mm)	8.12	40.2	0.089	0.090	-	0.76	7-11
F	0.6	UNSTUFFED W/SHELLS (3.0 mm)	8.12	40.9	0.071	0.096	-	0.80	4-7

ℓ = 1,0 fields balanced the toroidal force. [1] However, the plasma lifetime was limited to 4 to 6 μsec by a "ballooning" effect [or z dependence of the plasma sideward (m = 1) motion], which carried the plasma column to the wall periodically in each ℓ = 0 groove region. Probing of the ℓ = 1 fields showed them to be 35% stronger in the region of the 1.8-cm deep grooves due to differences in image current effects in groove and land regions. This electrical effect was anticipated in the original design; its considerable consequences for plasma behavior were not.

Reduction of the ℓ = 0 groove depths to 9 mm (Exp. C, Table I) and the associated reduction of the z dependence of the ℓ = 1 fields to 14% had a marked effect in largely eliminating the ballooning. The m = 1 (sideward) motion was nearly the same in the land and groove regions, with improved plasma containment times of 6 to 9 μsec. The streak photographs of Fig. 2A show the horizontal plasma motions without the ℓ = 1 coils excited. The motion is a simple toroidal "drift" to the walls with no observable effect induced by the bumpy ℓ = 0 fields. In Fig. 2B the ℓ = 1 coils were excited to 56 kA. Following the initial implosion the plasma column takes up an equilibrium position, which is shifted slightly inward in the groove regions, outward in the land regions and vertically in the planes between the groove and land regions as expected from the helical equilibrium shift of the plasma column. After remaining in equilibrium for 6 μsec, the plasma begins to drift outward in both the land and groove regions and strikes the wall in the land region.

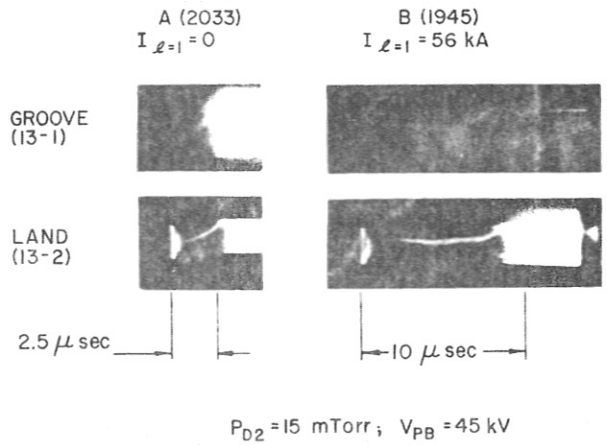

Fig. 2. Streak photographs near the center of the toroidal sector plasma showing horizontal motions (Exp. C, Table I).

In the experiments C through F of Table I with ℓ = 0 groove depths in the range of 6 to 9 mm, the transverse motions of the plasma column were quite similar. Comparison of the streak photographs of

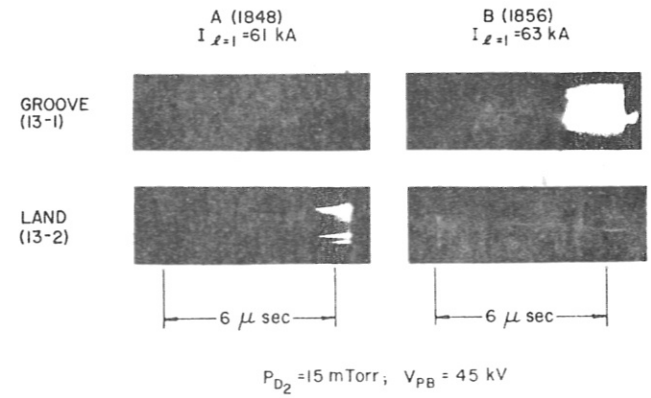

Fig. 3. Streak photographs of the toroidal sector plasma showing the effects of varying the ℓ = 1 coil currents on the horizontal motions (Exp. C, Table I). A (Left photographs): $I_{\ell=1}$ = 61 kA. (Right photographs): $I_{\ell=1}$ = 63 kA.

in the amplitude of the ℓ = 1 fields. A few percent

increase in the $\ell = 1$ current changes the plasma motion from being radially outward to inward in both land and groove regions. The streak photographs of Fig. 4 show two of the better discharges in terms of plasma containment with 7.5 mm, $\ell = 0$ groove depths and filler shells.

The observed transverse motions of the plasma at various positions around the torus show the following: (1) The plasma column takes up an initial helical shift and comes into an equilibrium position which lasts 4 to 11 μsec in contrast to a complete

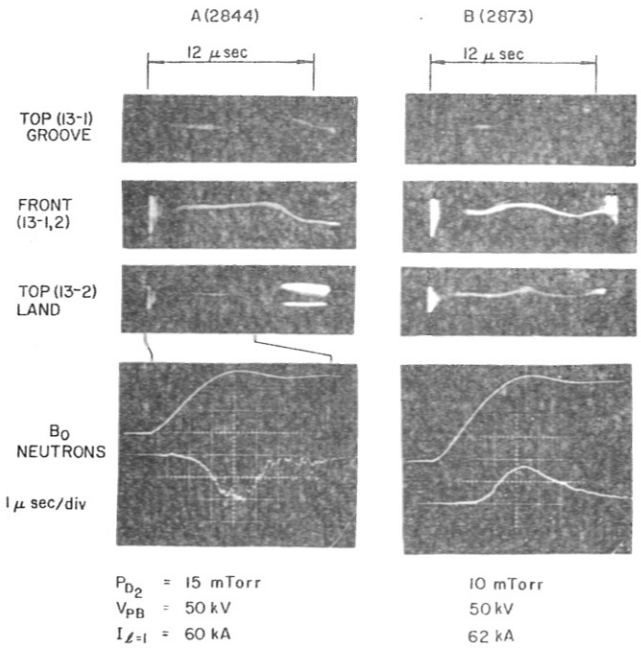

Fig. 4. Streak photographs of the toroidal sector plasma showing the horizontal (upper and lower photographs) and vertical (center photographs) motions (Exp. E, Table I). Oscillograms of main compression field and neutron-scintillator signal from Experiment E, Table I (lower left) and Experiment D, Table I (lower right).

absence of equilibrium without the $\ell = 1,0$ fields; (2) As the plasma moves away from the equilibrium position, the motion in the land and groove regions are usually similar, i.e., the column either moves radially outward or inward; and (3) The motion of the plasma column develops largely in the horizontal plane of the torus rather than in random directions. The values of the quantity $hRB_{\ell=0}B_{\ell=1}/B_o^2$ required experimentally to achieve equilibrium are in the range of 0.36 to 0.41 (Exps. C-F, Table I) compared with 0.62 to 0.33 for sharp boundary theory for respective β values of 0.6 to 0.8.

B. Neutron Emission The neutron emission usually begins to decrease at a time near the maximum of the magnetic field, Fig. 4, while the plasma remains confined. This is interpreted as follows: With reduced bank energy and with the neutron emission ($\sim 2 \times 10^6$/meter) near its threshold, the majority of neutrons result from an initially hotter plasma in the land regions. When temperature equilibration occurs between land and groove regions, the temperature and neutron emission decrease. Before axial equilibration the plasma is heated more in the land regions owing to: (1) The ~ 23% larger magnetic compression field in the land regions; (2) The ~ 11% larger azimuthal electric field in the land regions; and (3) In the unstuffed groove cases the observed enhanced δ_o (see below) which decreases the plasma density in the land regions and increases it in the groove regions. The neutron emission with the stuffed $\ell = 0$ grooves, Fig. 4B, has a slower decay than that of the unstuffed case, Fig. 4A, as expected from the elimination of effects (2) and (3).

C. Excluded Flux and Luminosity Measurements Fig. 5 shows the time variation for typical discharges of the excluded flux, plasma radius a, and computed beta

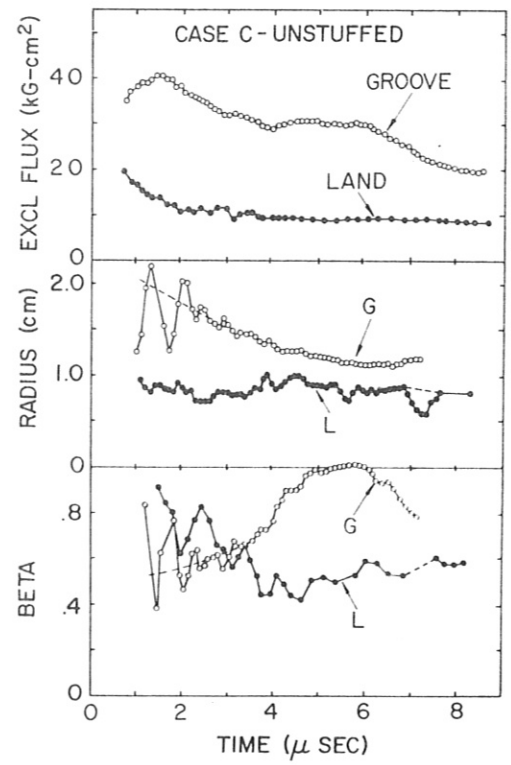

Fig. 5. Observed time variations of excluded flux, plasma radius from luminosity profiles, and computed beta on axis.

on axis (β). These data are derived from the side-on luminosity and balanced probe measurements by curve fitting, under the simplifying assumptions that the plasma has a Gaussian density profile and a uniform temperature. The Gaussian profile provides a good fit to the luminosity data, and the plasma radius a is taken as the inflection point of the density profile.

These data have been used to study the approach to axial pressure equilibrium as shown in Fig. 6 and Fig. 7 for the unstuffed case. In Fig. 6 is plotted the ratio β_L/β_G which should equal $(B_G/B_L)^2$ and $(b_G/b_L)^4$ if plasma pressure is independent of length along the column. (Here L and G refer to the center of the land and groove regions respectively, B is the measured compression field and b is the local compression-coil radius. At early times the ratio β_L/β_G is larger than the equilibrium value to which it relaxes in about 4 μsec. This corresponds to a

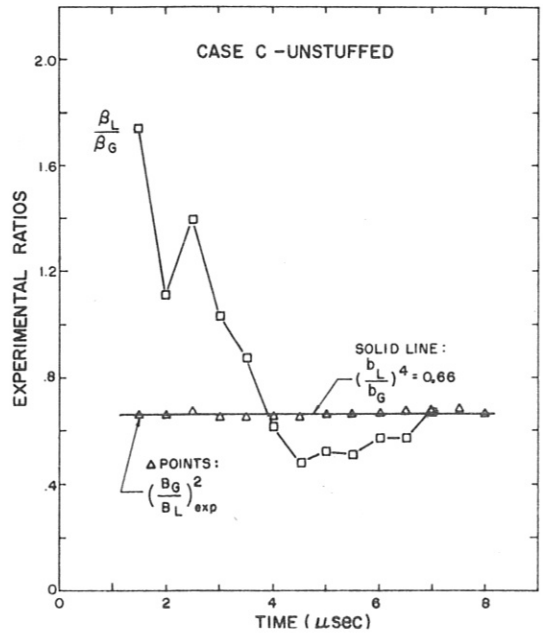

Fig. 6. Comparison of measured ratio of beta's in the land and groove regions with the values (horizontal line) corresponding to axial pressure equilibrium.

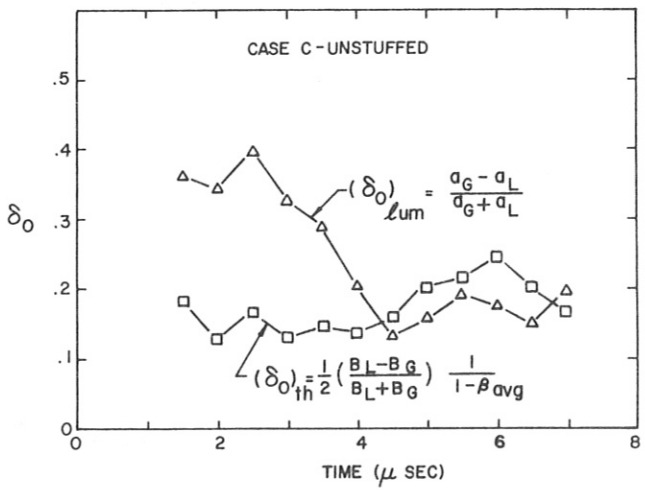

Fig. 7. Comparison of plasma column bumpiness $(\delta_o)_{lum}$ derived from the luminosity profiles with the value $(\delta_o)_{th}$ corresponding to the axial field variations in the land and groove regions.

transfer of energy density from the land to the groove regions.

The same phenomenon is also apparent in the plasma column bumpiness δ_o, as shown in Fig. 7. The values $(\delta_o)_{lum}$, directly measured as $(a_G - a_L)/(a_G + a_L)$, are initially greater than the values $(\delta_o)_{th}$ which should be the response to the fields B_L and B_G at axial pressure equilibrium. This indicates that the grooves are "overloaded" with plasma initially, corresponding to an "enhanced" δ_o.

IV. DISCUSSION

The plasma is observed to take up a helical toroidal equilibrium for approximately 5 μsec when the $\ell = 1$ fields are applied, in contrast to the case with no $\ell = 1$ field where the plasma accelerates immediately to the outer wall of the torus. At ~ 5 μsec an m = 1 plasma motion to the wall usually takes place, predominantly in the horizontal plane. No higher m unstable modes are observed. The m = 1 motion is the same in land and groove regions. Thus the "ballooning" observed earlier [1] with large δ_o has been eliminated. We conjecture that the m = 1 motion may have either of the following causes: (1) The k ≈ 0, m = 1 instability, observed when $\ell = 1$ fields are applied to a linear plasma column [8] may be occurring. In the present, toroidal case, however, the plasma remains stable for ~ 5 μsec, while in the linear case the instability sets in immediately; (2) A loss of equilibrium due to an imbalance in the applied $\ell = 1,0$ and toroidal forces may be developing, because of: (a) Failure of the $\ell = 1$ fields to "track" the toroidal B_ρ field in time (tracking is within ± 15%); or (b) Change of plasma β, radius, or δ_o with time (e.g. Figs. 5 and 7.) The plasma motion to the wall in case (2) may occur because the loss of equilibrium excites the m = 1 instability, or because it forces the plasma position outside the radial region near the toroidal axis (~ 2 cm) where the $\ell = 1$ fields produced by the helical windings have the required constant amplitude. The observed containment times are sufficient for the end effects (particularly the "wobble") observed in the linear case [8] to set in, initiating such a loss of equilibrium. (We note that the m = 1 plasma trajectory is best fit by a parabola rather than an exponential.)

A feedback stabilization system [2,9] is being prepared which is capable of compensating the m = 1 instability of case (1), the more difficult of the two cases to correct.

Work performed under the auspices of the U.S. Atomic Energy Commission.

REFERENCES.

[1]. S.C. Burnett, et al., Plasma Phys. and Controlled Nucl. Fusion Research 3, 201 (1971).
[2]. F.L. Ribe & M.N. Rosenbluth, Phys. Fluids 13, 2572 (1970).
[3]. H. Weitzner, Phys. Fluids 14, 658 (1971).
[4]. M.N. Rosenbluth, et al., Phys. Fluids 12, 726 (1969).
[5]. H. Grad & H. Weitzner, Phys. Fluids 12, 1725 (1969).
[6]. J.P. Freidberg & B.M. Marder, Phys. Fluids 14, 174 (1971).
[7]. J.P. Freidberg, Plasma Phys. & Controlled Nucl. Fusion Research 3, 215 (1971)
[8]. K.S. Thomas, et al., To be published Phys. Fluids, 15, Aug. 1972.
[9]. S.C. Burnett, et al., Paper G 1, these proceedings.

Toroidal High-Beta Stellarator Experiments on ISAR T 1

E.Fünfer, M.Kaufmann, W.Lotz, M.Münich

J.Neuhauser, G.Schramm, U.Seidel

Max-Planck-Institut für Plasmaphysik, Euratom Association

Garching bei München, Germany

Abstract: Toroidal theta pinch experiments on ISAR T 1 using different combinations of $\ell = 1$, $\ell = 2$, and partly $\ell = 0$ fields are described. Best results are obtained with a mixture of all field components. For better understanding of the dynamical phase, forces of the stellarator fields on a not deformed plasma cylinder were calculated.

I. Introduction: $\ell = 1$ stellarator fields combined with smaller magnetic field components of other symmetry (e.g. $\ell = 2$, $\ell = 0$)/1/ can produce M&S-like toroidal equilibria with a non-planar axis and without net plasma current. For high aspect ratio ($A = R/r_p$, r_p = plasma radius, R = major radius) and intermediate β such equilibria are much less m = 1 unstable than the classical M&S/2/ and can be wall stabilized /3/. At lower β ($\beta \approx 0.1$) an average minimum B stabilization by $\ell = 2$ fields should be possible, too /4/. For stability reasons a $\ell = 2$ admixture seems to be favourable and was therefore in the centre of this investigation.

II. The ISAR T 1 configuration: With the ISAR T 1 toroidal theta pinch (bank energy 2.6 MJ, R = 135 cm, B_{max} = 34 kG, T/4 = 7.5µs) we can produce a strong $\ell = 1$ magnetic field as well as moderate $\ell = 2$ and $\ell = 0$ fields in addition to the main toroidal field. The $\ell = 1$ and $\ell = 2$ fields are produced by helical conductors ($\ell = 1$: $\lambda_1 = 2\pi/h_1 = 35.5$cm, 24 periods; $\ell = 2$: $\lambda_2 = 2\lambda_1$). The $\ell = 0$ field is generated by copper inserts (Fig.1; $\lambda_0 = \lambda_1$). As we use asymmetrical inserts, we get additional but comparable small $\ell = \pm 1$ components. In the first experimental run the $\ell = 2$ and $\ell = 0$ fields have been restricted to one-fourth of the torus in order to try different combinations with less technical effort.

The equilibrium plasma surface (sharp boundary) for the general case may be written (neglecting toroidal effects) as:

$$r = r_p\left[1 + \delta_1 \cos(h_1 z - \theta) + \delta_2 \cos\left[2(h_2 z - \theta)\right] + \delta_0 \cos h_0 z\right]; h_0 = h_1 = 2h_2$$

Fig. 2 shows a side-on view of the plasma column for each component and the resulting M&S-like structure, producing a force $F = F_{1/2} + F_{1/0}$ opposite to the toroidal drift force F_R.

III. Dynamic effects: The possibility of producing a helically deformed plasma column by shock heating was shown in linear experiments /5/. Additional problems may arise in a toroidal experiment, because $F_{1/2}$ and $F_{1/0}$ are time dependent as a consequence of dynamical effects. Using a cylindrical quartz tube the initial plasma surface and the surface of the compressed plasma will be cylindrical rather than helical. Calculating the interference forces acting upon a

conducting cylinder we get (per unit length):

$$F_{1/2\ cyl} \approx I_1\ I_2\ r_p^2\ \mu_o\ .\ 2/\pi.r_w^3 \text{ and } F_{1/o,cyl} \approx \tilde{B}_o\ I_1\ h_1\ h_1 r_p^2/r_w$$

while the equilibrium forces /1/ are:

$$F_{1/2} = F_{1/2,cyl}\ .\ 2\beta/2-\beta \text{ and } F_{1/o} = F_{1/o,cyl}\ .\ \beta(3-2\beta)/\left[(1-\beta)(2-\beta)\right].$$

($I_{1/2}$ = helical currents, $\tilde{B}_o$ = amplitude of the $\ell = 0$ field, r_w = radius of helical windings). If β is near 0.5 the force on a cylindrical plasma is nearly equal to the equilibrium force. Therefore one should expect, that stellarator fields of the right magnitude compensate the toroidal drift already during the built up of the helical deformations.

IV. Plasma parameter: Most experiments were performed using only 1/3 of the bank (0.5 MJ). The deuterium gas was preionized by a toroidal z-pinch, where special care was taken to avoid net toroidal plasma current after the driving z-current pulse was switched off.

The sum of the ion and electron temperatures (T_i+T_e) was determined from the toroidal drift of the pure theta pinch assuming sinusoidal time dependence. For 0.5 MJ, 20 microns there was $(T_i+T_e)_{max}$ = 140 eV (degree of preionization α = 15%). T_e was also determined from the time dependence of oxygen impurity lines by solving the rate equations, giving $T_e \approx T_i$. The density was measured with a feedback laser interferometer (infrared, λ = 3.4 µm) or with a microwave Michaelson interferometer (λ = 1mm). For the above parameters the maximum density on the axis was $n_A \approx 1.2 \times 10^{16} cm^{-3}$ (r_p = 1.0 cm) giving $\beta(t = 5\ \mu s) \approx 0.4$.

V. Experiments with different field admixtures

(a) Theta pinch with $\ell = 2$ or with $\ell = 0$ (inserts): The gross toroidal drift motion was the same as in the pure theta pinch. The plasma deformations δ_2, δ_o have not yet been measured. Theoretical values were $\delta_o \approx 0.02/(1-\beta)$, $\delta_2 \approx 0.4(2-\beta)$.

(b) Theta pinch with $\ell = 1$: The plasma helix was formed as in linear experiments but the centre of the helix showed nearly the same drift as the pure toroidal theta pinch. The averaged δ_1 was $\langle \delta_{1\ exp} \rangle \approx 1.5 \ldots 2$ (depending on the retardation of the $\ell = 1$ field) compared with a theoretical value of $\delta_1 \approx 3.0/(2-\beta) \approx 1.9$.

(c) Theta pinch with $\ell = 1$ and $\ell = 0$: Because of the very small $\ell = 0$ there was nearly no difference compared to the pure $\ell = 1$ case in qualitative agreement with theory.

(d) Theta pinch with $\ell = 1$ and smaller $\ell = 2$: From theory /1/ we get the equilibrium condition $\delta_1\ .\ \delta_2 = 2r_p/(2-\beta)\ (h_1 r_p)^2$. $R \approx 0.53/(2-\beta)$. Starting with $\langle \delta_1 \rangle \approx 1.5$, we found a strong effect of the $\ell = 2$ even with a very small $\ell = 2$ admixture. By increasing δ_2, however, only a relatively small improvement could be achieved. Even with $\delta_1\ .\ \delta_2$

higher than claimed by theory, the lifetime of the plasma was not much longer than the toroidal drift time (Fig.3;phase I/III: local helical displacement inward/outward). From smear pictures at different slits a long the torus sector with $\ell = 2$ windings, we concluded that end effects should not have caused the early wall contact. Smear pictures seem to show an initial disturbance in the outward direction of the plasma helix during the dynamic phase. Such a disturbance enhanced by instabilities could lead to the observed behaviour. A final experimental prove and an explanation of the disturbance is still necessary.

VI. Theta pinch with $\ell = 1$, $\ell = 2$, and $\ell = 0$: The best result was achieved by combining $\ell = 1$, $\ell = 2$, and $\ell = 0$. Smear pictures at opposite phases are given in Fig.4a compared to the toroidal drift of the theta pinch. In this case $\delta_{1\ exp} \approx 1.1$, while theoretical value were about $\delta_1 = 1.25$, $\delta_2 = 0.25$, $\delta_0 = 0.033$. Similar results were obtained if δ_1 was increased and δ_2 appropriately decreased. By increasing only one component by 25% the plasma helix was driven inward (Fig.4b). Also net toroidal plasma currents $/I_p/ \geq 1$ kA changed the plasma behaviour.Again we examined end effects. In Fig.5 smear pictures at the same phase but 0.5 λ_1 and 1.5λ_1 away from the centre of the torus sector are shown. The end effect is readily seen. The end effect may be enhanced by unstable forces.

We should mention that the $\ell = 1/\ell = 0$ interference force seems to contribute only a small part to the balance of forces at late times. Nevertheless, the $\ell = 0$ seems to be favourable during the dynamic phase to avoid large initial displacement of the plasma column, while later on the equilibrium is mainly governed by interference of $\ell = 1$ and $\ell = 2$ fields. The most favourable configuration found in this sector experiment will be furnished all around the torus in the near future. In this experiments the influence of the small $\ell = 0$ fields on the equilibrium in particular at early times will be further investigated.

We gratefully acknowledge helpful discussions with Dr.J.Nührenberg and Dr.F.Herrnegger and thank W.Ochem for numberical calculations.

References:

/1/ Ribe,F.L., M.N.Rosenbluth; Phys.Fluids 13, 2572 (1970)
/2/ Meyer,F., H.U.Schmidt; Z.f.Naturf.13a, 1006 (1958)
/3/ Weitzner,H., Plasma Phys.Contr.Nucl.Fus.Res., Vol.III,CN 28/J-6 Vienna (1971)
/4/ Freidberg,J., B 9 this conference
/5/ Fünfer,E. et al.; Plasma Phys.Contr.Nucl.Fus.Res., Vol.III, CN 28/J-3, Vienna (1971)

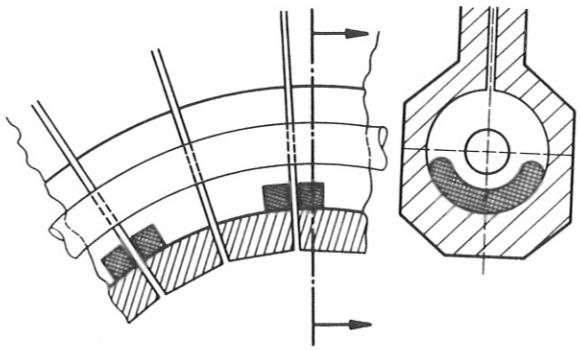

Fig. 1

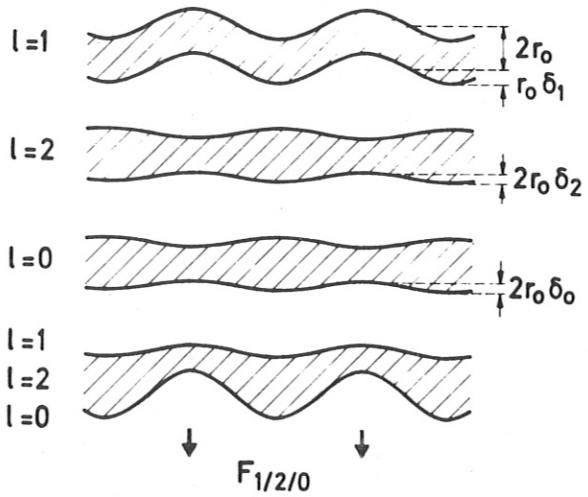

$$r_p = r_0 [1 + \delta_1 \cos(h_1 z - \Theta) + \delta_2 \cos[2(h_2 z - \Theta)] + \delta_0 \cos(h_0 z)]$$

$$h_1 = h_0 = 2h_2$$

Fig. 2

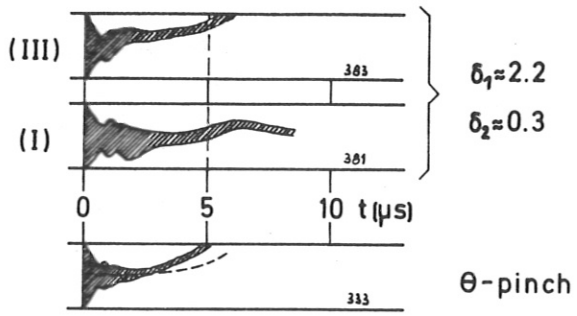

Fig. 3

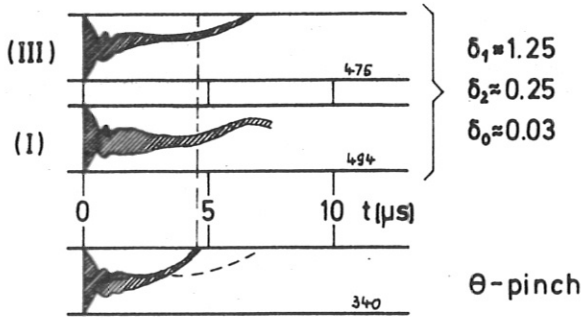

Fig. 4a

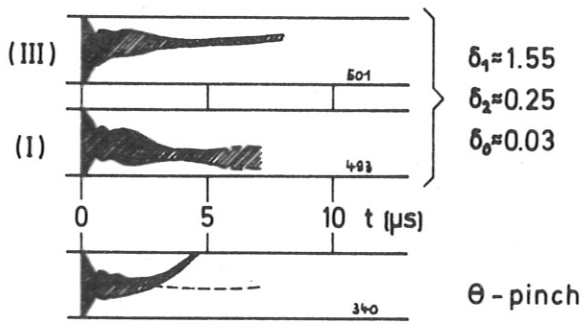

Fig. 4b

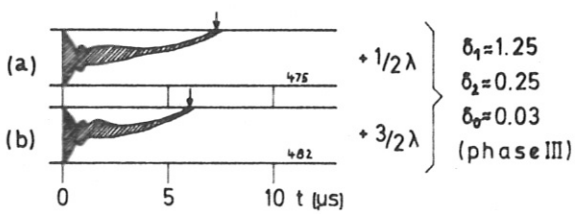

Fig. 5

HIGH-BETA REVERSED FIELD DISCHARGES WITH EXTENDED LIFETIMES

C.W. Gowers*, G.F. Nalesso+, A.A. Newton, D.C. Robinson, A.J.L. Verhage, H.A.B. Bodin
UKAEA, Culham Laboratory, Abingdon, Berks.

ABSTRACT Criteria for setting up stable reversed field distributions are discussed and experiments described in which such configurations have been generated without instability or wall contact. The plasmas have $\beta_\theta \sim 0.8$ and lifetimes $\sim$ 30-40 μsec, the classical resistive decay time of the confining magnetic fields.

INTRODUCTION Further studies of the confinement of high-beta plasma in the reversed field pinch configuration[1-4] are described in this paper. Theoretically[2] this configuration can be stable to all ideal M.H.D. modes with $\beta \sim 0.3$-0.4; stability with $\beta \sim 0.1$ was observed for 3 milliseconds in Zeta[4], where the configuration set itself up following both instability and wall contact, with little external control. Reversed field distributions can be set up in a controlled fashion using programming[1]. Although evidence was obtained that the mode which grew in the outer regions, due to a minimum in the pitch, was suppressed, the plasma lifetime was short-typically $\lesssim$ 10 μsec. In no case were the four necessary criteria (see below) all fulfilled together.

CRITERIA FOR SETTING UP STABLE DISTRIBUTIONS USING PROGRAMMING In principle, a conventional stabilised z-pinch is first set up and then the B_z outside the plasma is reversed. Four criteria must be satisfied in order to generate quasi-stationary reversed field distributions in this way:

(1) The reversed B_z must be applied before local current driven M.H.D. instabilities, which grow if there is a pitch minimum[2] in the outer regions, develop.

(2) Wall contact, due to the outward expansion which can result from the application of the reversed field, must be minimised.

(3) Overcompression, which will lead to a violation of conducting wall stabilisation, must be avoided.

(4) Current diffusion (of I_z) near the axis leading to a negative pressure gradient in that region and instability, as observed[1] must be avoided. (Theoretically in pinch discharges with $q < 1$ $p'_{r\to 0} < 0$ always gives instability.)

Criteria (2) and (3) are difficult to fulfill together, as they have conflicting requirements on the timing and rate of rise of B_z with respect to B_θ. The radial motion depends on the value of $E_\theta B_z - E_z B_\theta$ at the walls, and it is this quantity whose time variation must be optimised.

---

* A.W.R.E. Aldermaston, Berks; + University of Padua, Italy.

In previous work[1] for "well compressed pinches" (1) was satisfied, because of the slow growth of the mode, and (2) was easily fulfilled but (3) and usually (4) were violated. In "weakly compressed pinches" (1) could be satisfied, but the plasma was driven outwards against the walls; there was rapid mixing of the opposed B_z fields and collapse of the column (often violating (3)). This behaviour was similar to that in some early reversed field experiments[5,6].

EXPERIMENTAL DETAILS The quartz torus, of 2 m major diameter and bore 12 cm, was encircled by a conducting shell of bore 15 cm. The I_z current was between 40 and 90 kA with fast and slow B_z fields of 3-6 kG. Deuterium at a filling pressure of 30 or 40 mtorr was used. Diagnostics included magnetic field measurements in uncrowbarred* discharges using a magnetic probe (diameter of quartz envelope 9.5 mm) containing five sets of B_θ and B_z coils, each 2.8 mm diameter spaced 1.5 cm apart and two B_r coils; helical sin/cosine Rogowski[7] coils; and laser light scattering.

EXPERIMENTAL RESULTS Electron temperature and density distributions have been measured in similar conditions in both stabilised pinches (the "initial plasma" before the reversed field is applied) and reversed field discharges. Fig.1 shows temperature and density distributions in a stabilised pinch at 4.5 μsec. Both distributions are hollow, the latter peaking at slightly smaller radii. Similar distributions are observed in reversed field plasmas. In stabilised pinches[8] $T \propto \beta_\theta I_z^2$, with β_θ approximately constant about 0.4 as expected for a resistively heated pinch; the peak electron temperature, at 90 kA, was about 30 eV. In reversed field discharges additional heating due to j_θ currents yields $\beta_\theta \sim 0.8$, with peak electron temperature about 20 eV at 50 kA.

Fig.2 shows tracings of the current and B_z field oscillograms for a crowbarried reversed field discharge. The programming sequence used (with the present capacitor bank arrangement) is as follows: the slow B_z is switched on first, followed by the fast reversed B_z with unpreionized gas. Ionization is by means of the main I_z current, which begins to rise about 1 μsec after the fast B_z was switched on. By varying this time delay the relative magnitudes of E_θ and E_z can be controlled. The plasma does not expand outwards and the pitch minimum is either avoided or its duration minimised because there is essentially no compression until the external B_z has reversed. Application of the I_z and B_z crowbars, whose jitter must be less than 200 nsec, leads to a quasi-stationary reversed field configuration.

The time evolution of such magnetic field configurations (for uncrowbarred discharges) is shown in Fig.3. The pressure distribution shows compression is

* For times exceeding 5-10 μsec the probe often perturbed the plasma.

underway at 2 μsec, 0.5 μsec after the B_z reversal at the walls; thereafter the distribution is of annular form (see 3 or 4 μsec) with mean radius about 2 cms, in approximate agreement with scattering data; some overcompression has occurred because the crowbar was not used. Typically, in crowbarred discharges, the annulus is about 3 cms radius, which satisfied wall stabilisation; the pressure gradient near the axis is positive. The parallel conductivity, estimated from magnetic probe data and the measured volts/turn, shows no evidence of anomalous effects when compared with Thomson scattering values at the peak of the pressure distribution (note that usually $v_D < c_s$); $\sigma_\perp$ has been estimated within an uncertainty of about a factor of three and is of the order of $\sigma_{//}$.

Fig.4 shows streak photographs with and without the crowbar; reversed field discharges with lifetimes extending to 30 or 40 μsec have been observed which is to be compared with the classical lifetime of the field configuration of about 37 μsec. A weak m = 1 instability is sometimes evident in the later stages, possibly because $\beta_\theta \sim 0.8$ exceeds the stability limit. Both the total I_z and B_z at the walls decay approximately together (see Fig.2), the decay time being primiarly determined by the plasma temperature; this suggests that the configuration retains the form shown in Fig.3. Scattering measurements at 16 μsec show no significant cooling and a balance between joule heating and losses is evidently set up. Tentative estimates from the decay of the field configurations yield a value of energy confinement time typically a factor of two or three shorter than the lifetime of the column.

CONCLUSIONS Reversed field configurations with $\beta_\theta \sim 0.8$ have been set up without wall contact or instability. Their lifetime of 30-40 μsec corresponds to the classical resistive decay time of the fields; this is to be compared with 3 msec in Zeta where the plasma diameter is much larger. For similar plasma parameters (n, T, β) the lifetime of the reversed field discharge considerably exceeds that of other configurations studied[1] in the present experiment.

REFERENCES

1. H.A.B. Bodin et al. Proc. IAEA Madison Conf. 1, 225 (1971).
2. D.C. Robinson, Plasma Physics 13, 439 (1971).
3. T. Ohkawa et al., Phys. of Fluids 6, 46 (1963).
4. D.C. Robinson, R.E. King, Proc. IAEA Novosibirsk Conf. 1 263 (1968).
5. S. Berglund et al., Arkiv für Fysik 27, 17 (1964).
6. A.P. Babichev et al., J.E.T.P. 14, 983 (1962).
7. R.E. King et al., Culham Preprint CLM-P 302 (1972).
8. C.W. Gowers et al. Paper A4 this Conference.

FIGURE CAPTIONS

Fig.1 Electron temperature and density distributions in an unpreionized stabilised pinch at 4.5 μsec, p_0 = 30 mtorr.

Fig.2 Tracings of current and external B_z field oscillograms for a crowbarred reversed field pinch. p_0 = 40 mtorr.

Fig.3 Magnetic field and pressure distributions for an uncrowbarred reversed field pinch. Graphical output from a computer programme used to analyse the data is shown. The data is normalised with p = 0 at the inner quartz wall, radius 6 cms; the pressure points at larger radii should be ignored.

Fig.4 Streak photographs with (below) and without (above) crowbar of reversed field discharges.

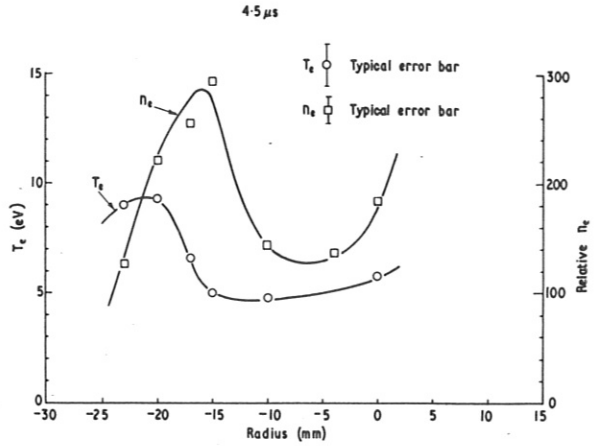

Fig.1

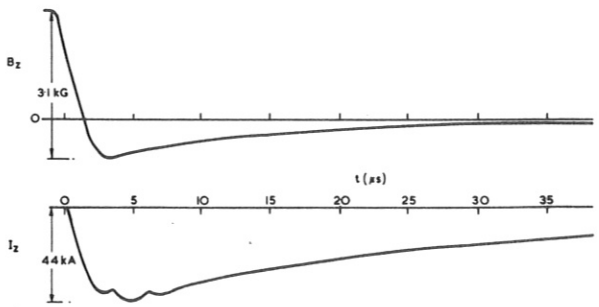

Fig.2

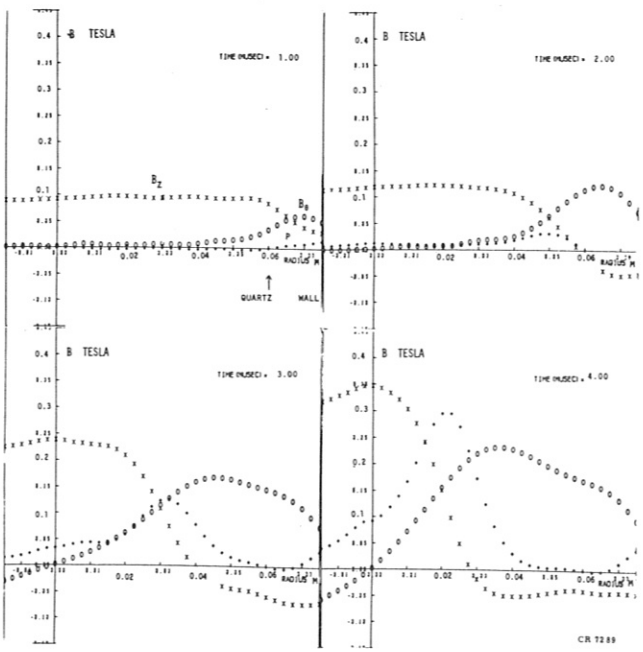

Fig.3

Two stereo views, 26 cms apart

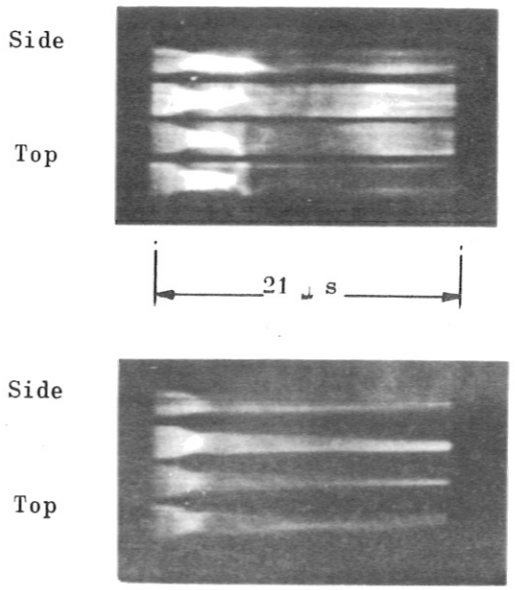

Fig.4

THEORETICAL AND EXPERIMENTAL STUDY OF HEATING AND ENERGY LOSSES IN PINCH DISCHARGES

C. W. Gowers*, G. E. Nalesso≠, A. A. Newton, D. C. Robinson
A. Verhage, A. Wootton+, H. A. B. Bodin
UKAEA, Culham Laboratory, Abingdon, Berkshire, England
*AWRE, Aldermaston
≠Universita di Padova
+Royal Holloway College

ABSTRACT

In HBTX z-pinches, screw-pinches and reversed field-pinches have been investigated with probes, Thomson scattering and spectrally resolved photography. The measured electron temperature and density distributions have been compared with predictions from an MHD code using the full circuit. Agreement within experimental error is obtained in all cases for the compressed regions of the column starting with partially ionised initial conditions corresponding to the preionization plasma. For example, for stabilized pinches both computation and experiment show that the temperature increases as I_z^2 with $\beta_\theta \sim 0.5$; the peak value obtained at 30 mtorr with a current of 90 kA is about 30 eV. Observed electron temperatures in the outer plasmas are lower than predicted even when strong turbulent electron thermal conductivity is assumed in the computation; this will be discussed.

The effect of partial ionization in B_z compression heated systems has been studied in positive and negative bias field in order to investigate ways of controlling beta. Experimentally and theoretically the rate of rise of temperature becomes sensitive to the degree of ionization when the electric field is reduced; in these conditions the heating rate is also very sensitive to the addition of small amounts of negative bias field.

Introduction

Investigations of the evolution and heating of various pinch configurations have been made on HBTX[1] where compression by axial currents, I_p, and axial magnetic fields, B_z, can be used either separately or together in several different ways. A parallel study using the partially ionised 1-D MHD code[2], which has been extended to include multiple arm circuits and inductive coupling for energetically consistent calculations of the B_z and B_θ magnetic fields, has been pursued to understand the formation stages of the pinch. One important type of discharge using both I_p and B_z is the Reversed Field Pinch in which B_z on axis is oppositely directed to B_z at the confining metal wall; hydromagnetic stability is expected and is observed for long times in this pinch[3].

On HBTX B_z pinches (theta pinch and screwpinch) are preionised, but for I_p pinches (z-pinch and reversed field pinch) preionisation is optional and is not used in many cases[3]. Measurements of the preionisation discharge, which carries a "trapped" axial current[4] of about 6 kA, show electron density, n_e, equivalent to 50 per cent ionisation of the filling gas[5] distributed parabolically with a maximum on axis. The electron temperature, T_e, is about 1.5 eV on axis falling to a low value at the wall. The initial distribution of neutrals has not been measured but computations of the partially ionised state[6] (without confining magnetic fields) show that a dense atomic layer accumulates close to the wall in a few μs. Initial conditions for the MHD computations are inferred from these results and comparable, but isothermal, parabolic distributions of density with 90 per cent ionisation on axis are used. Unpreionised discharges are approximated with 10 per cent uniform ionisation.

Stabilised z-pinches

Measurements have been made of the preionised "stabilised" z-pinch with 0.38 kG of initial and fixed B_z and I_p rising to 90 kA in 6 μs in 30 to 40 mtorr deuterium. (90 μF at 36 kV in the z-circuit). Thomson scattering results show initially hollow temperature and density distributions with the maximum of T_e occurring at somewhat larger radii than that of n_e. In Fig. 1 T_e on axis is compared with computations for the preionised and unpreionised cases. After 1.8 μs the effects of compression can be seen and during the bounces the observed and predicted temperatures agree until 6μs when a gross MHD instability destroys the configuration. In unpreionised discharges the electron temperature rises more slowly and the bounces, which are heavily damped in this case, are less apparent.

Coupled measurements of n_e and T_e on axis for the preionised case, when displayed on a log plot (see fig.2) exhibit an effective γ of 1.88 ± 0.17 which is significantly larger than that expected from adiabatic compression of a collision dominated plasma. Since ionisation of the neutrals trapped by charge exchange should reduce the effective γ significant Joule heating is expected.

The observed and predicted sheath structure is also indicative of joule heating in the outer regions of the plasma where $V_D \gtrsim V_S$. Computations show that outside the sheath region the uncollected neutrals maintain a cold layer and the temperature falls to a low value in the vicinity of the wall.

Integrations of the pressure distribution obtained either by Thomson scattering or by magnetic probes which measure B_θ and B_z show that $\beta_\theta \sim 0.3$ to 0.4 ($\beta_\theta = 2Nk(\bar{T}_e+\bar{T}_i)/I^2$) in the compressed stages of the pinch. Figure 3 shows that $T_e \propto I^2$ at this time. Computations show a mean $\beta_\theta \sim 0.55$ with strong excursions superimposed due to radial oscillations. The latter are much stronger in the computation as shown in Fig. 4 where observed and predicted I_p waveforms are compared.

The computation predicts the general properties and the temperature and density of the central regions of the pinch reasonably well. However the code appears to underestimate the damping of radial oscillations and this may be due to either the choice of initial conditions or the approximate forms of the rate coefficients which are used.

Screw Pinches and Theta Pinches

MHD computations of fully ionized theta-pinches have shown high electron temperatures in the outer density regions of the plasma

due to high values of $E^2\sigma/n_e$. This anomaly is removed when partially ionized initial conditions are used, and the distributions of T_e obtained are approximately uniform in the well compressed plasma and fall in the low density outer regions to low values at the wall.

Earlier numerical investigations of the effect of partial ionization on a theta pinch[7] (4 cm radius, 3.5 m length, 20 mtorr D_2) showed that a cooling effect dependent on the initial rate of rise of magnetic field, B_o, could be expected. A threshold $\dot{B}_z \sim 1.5$ kG/μs was predicted below which a 10 per cent uniformly ionized plasma would not be heated. At 10 kG/μs this cooling effect was small and for $\dot{B}_z \geq 15$ kG/μs it was essentially negligible[8]. These effects were studied on HBTX and the 3.5 m theta-pinch where extreme sensitivity to $\dot{B}_z$ was found.

On HBTX, at $\dot{B}_z$ of 1.5 to 3.1 kG/μs, 20 to 60 per cent of the filling gas, estimated from the radial oscillation frequency, was imploded. The mass collected on the 3.5 m theta-pinch varied from 12 per cent at 2.2 kG/μs to 70 per cent at 3.3 kG/μs. The power input decreased less than the mass collection with $\dot{B}_z$ so that higher diamagnetic temperatures were estimated for the lower $\dot{B}_z$. In Fig. 5, which shows measurements of the 3.5 m theta-pinch, comparison of curves 3a and 3b (diamagnetism at 4 μs and at 8 μs) shows a fall of temperature during the half cycle. At the lowest values of $\dot{B}_z$ a cold low-β plasma remains after a few μs. (Such effects have not yet been identified at higher $\dot{B}_z$ where longer decay times are expected). Curves 1 and 2 of Fig. 5 show that small reversed bias fields give an appreciable increase in the diamagnetism; the mass collection remains unchanged. In addition, the decay of diamagnetism is considerably reduced and a fully diamagnetic plasma persists for the full 18 μs half cycle of the discharge.

Fig. 6 shows a plot of diamagnetic temperatures at 4 μs estimated from the diamagnetic signal for various initial bias fields. (The data is for $\dot{B}_z = 3.3$ kG/μs with 30 mtorr deuterium filling pressure). The maximum reversed bias field usable was limited to ~0.5 kG by m = 0 resistive tearing modes and this is considerably less than the critical value, $B_c \sim (4\dot{B}_z^2 M)^{\frac{1}{4}}$ [9] (M is the line mass and $B_c \sim 1.5$ kG in the present case). Results are shown for two preionisation conditions; crosses denote measurements of discharges started in a high level of preionisation with theta pinch initiation during the axial current pulse; a smooth variation with bias can be seen and there is agreement with computation predictions (shown by curve a) for fully ionised start. In contrast the dots show discharges with delayed preionisation; sufficient time had elapsed for the preionised plasma to interact with the walls when the bias field was less than or of the order of 0.1 kG. With zero bias field there is agreement between experiment and computations (curve b) for a partially ionised start with parabolic distributions of electron density at an average ionisation level of 40 per cent.

The results demonstrate the usefulness of small bias fields in controlling the plasma temperature and beta. They also show the importance of initial conditions when heating is to be achieved at low rates of rise of driving magnetic field.

In toroidal $\dot{B}_z$ compression configurations (i.e., screw pinches) other processes can influence the plasma, especially its outer regions e.g. joule heating by axial currents and turbulent thermal conduction losses[1]. Computed radial distributions of T_e at 5 μs are shown in Fig. 7 for a preionized HBTX screwpinch with 84 μF 27 kV in I_z circuit and 168 μF 30 kV in I_θ circuit. Curve b is for zero initial B_z while curves c and d show the effects of -0.5 and +0.5 kG. At 5 μs the reversed trapped field in case c has been annihilated by diffusion, and the effect of bias on the heating noted above is apparent.

An outer maximum of T_e is dominant in all three cases (not shown for b and c) and the compressed plasma is located within a radius of 1.5 cm. For curve e the B_θ was "switched off" showing that E_z contributes to the heating of the outer regions in b, c and d. (With B_θ "off" and a fully ionized start a distribution similar to b is obtained). Thermal loss due to turbulence is simulated in curve a by setting $K_{e\perp} = 0.1\, K_{e\parallel}$ which removes the anomaly in T_e and slightly reduces T_e in the compressed column.

Scattering measurements of T_e on HBTX agree with predictions of case b for the central column. In the outer region T_e has been estimated from the resistivity assuming classical behaviour; the mean temperature at peak I_z is ~ 5 eV while magnetic probe results show a much lower value close to the wall.

Data from Thomson scattering has also been examined to determine the effective γ (see above); analysis of the points in Fig.8 gives $\gamma = 1.59 \pm 0.11$. Thus collision dominated adiabatic behaviour is indicated and a small energy loss may be present.

Reversed Field Pinches

In establishing reversed field pinches one of the critical factors is the balancing of the outward expansion (driven by the initially fallling B_z) by the compression due to B_θ without producing subsequent over compression. Long lived discharges so far obtained are unpreionised resulting in strongly annular plasmas as shown by the parallel resitivity temperature derived from magnetic probe data. The $j_\theta B_z$ and $j_z B_\theta$ components on either side of the plasma must balance to cancel radial motion after the plasma has been compressed from the wall.

The reversed field discharges can be characterised by the ratio of initial B_z to the critical value for theta pinch expansion (see above) and the relative rates of change of B_z and B_θ at the wall. A stable distribution must be established in less than an instability growth time, $\sim[B_\theta\, f(B_\theta(r), B_z(r))/M^{\frac{1}{2}}]^{-1}$ (f takes account of the distribution of fields and other effects such as inertia and is of the order of or less than unity) which requires $2f(B_{zo}/B_c)^2\ (\dot{B}_\theta/\dot{B}_z) \leq 1$. Fig 9 shows the regime in which long-lived reversed field discharges can be established in relation to other types of pinch. (For the example given in (3) $\dot{B}_\theta/\dot{B}_z \sim 0.9$ and $B_{zo}/B_c \sim 0.75$).

MHD computations reproduce the formation of the annular plasma. A large amount of neutral gas is trapped within the ring and the subsequent behaviour of the latter is sensitive to ionisation losses and β_θ rises to ~0.5 at the time when B_z reaches its maximum reversal. The formation proceeds with a considerable loss of the reversed B_z flux as is observed in experiment.

Conclusions

The measured heating rate and the time variation of the axial currents in stablised z-pinches and screw pinches is in broad agreement with the predictions of MHD calculations using partial ionization and an electrical circuit. In stabilised pinches the temperature increases as the square of the current with $\beta_a \sim 0.4$ and a maximum temperature of 30 eV was measured. Screw pinch temperatures in the range 30-200 eV were obtained. Strongly annular reversed field pinches are predicted as observed.

For the outer regions of the plasma the limited amount of experimental data available indicates low temperatures in qualitative agreement with computation. Predictions are sensitive to the initial conditions and rate coefficients used.

References

1. H. A. B. Bodin et al. Plasma Physics and Controlled Nuclear Fusion Research, IAEA Vienna, 1971, vol. 1, p 249.
2. K. V. Roberts, Plasma Physics 5, 365 (1963).
3. C. W. Gowers, G. F. Nalesso, A. A. Newton, D. C. Robinson A. Verhage and H.A.Bodin. Paper A3, this conference.
4. W. R. Ellis and A. A. Newton, Plasma Physics (to be published)
5. F. E. Irons, W. R. Ellis and A. A. Newton, Plasma Physics 14, 717 (1972).
6. J. W. Long, and A. A. Newton. Phenomena in Ionized Gases, Parsons, Oxford.
7. A. Wootton, G. F. Nalesso and A. A. Newton. Paper C4 at this conference.
8. See Fig. B 19, Culham Laboratory Report. CLM-PR14.
9. T. S. Green and A. A. Newton, Physics of Fluids 9, 1386 (1966).

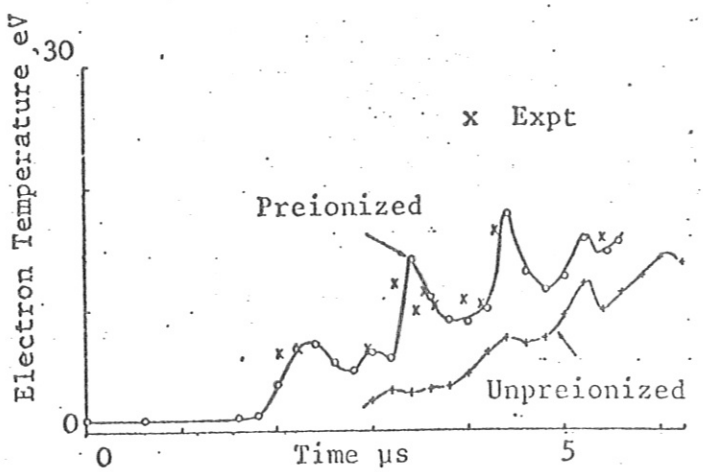

Fig.1. Computed and measured temperature on axis of the z-pinch

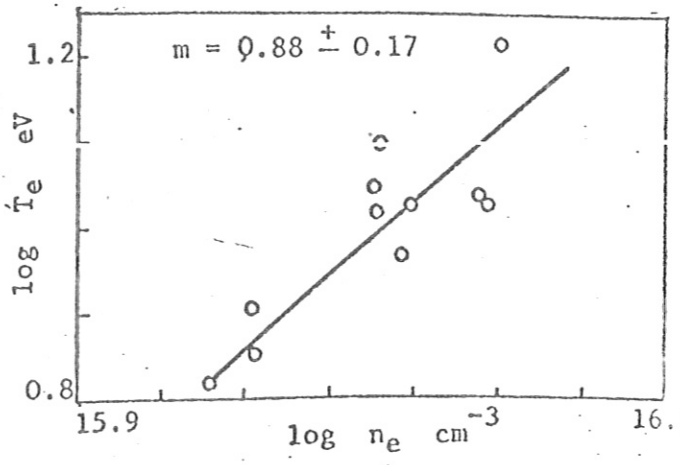

Fig.2. Measured electron temperature and density in a z-pinch

Fig 3. Plot of Electron Temperature near the axis vs. axial current.

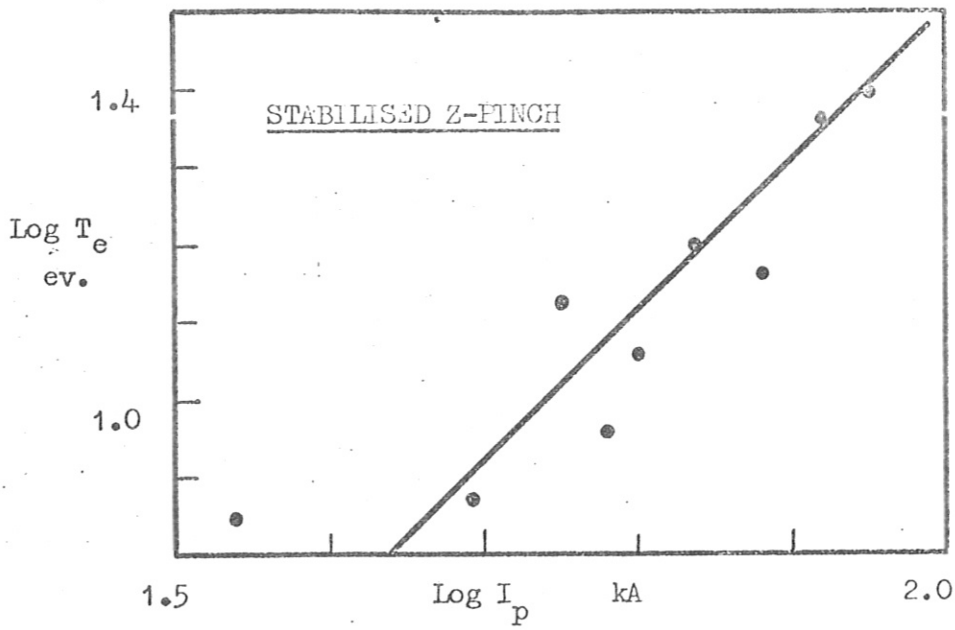

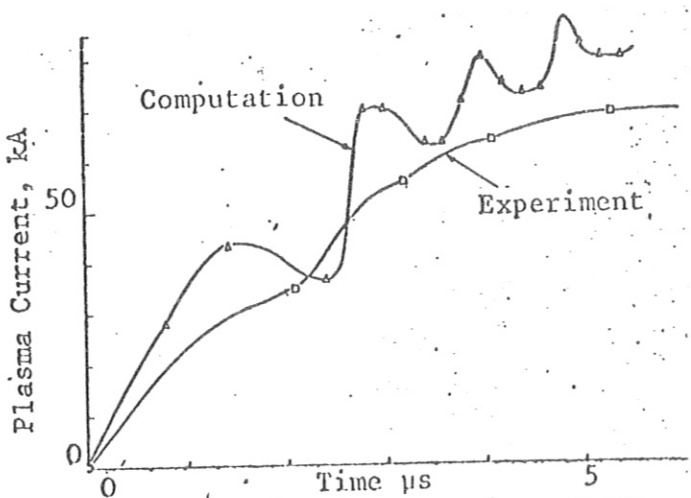

Fig.4. Computed and measured currents in a z-pinch.

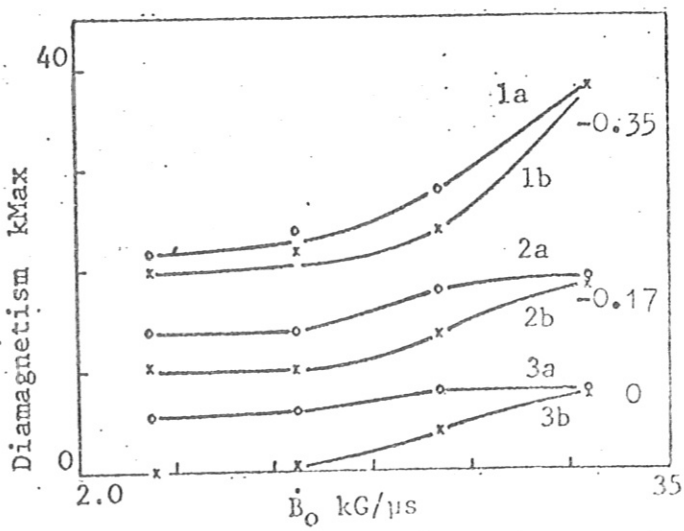

Fig.5. Measured theta pinch diamagnetism at 4 μs (curve a) and 8 μs (curve b). Figures show the initial bias field.

Fig 6. Plot of the Diamagnetic Temperature vs. initial bias field for the 3.5 metre theta-pinch. Curves a and b are computed for fully and partially ionised starts.

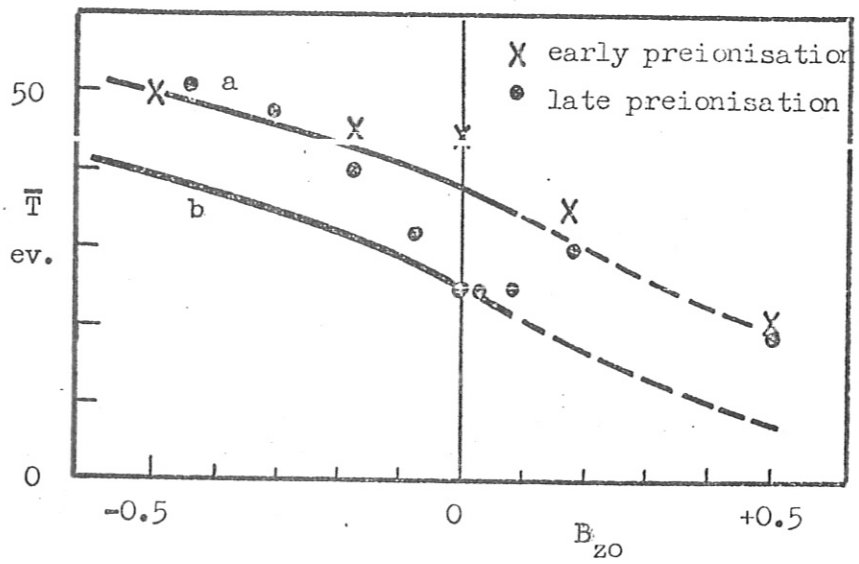

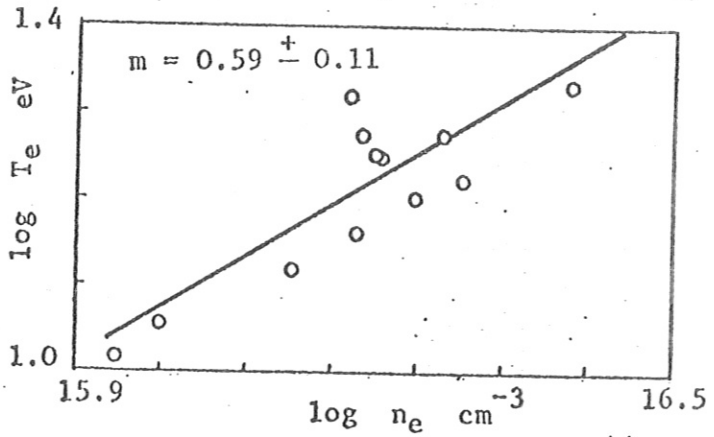

Fig.8. Measured electron temperature and density in a Screw Pinch

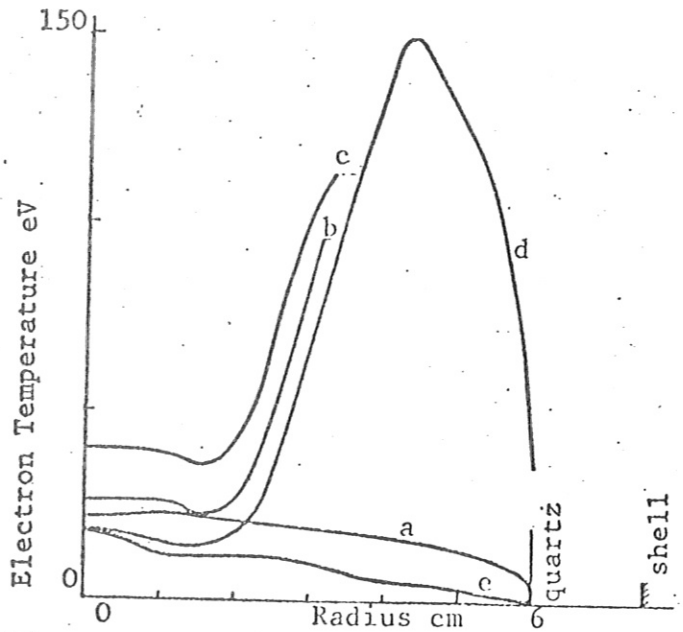

Fig.7. Computed radial temperature distributions for Screw Pinches

Fig 9. Plot showing Pinch Regimes.

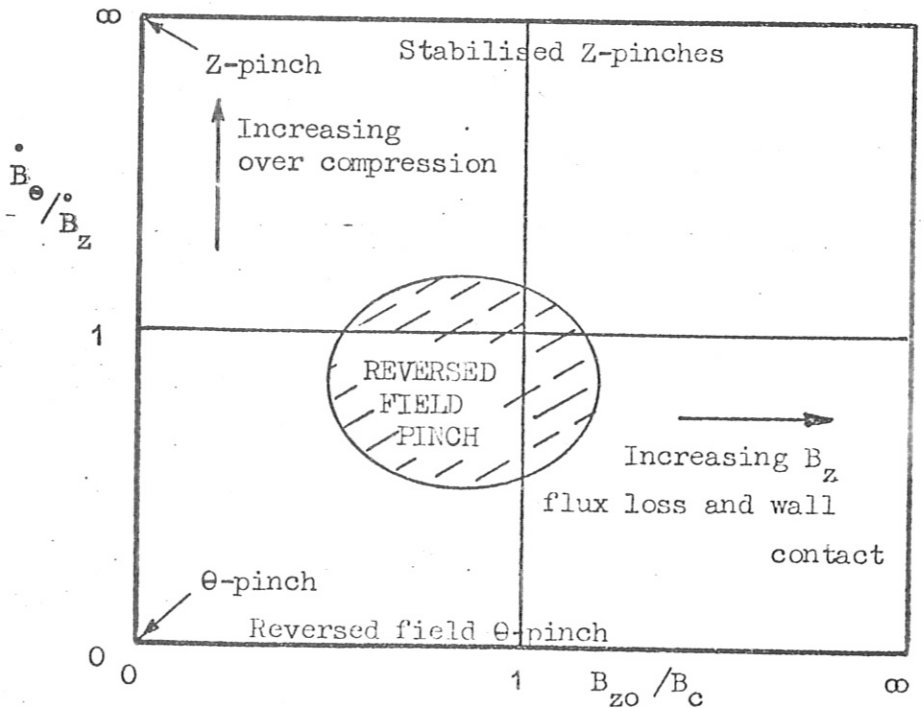

RECENT RESULTS FROM THE SHOCK-HEATED TOROIDAL Z-PINCH EXPERIMENT ZT-1

by

L. C. Burkhardt, J. N. Di Marco, P. R. Forman, A. Haberstich, H. J. Karr, J. A. Phillips

Los Alamos Scientific Laboratory, University of California

Los Alamos, New Mexico USA

ABSTRACT

Preionization in this experiment is produced by a $\lesssim$ 20 kA z-current of period ~ 30 μsec. The degree of ionization and radial distribution of current density are functions of the filling pressure and strength of the preionization current. After the start of the main z-current, with initial $\dot{B}_\theta$ (wall) of ~ 60 kG/μsec and peak currents of ~ 200 kA, plasma pressure profiles show a positive pressure gradient on axis, as required for MHD stability, existing for times of at least 8 μsec (current zero at ~ 11 μsec). The plasma β_θ is ~ 0.4 at 5 mTorr filling pressure and increases with the filling pressure. Plasma temperatures ($T_i + T_e$) of 1-4 keV are inferred from the pressure profiles and initial gas filling densities with the higher temperatures corresponding to the lower pressures (2 mTorr). When the B_z field outside the pinch column is reversed, streak photography and MHD stability analysis show significant improvement towards stability. High plasma conductivity prevents the zero in B_z from moving away from the wall more than ~ 0.5 cm.

The ZT-1 toroidal experiment[1] is designed to achieve MHD stable magnetic profiles[2,3] for a high temperature (1 keV) pinch. This experiment uses shock-heating by the magnetic field of the fast rising z-current. Some experimental parameters are listed in Table I.

TABLE I

Discharge tube radius	5.2 cm
Major torus radius	76.4 cm
Initial longitudinal electric field	~ 1 kV/cm
Initial rate of rise of discharge current	~1.5 x 10^{12} A/sec
Discharge current, I_z	$\lesssim$ 200 kA
Quarter period of I_z	$\gtrsim$ 11 μsec
Bias B_{z0} field	$\lesssim$ + 4 kG
Reversed B_z field external to the pinch	$\gtrsim$ - 4 kG

A magnetic energy storage technique using fuses is used to develop the high longitudinal electric field as discussed elsewhere.[1]

This paper describes, I) the pre-ionization phase, II) the z-pinch characteristics when operated (a) without B_z reversal and (b) with reversal, and III) an MHD stability analysis of measured magnetic field profiles.

I. PREIONIZATION

The preionization circuit drives a z-current of $\lesssim$ 20 kA and half period ~ 15 μsec which precedes the main z-pinch current. The electron line density is determined by He-Ne laser interferometry[4] across a minor diameter through the vacuum ports. The degree of ionization is found to be proportional to the energy in the preionization circuit. At 30 mTorr filling pressure and 2.5 kG B_z bias field ~ 100% ionization is reached after the first half period of the z-current of peak amplitude ~ 13 kA. B_θ magnetic field distributions show that if the z-current is held constant and the filling pressure reduced the uniform z-current density becomes

peaked on axis.

When the experiment is run in a "slow" mode by connecting the main z-capacitor bank directly to the pinch, peak z-current ~ 150 kA and $\pi/4 \sim 10$ μsec, the degree of ionization has a significant effect on the radial pressure profiles. A pressure peak appears at large radii when the ionization is low (~30%) and only with high ionization ($\gtrsim$ 80%) is there efficient gas accumulation with one pressure peak on axis. These problems can be avoided by choosing parameters to give ~ 100% preionization.

IIa. FAST Z-PINCH WITHOUT B_z REVERSAL

B_θ and B_z magnetic field distributions are measured by probes located across a minor diameter parallel to the major axis. The reproducibility of traces from discharge to discharge at 5 mTorr and 4 kG bias field is found to be within experimental error and we infer that no large scale kink instability develops. (This is not true when the experiment is run in the "slow" mode).

Pressure profiles calculated for two discharges are shown in Fig. 1. The pressure profiles are hollow with a pressure peak off axis which exists up to ~ 8 μsec; z-current zero is at ~ 11 μsec. Stabilization against modes driven by the pressure gradient requires that the gradient near the axis be positive or equal to zero. Fig. 1 shows that with 4 kG B_z bias field and 2 and 5 mTorr filling pressure the necessary positive pressure gradient exists.

The plasma temperature ($T_i + T_e$) is calculated from the pressure by the equation;

$$T_i + T_e = \frac{1}{Nk} \int_0^{r_w} 2\pi\, r\, p\, dr,$$

where N the total line density is assumed constant and equal to the initial line density. In addition the temperature is assumed independent of radius. β_θ as defined by the Bennett relation is

$$\beta_\theta = (200 \int_0^{r_w} 2\pi\, r\, p\, dr)/I^2.$$

Numerical integration leads to the data shown in Fig. 2 for a 4 kG B_z bias field and three filling pressures. The temperatures show an inverse dependence on filling pressure and decrease with time.

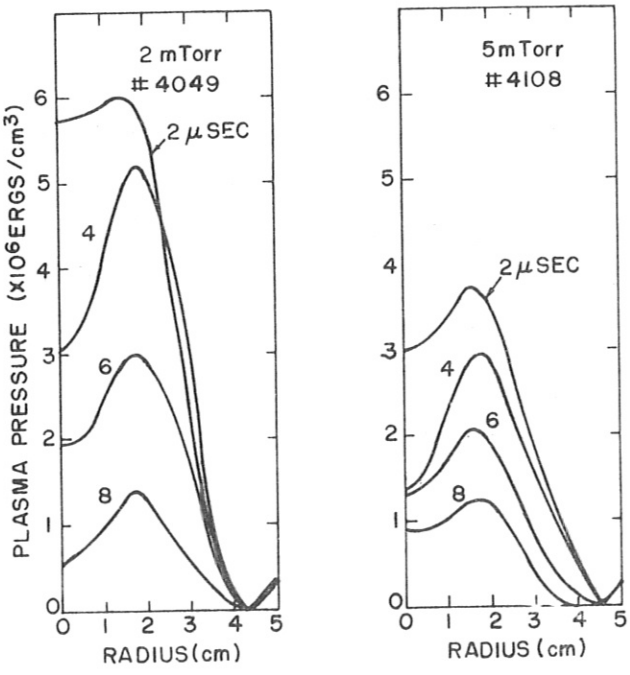

Fig. 1. Radial pressure profiles as a function of time for two filling pressures. B_z bias field = 4 kG.

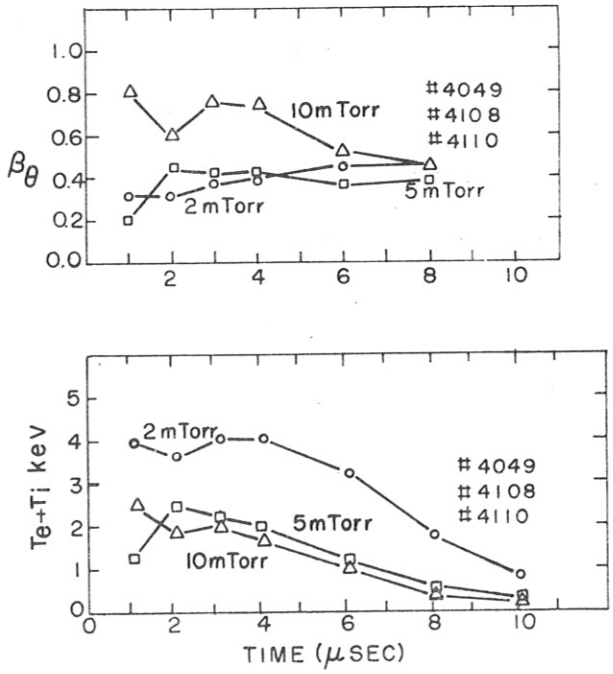

Fig. 2. Calculated β_θ and plasma temperature ($T_i + T_e$) as a function of time for three filling pressures. B_z bias field = 4 kG.

These temperatures are optimistic since the line density may have increased by a factor of 2-3 as seen by the interferometer. However, the contribution to the line density by plasma in the pump ports is not known.

MHD theory predicts that β_θ must be less than 0.5 for stability while the highest stable profile obtained numerically[2] has $\beta_\theta \approx 0.31$. The experimental β_θ's in Fig. 2 do not exceed those required for stability. In summary, we find that the field configurations having the lowest $\beta_\theta \sim 0.4$, the least variation in the value of β_θ with time and having a positive gradient near the axis, are obtained with $B_z \sim 4$ kG and 2-5 mTorr filling pressure.

If temperatures $\sim$ 1 keV and densities $\sim 2 \times 10^{15}$/cc exist a detectable yield of neutrons should be produced. Neutrons are seen in numbers compatible with these plasma conditions.

IIb. FAST Z-PINCH WITH B_z REVERSAL

The current in the B_z winding is reversed $\sim$ 1 μsec after the initiation of the main z-current. The peak reversed B_z is $\sim$ 1.5 kG with $\tau/2 \sim 10$ μsec Magnetic field distributions and pitch of field lines are shown in Fig. 3 with and without field reversal. Because of high plasma conductivity the reversed B_z is separated from the forward B_z and the plasma column is compressed, increasing the B_z on axis, and moving the B_θ field radially inward. The resulting equilibrium prevents the zero in B_z from moving away from the wall more than $\sim$ 0.5 cm.

Four typical streak photographs taken across a minor diameter with and without B_z reversal are shown in Fig. 4. With field reversal the streaks are significantly fainter with a marked decrease in the bright filamentary structure seen without reversal; rather, bands of light separated by dark spaces spread across the discharge tube. These bands of light can be correlated with B_z passing through zero and with the peak B_z reversal.

III. STABILITY ANALYSIS

The measured magnetic field profiles have been analyzed for MHD m=1 stability. Use is made of the theory of Freidberg[5] to calculate the eigenmodes of the radial displacement from equilibrium and the

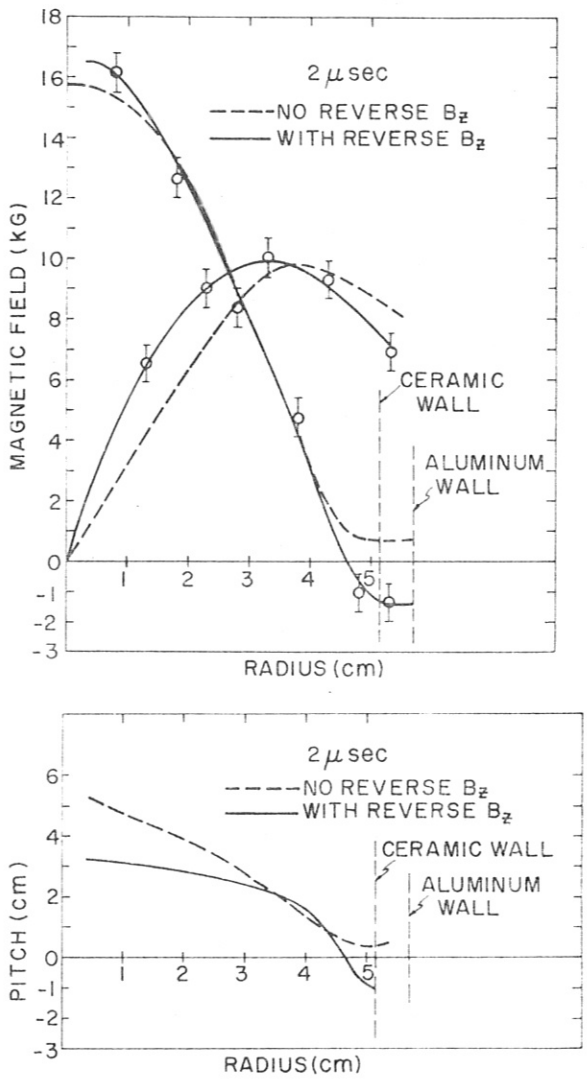

Fig. 3. Measured B_θ and B_z magnetic field distributions and pitch of magnetic field lines with and without B_z reversal.

theory of Robinson[2] to interpret the results.

These are shown in Fig. 5(a) for a no reverse B_z case and in Fig. 5(b) for a reversed field case. k is the wave number along the major circumference and r is the minor radial position. The lines g=0 correspond to the roots of the factor g(r,k) appearing in the energy integral.[2] The horizontal lines indicate stable wavenumbers while the shaded areas represent unstable modes. The amplitude of these modes has been made proportional to their growth rate. The shortest growth time is of the order of 0.5 μsec in case (a) and 1.5 μsec in case (b).

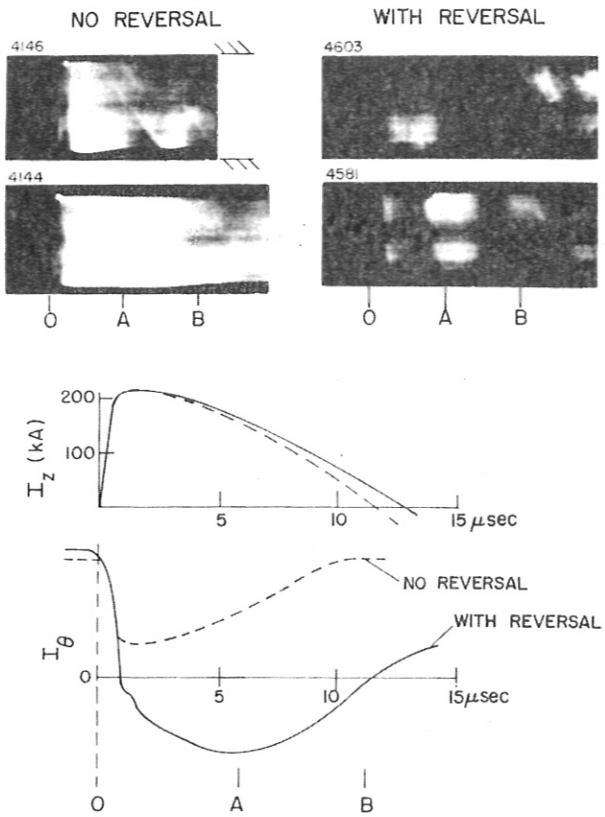

Fig. 4. Four streak photographs across a minor discharge tube diameter with and without field reversal. The main z-current and current in the B_z winding are also shown.

The purpose of reversing B_z is to form a plasma with no minimum in the pitch and no current or pressure at the wall. That the first of these goals has been achieved can be seen in Fig. 5(b). In view of the slow penetration of the reversed field, it is doubtful that the azimuthal current vanishes at the wall. More important perhaps, the smoothed magnetic field profiles used in computing Fig. 5(b) imply a residual pressure at the wall. Whether this pressure exists in the experiment is not clear. Removal of the wall pressure by a slight alteration of the B_θ profile makes the pinch less stable. Programming of our profiles has just begun and it is clear that much work remains to be done.

Work performed under the auspices of the United States Atomic Energy Commission.

REFERENCES

1. D. A. Baker, et. al. paper CN-28/B-2, Plasma Physics and Controlled Nuclear Fusion Research, Conference Proceedings, Madison 1971, IAEA, Vienna, page 203, 1971.
2. D. C. Robinson, Plasma Physics, 13, 439, (1971).
3. J. P. Freidberg, private communication.
4. D. E. T. F. Ashby and D. F. Jephcott, App. Phys. Letters 3, 13 (1963).

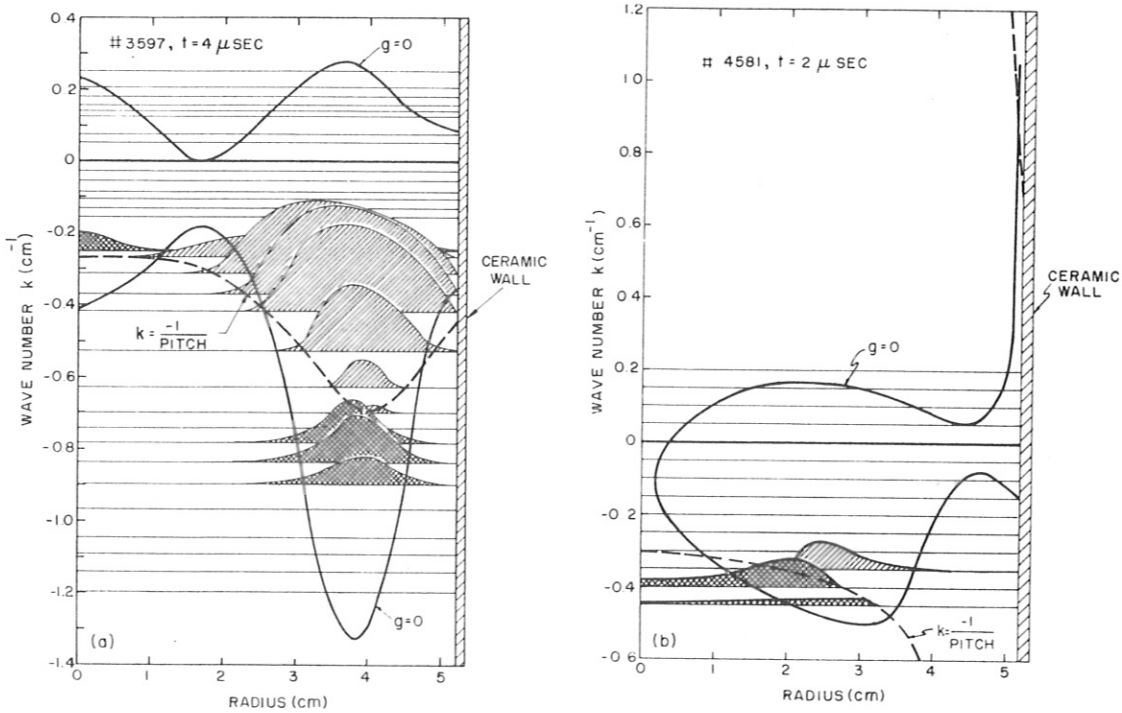

Fig. 5. Stability diagrams for z-pinches a) without B_z reversal and b) with reversal.

OBSERVATIONS OF M.H.D. INSTABILITIES NEAR THE KRUSKAL-SHAFRANOV LIMIT IN LINEAR AND TOROIDAL HIGH BETA PINCHES

by

I K Pasco, D C Robinson, P P L A Smeulders

UKAEA Culham Laboratory, Abingdon, Berks. England.

Abstract: The growth rate and wavelength of M.H.D. instabilities have been measured in the High Beta Toroidal Experiment and its linear 2 metre counterpart over a wide range of pitch lengths ($2\pi r\, B_z/B_\theta$). Optical and electrical measuring techniques are used. The wavelength of the Kruskal Shafranov m = 1 instability varies in accordance with $q(= \frac{r\, B_z}{R\, B_\theta}$, toroidal, $= \frac{\pi r}{L} \cdot \frac{B_z}{B_\theta}$ linear). The growth rate of the instability is found to be approximately proportional to the axial current in the straight system, and this agrees with theory for small plasma displacements.

The m = 1 instability disappears in both cases at the Kruskal-Shafranov limiting value of $q(r_m) = 1$ where r_m is the radius at which q is a minimum. This lies near the plasma boundary in the linear case and further out in the torus . Values of q up to 3 were studied and in the toroidal experiment evidence of an m = 2 instability was obtained when $q \sim 2.5$.

The field configuration was varied by altering the preionisation current induced in the plasma, and configurations were usually of the screwpinch type, with the current flowing principally in the outer regions. In the linear device measurements below 12 kA were made with the current flowing principally in the plasma column.

Introduction: The growth rate and wavelength of the m = 1 Kruskal-Shafranov helical instability have been previously studied in linear[1,2] and toroidal geometry[3] and the results compared with hydromagnetic theory. The measured growthrates were then found to be an order of magnitude lower than those predicted by sharp boundary theory. Incompressibility and a vacuum field configuration outside the plasma were assumed.

Measurements of the growth rate, wavelength and field configuration have been made on the High Beta Toroidal experiment[4] and its linear 2m counterpart[5].

Experimental conditions and Plasma Properties

Peak Axial Magnetic fields of 4 - 18 kG rising in 4-7 μs produce plasmas in preionised H_2 or D_2 at 30 mtorr with the possibility of the addition of

bias to control Beta. Axial currents of 2 - 80 kA rising in 4-7 μs provide the azimuthal component of the field. The magnetic field configuration has been obtained in both devices using inserted multi-coil magnetic probes.

Fig. 1(a) shows a typical field configuration from the linear device. The form of the pitch variation ($r B_z/B_\theta$) is very sensitive to the timing and form of the preionisation pulse. It is possible to obtain pitch minima anywhere between the plasma and insulating wall (4 cm), depending on whether the current flows within the plasma or outside it. Fig. 1(b) shows the field configuration in the torus. In this case the pitch minimum occurs near the insulating wall, (6 cm) and most of the axial current flows in the outer regions whose conductivity temperature is about 3 eV.

The Electron temperature ranges from 10 to 100 eV as measured diamagnetically in both devices and by Thomson scattering in the case of the torus. Electron densities are $\sim 2.10^{16}$ cm^{-3}.

Measurements. Wavelengths and growth rates are derived from temporal changes in the plasma position obtained by optical and electrical techniques.

Optically the emitted continuum radiation is collected by stereo pairs of keyholescopes[6] allowing multiple streak photographs to be taken through holes in the metal wall of 8 mm diameter. Fig. 2(a) shows a streak picture from the linear device and fig. 2(b) from the torus. The photographs yield the position and wavelength after distortion corrections are made.

Electrically the output from three pairs of Rogowski coils with winding densities varying as $\sin\theta/\cos\theta$[7] positioned around the major circumference of the torus and along the axis of the linear device, has been used to determine the displacement and instability wavelength. Since the current in the outer regions is larger for a screwpinch field than it is for a vacuum field, equal displacements of the plasma will yield a larger sin/cos signal in the vacuum field case. Comparison with optical measurements can then be used to determine the form of the field configuration without inserting a magnetic probe.

Results: Figs. 2(a) and (b) show exponential growth of an m = 1 instability. The wavelengths in the torus are obtained after taking into account the equilibrium motion seen in Fig. 2(b), upper.

Fig. 3 shows the measured wavelengths for the two devices as a function of the minimum value of $q = \frac{rB_z}{RB_\theta}$ for the torus and $q = \frac{\pi r}{L}\frac{B_z}{B_\theta}$ in the linear case. The measured wavelength of the instability is proportional to the pitch length, or q, at the pitch minimum as predicted by stability theory[8]. Growth rate computation[9] for field configurations as in Fig. 1 gives the fastest growth

at this particular wavelength where $\underline{K}.\underline{B} = 0$. It is to be expected that periodicity around the major circumference will govern the number of possible wavelengths in the torus but to a lesser extent in the linear machine due to the ill-defined end points.

The maximum wavelength observed in the torus is equal to the circumference or 620 cm and in the linear case it is measured to be $\sim$ 400 cm or approximately twice the machine length. Experimental results indicate that the wavelength λ shows discrete steps: 6.28 m ($n = (2\pi R/\lambda) = 1$), 3.14 m ($n = 2$), 2.09 m ($n = 3$), etc, in the torus. In the linear case the minimum value of q usually occurs close to the edge of the plasma. Thus a much lower current ($\leq$ 4 kA) is required in this case to reach the Kruskal-Shafranov limit than in the torus ($\leq$ 28 kA). For $q > 1$ growth still exists but there is a tendency for the plasma to change its shape as it goes unstable suggesting the presence of $m = 2$, which would be expected.

The growth rates predicted by the computation[9] are in good agreement for both devices and Fig. 4 shows such a comparison for the linear device, the straight line is, obtained from a computed growth rate and assumes that $\omega \sim B_\theta a^{-1}(4\pi\rho)^{-\frac{1}{2}}.\beta^{\frac{1}{2}}$ or that the growth rate is proportional to the current.

Conclusions:

The measured wavelengths of Kruskal-Shafranov $m = 1$ instabilities in both linear and toroidal geometries have been found to be in good agreement with theory for values of q_{min} less than unity. When q is equal to one the wavelength is equal to twice the linear machine length and once around the torus respectively

The measured growth rates are found to be in agreement with theory for a variety of screwpinch configurations. There is evidence that instabilities having $m > 1$ are generated in cases where $q > 1$.

References:

1. Little, E M, et al. Proc. 3rd Int.Conf.Plasma Phys. & Contr.Nuc.Fus.Res. Novosibirsk (IAEA Vienna) Vol.2, P.555 (1968).
2. Kvartskhava, J F, et al, Proc.4th Int.Conf.Plasma Phys. & Contr.Nuc.Fus.Res. Madison (IAEA Vienna) Vol. 1, P.157 (1971).
3. Wilhelm, R and Zwicker, H. Zeits fur Phys.Vol.240, P.295 (1970).
4. Bodin, H A B, et al, Proc.4th Int.Conf.Plasma Phys. & Contr.Nuc.Fus.Res. Madison (IAEA Vienna) Vol. 1, p.225 (1971).
5. Pasco, I K, Ph D Thesis, Polytechnic of N. London (1972).
6. Evans, D E, Pasco, I K, J Sci. Insts. Vol. 3, P.258 (1970).
7. King, R E, Robinson, D C, Verhage, A J L, Culham Laboratory Report CLM P.302 (1972).
8. Robinson, D C, Plasma Phys. Vol.13, P.439 (1971).
9. Crow, J E, robinson, D C, See this conference.

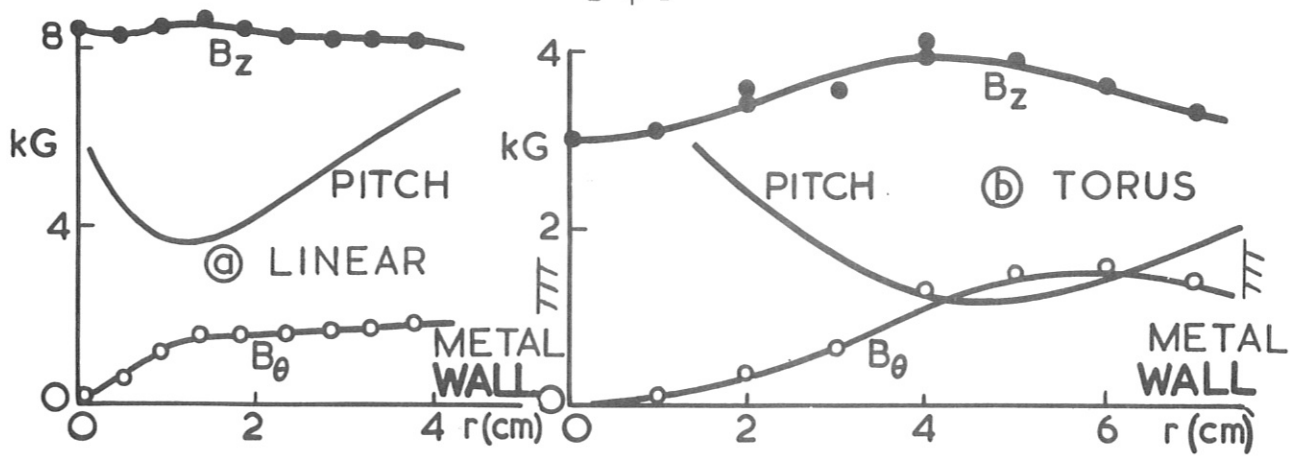

FIG. 1: MAGNETIC FIELD AND PITCH PROFILES WITH RADIUS, (a) LINEAR AND (b) TORUS

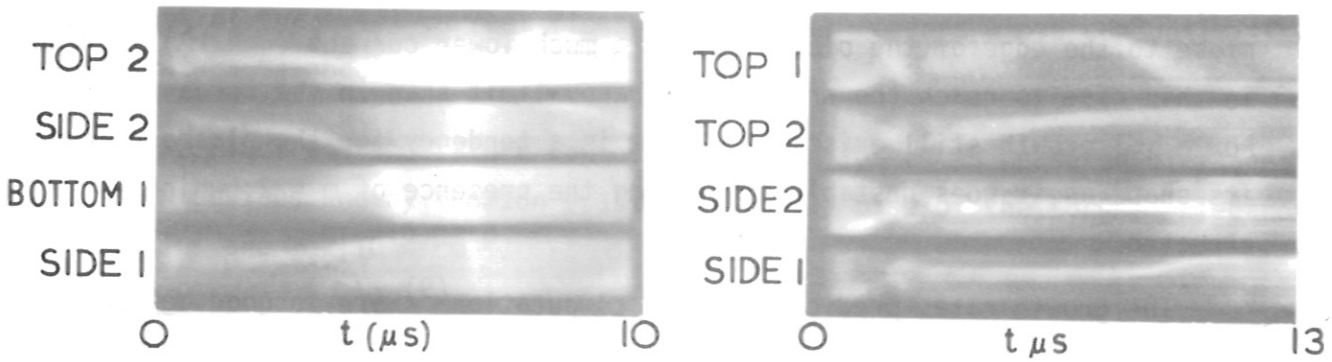

(a) B_z = 18.3 kG: B_θ = 0.69 kG: Po = 30 mT. (b) B_z = 8.55 kG: B_θ = 0.80 kG: Po = 30 mT.

FIG. 2: DUAL STEREOSCOPIC PLASMA STREAK PHOTOGRAPHS, (a) LINEAR AND (b) TORUS

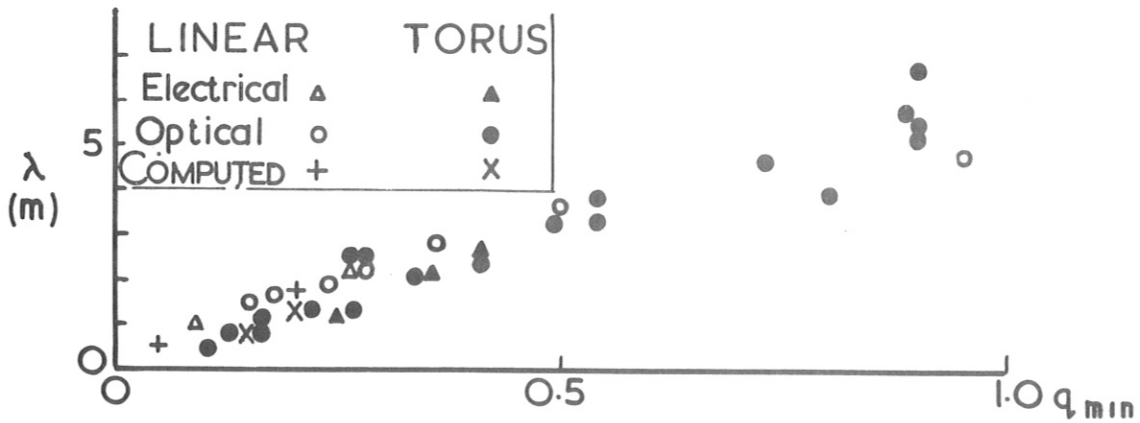

FIG. 3: MEASURED AND COMPUTED INSTABILITY WAVELENGTH WITH CALCULATED q

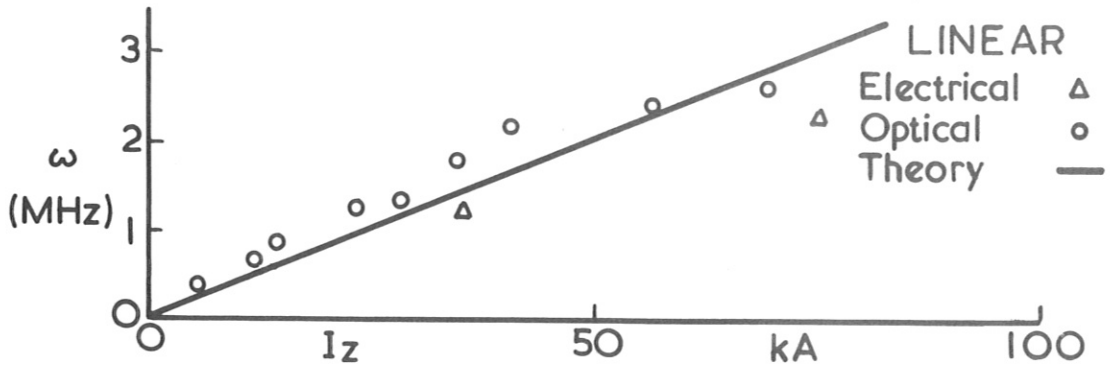

FIG. 4: MEASURED AND COMPUTED INSTABILITY GROWTHRATE WITH AXIAL CURRENT.

EXPERIMENTAL RESULTS ON THE HIGH-ß COMPACT TORUS EXPERIMENT TEE

H.J. Belitz, E. Kugler, P. Noll, F. Sand, G. Waidmann, F. Waelbroeck
Institut für Plasmaphysik der Kernforschungsanlage Jülich GmbH
ASSOCIATION EURATOM-KFA

Abstract. A plasma is produced by fast rising magnetic fields in a Tokamak-like configuration to study its stability for the case $ß_J > 1$ (poloidal ß) and $q = \frac{2\pi}{\iota} \gtrsim 1$. With B_{max} = 4,3 kG and a filling pressure p_o = 1 mtorr D_2, an initial plasma with an aspect ratio $A_p \approx 5$, a major radius $R_p \approx 28$ cm, $\bar{ß} \approx 0.1$, $\bar{T} \approx 150$ eV and $q(a) \approx 0.8$ was obtained. After crowbar, the plasma current I_p decreases in $\sim 10^{-4}$ sec and no major MHD instabilities were found when I_p is smaller than the Kruskal-Shafranov limit.

1. INTRODUCTION. In this experiment, fast and simultaneously rising toroidal and poloidal magnetic fields B_φ and B_ω produce a plasma with $\bar{ß} = 8\pi\bar{p}/B^2_\varphi \gtrsim 0{,}1$ in a Tokamak-like configuration. The confinement of this plasma, in particular its MHD equilibrium and stability behaviour, is investigated in the domain where $ß_J = 8\pi\bar{p}/B^2_\omega(a)$ is near the equilibrium limit $\approx R_p/a$ (R_p,a, = major, minor plasma radii) and where the reciprocal rotational transform $q(a) = aB_\varphi/R_pB_\omega(a)$ is close to one. These $\bar{ß}$ values, which are about those required in a reactor, have not been accessible so far in Tokamak experiments. In screw pinches, improved stability was observed [1,2] when $q \gtrsim 1$, but the plasma aspect ratio was large and $\bar{ß}$ probably still too high for complete stability. In TEE, by using a short rise time and a compact vessel (R_o = 25 cm, minor inner radius r_w = 9,5 cm), the adiabatic compression is reduced, and the aspect ratio of the resulting plasma is reasonably small ($R/a \approx 5$). After crowbar of the external currents, plasmas with $\bar{ß} \gtrsim 0{,}1$ should then be confinable. No power is applied to the discharge during the confinement phase, and the decay of the plasma and coil currents play a significant role on the plasma evolution. An initial gas pressure of $\sim$1 mtorr D_2 was chosen to reduce the $\bar{ß}$ by fast anomalous field diffusion during the implosion phase [3] and to produce confinable plasmas with $\bar{T} > 100$ eV at the available magnetic field strengths $B_\varphi \lesssim 10$ kG. The use of a positive initial bias field B_o allows to reduce further $\bar{ß}$.

2. APPARATUS [4]. The main coil consists of 36 parallel helical wires with a pitch length of 1.74 R. The shape of the winding is such that the vacuum vertical field $B_\perp \approx 0{,}01\ B_\varphi$. The gas, ionized by r.f. electric fields, is preheated by a discharge of condensers through the coil ($\omega = 2\cdot10^5\ s^{-1}$, $B_{\varphi\,max} \lesssim 1$ kG). The fast discharge ($\omega = 10^6\ s^{-1}$) of the main bank produces, at a charging voltage of 30 kV, a toroidal field of 4,3 kG and induces the plasma current. After crowbar

by metal to metal switches, the main current decreases to I_{max}/e in about 1 msec; the initial decay is more rapid (characteristic time 100-200 μsec) because of the skin effects in coils and collectors. A copper shell is used to achieve a toroidal equilibrium. This shell covers the outer periphery of the torus, allowing to apply rapidly varying external $B_\perp$ fields to control the plasma position during the implosion phase and later. The induced plasma current can be varied at constant $B_{\varphi max}$ by placing toroidal metal rings close to the main windings. When these rings are concentrated near the inner periphery of the main coil, a fast rising $B_\perp$-field results, which partly compensates the effect of the $I_p \times B_\perp$ reduction. By proper selection and distribution of the resistance of these rings, a time-programming of the Volt.sec seen by the plasma (i.e. a type of inductive power crowbar) can be obtained; in particular, a controllable compensation of the negative toroidal electric field exerted on the plasma by the decaying coil current I_o in the main winding can be achieved.

EXPERIMENTAL RESULTS AND DISCUSSION.

- The preheat phase has been studied [5] in an auxiliary experiment with similar dimensions. At p_o = 1 mtorr, more than 60% of the gas initially present in the vessel is ionized and the measured electron temperature T_e is 5 eV.
- At the end of the fast compression (t = 1,6 μsec), magnetic measurements [6] yield for the plasma radius, depending on the initial conditions, 5 cm< a< 7 cm, a being defined from the region where an appreciable current flows. In experiments without toroidal metal rings, values $q(a) \lesssim 0.4$ were found. With 5 inner rings and B_o = 0 Gauss, a plasma with $\bar{\beta} \approx 0.4$ is produced. Strong skin effects and a large displacement towards the outer wall are observed. From similar experiments with B_o = 270 G, (the condition mainly discussed here), we deduce a = 6,5 cm, R_p = 28 cm, and an approximately triangular pressure profile with $\bar{\beta}$ = 0,11. The skin effect is less pronounced and the q(a)-value is 0.8. From the Doppler width of HeII, CIII and CV lines a temperature T_{D^+} = 70 $\pm$ 15eV was estimated . With B_o = 0 G, a value T_e = 250 eV was obtained from soft X-ray measurements. The average temperature deduced from pressure balance is somewhat higher.
- Fig. 1 shows the evolution of the plasma current I_p for three different cases. I_p drops during the first two μsec after crowbar by a factor 2.7 without, and about 1.5 with metal rings. During this initial period, the B_ω and B_φ signals of probes in the plasma present strong fluctuations which indicate erratic motions of the magnetic axis. At t = 4 μsec , the I_p-values are approximately the same for the three experiments. For all similar experiments, the rapid initial decrease of the plasma current stops when $I_p \lesssim$ 20kA. This can probably be correlated to the fact that, for a reasonable plasma radius ($a \approx 6$ cm) the Kruskal-Shafranov

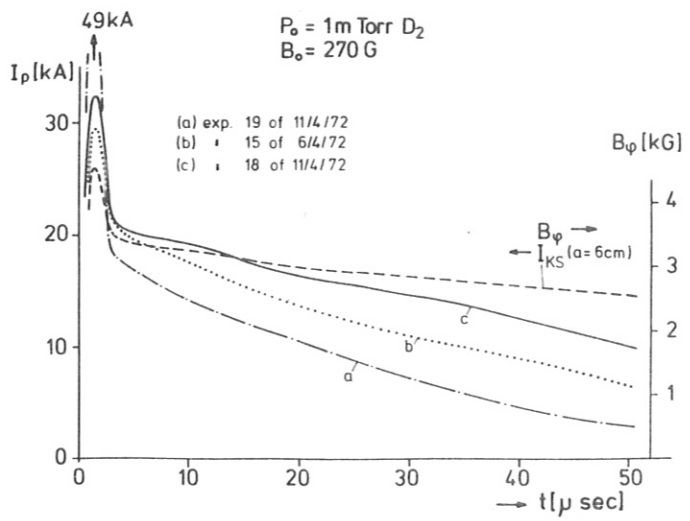

Fig. 1. Plasma current I_p and Kruskal-Shafranov-limiting current I_{KS} for a = 6 cm (B_φ on right scale) for 3 cases: $I_{p\,max}$ not reduced (a), reduced with 5 copper rings (b) and 5 resistive rings (c).

limit corresponds to this I_p-value. The later current decay is, to a large extent, determined by the toroidal electric fields E_φ caused by the I_o decrease in the helical main winding. E_φ is large ($\approx$1 V/cm for case a) immediately after crowbar. The copper rings reduce E_φ by ~40%. A further decrease has been achieved (case c of fig. 1) through the current decay in the resistive rings for which L/R = 60 μsec. The characteristic decay times of the current $\tau_I = (d\,\ell n\, I/dt)^{-1}$ deduced at the 20th μsec are 30, 50 and 80 μsec for cases a,b,c. The observed continuum radiation is almost proportional to I_p. The plasma current cannot be maintained constant in the last experimental case, since q is close to 1 at the 4th μsec, and since B_φ decreases. Fig. 1, c shows that, assuming that a does not vary, we achieve within $\pm$ 10% a constant q-value over about 35 μsec. During the slower decay phase of I_p, the current and the B_ω-probe signals are smooth in the cases a and b. For experiments similar to that of case c), fluctuations are observed on the B_ω-probe signals during the first $\approx$30 μsec, which disappear abruptly afterwards. These might result form a too effective "power crowbar" which tend to maintain the plasma in a weakly unstable domain. At t = 10 μsec, the current is distributed in the whole plasma (no detectable skin effects), and the magnetic axis lies at R = 29 cm. A smooth outwards drift of this axis follows; it reaches 29.5 cm at the 60th μsec ; at the end of the current life-time (>100 μsec), the outward motion becomes more rapid. If we assume that β_J cannot surpass a critical limit, of the order of R/a, the maximum confinable plasma energy is proportional to I_p^2/a. Thus, if the energy containment time is larger than half of the current decay time τ_I, the β_J will at first increase [7]. The equilibrium limit could thereby be reached, and the plasma containment should then mainly be governed by losses to the glass wall resulting from the large β_J value. The observed slow outward drift of the magnetic axis indicates that this may well be the case in TEE.

CONCLUSIONS.

The first experiments in TEE have shown that the production of a hot compact plasma with $\bar{\beta} \gtrsim 0{,}1$ and $\beta_J > 1$ can be achieved. An MHD-stable behaviour was not found when $q < 1$. An inductive "power crowbar" allows to extend to 50 µsec the period during which plasmas with $q < 2$ can be studied and to reduce the rate of increase of β_J which results from the decrease of the toroidal plasma current. The plasma appears to be MHD-stable during the time where q increases from 1 to 2.

REFERENCES

[1] R.F. de Vries et.al., 3rd Eur. Conf. Fusion and Plasma Phys., Utrecht, (1969), p. 88

[2] H. Zwicker et.al., Plasma Phys. and Contr. Nuclear Fusion Research, IAEA Vienna (1971), Vol. I, 251

[3] H.A.B. Bodin et.al., Plasma Phys. and Contr. Nuclear Fusion Research, IAEA Vienna (1969), Vol. II, 533

[4] H.J. Belitz et.al., Plasma Physics and Controlled Nuclear Fusion Research, IAEA Vienna (1971), Vol. III, p. 179

[5] F. Sand et.al. submitted to Nuclear Fusion

[6] H.J. Belitz et.al. to be presented at the 5th European Conference on Controlled Fusion and Plasma Physics, Grenoble (1972)

[7] S.V. Mirnov ZhETF Pis. Red. 12, 2 (1970) 92

A VLASOV-FLUID MODEL FOR STUDYING GROSS STABILITY OF HIGH-BETA PLASMAS

by

J. P. Freidberg and H. R. Lewis

University of California, Los Alamos Scientific Laboratory

Los Alamos, New Mexico

ABSTRACT

A formulation of the Vlasov-fluid model in a way suitable for numerical computation is described, and application to equilibria with axial and translational symmetry discussed.

The Vlasov-fluid model has been proposed recently[1] for making a more realistic study of the gross stability of high-beta plasmas than is possible in terms of the usual ideal MHD approximation. In the Vlasov-fluid model the ions are treated as collisionless, the electrons are treated as a massless fluid, charge neutrality is assumed, and the displacement current in Maxwell's equations is neglected. The basic equations of the model are

$$\underline{E} + \frac{1}{c}\,\underline{u}_e \times \underline{B} = 0 \ , \tag{1}$$

where $\underline{u}_e$ is the velocity of an electron; and

$$\nabla \times \underline{E} = -\frac{1}{c}\frac{\partial \underline{B}}{\partial t} \ , \tag{2}$$

$$\frac{\partial f}{\partial t} + \underline{v}\cdot\nabla f + \frac{Q}{M}\left(\underline{E} + \frac{1}{c}\,\underline{v} \times \underline{B}\right)\cdot\nabla_{\underline{v}} f = 0 \ , \tag{3}$$

and

$$(\nabla \times \underline{B}) \times \underline{B} = 4\pi Q \int d^3\underline{v}\,\left(\underline{E} + \frac{1}{c}\,\underline{v} \times \underline{B}\right) f \ , \tag{4}$$

where f is the ion distribution function, and Q and M are the ionic charge and mass. We consider the equilibrium ion distribution function to be a function only of the total energy in order that there be no stationary flow in equilibrium. Then, as was shown in ref. 1, the allowed equilibria, the criterion for marginal stability, and an estimate of the m = 1 growth rate are identical in the Vlasov-fluid model and ideal MHD. However, estimates

of the growth rates for $m \geq 2$ can be much smaller in the Vlasov-fluid model than in ideal MHD, in qualitative agreement with experimental observations on hot θ-pinches.

Our purpose here is to propose a method for solving the Vlasov-fluid model for the actual eigenfrequencies and eigenfunctions, since only crude estimates were obtained in ref. 1. We have reformulated the linearization of the Vlasov-fluid model in a way that has two very important practical features which make the study of exponential stability feasible. Firstly, although equilibrium particle trajectories do enter the formulation, they enter more simply than in the usual procedure in which integrations along equilibrium trajectories must be carried out. Secondly, the truncated algebraic equations that result from the formulation and which must be solved numerically are in a form that is convenient for computation, even when the dimension of the algebraic problem is very large. The new formulation can be derived in part from a treatment of linearized Vlasov plasmas that is based on Hamilton's variational principle.[2]

The Basic Equations

Consider an equilibrium defined by an ion distribution function $f_o(\epsilon)$, pressure p_o, number density n, scalar potential $\phi^{(0)}$, vector potential $\underline{A}^{(0)}$, and fields $\underline{E}^{(0)} = -\nabla\phi^{(0)}$ and $\underline{B}^{(0)} = \nabla \times \underline{A}^{(0)}$, where $\epsilon = \frac{1}{2} Mv^2 + Q\phi^{(0)}$. As in ref. 1, the gauge is defined by $\underline{B}^{(0)} \cdot \underline{A}^{(1)} = 0$ and the perturbed scalar and vector potentials are related by $\phi^{(1)} = \underline{E}^{(0)} \times \underline{B}^{(0)} \cdot \underline{A}^{(1)}/B^{(0)2}$.

The basic linearized equations can be brought into the form

$$\underline{F}(\underline{\xi}) = Q \int d^3\underline{v}\, (\partial f_o/\partial\epsilon) \left[\underline{E}^{(0)} + \frac{1}{c}\, \underline{v} \times \underline{B}^{(0)}\right](\partial s/\partial t) \tag{5}$$

and

$$\left[\frac{\partial}{\partial t} + \mathcal{L}(\underline{r},\underline{v})\right] s = M\underline{v} \cdot \left[\frac{\partial}{\partial t} + \underline{v}\cdot\nabla\right] \underline{\xi}\ , \tag{6}$$

where $\underline{\xi}(\underline{r},t) = \underline{B}^{(0)} \times \underline{A}^{(1)}/B^{(0)2}$, $\underline{F}(\underline{\xi})$ is the incompressible MHD operator, and $\mathcal{L}(\underline{r},\underline{v})$ is the equilibrium Liouville operator. The perturbed distri-

bution function can be expressed in terms of the potentials and $\partial s/\partial t$, but the function $s(\underline{r},\underline{v},t)$ itself has no obvious direct physical interpretation.

The numerical treatment of Eqs. (5) and (6) is facilitated by representing $\underline{\xi}$ as an expansion in orthonormal eigenfunctions $\underline{\xi}_\ell$ of $\underline{F}(\underline{\xi})$, $\underline{F}(\underline{\xi}_\ell) = \lambda_\ell n(\underline{r})\underline{\xi}_\ell$, and s as an expansion in orthonormal eigenfunctions s_k of the hermitian operator $(1/i)\mathcal{L}(\underline{r},\underline{v})$, $\mathcal{L}(\underline{r},\underline{v})s_k = i\mu_k s_k$. Because of the close connection with ideal MHD, it is expected that only a few eigenfunctions $\underline{\xi}_\ell$ will be required. With these expansions, Eq. (5) can be solved for $\underline{\xi}$ and substituted into Eq. (6), which can then be written in a matrix representation in the space of eigenfunctions of $(1/i)\mathcal{L}(\underline{r},\underline{v})$. Taking the time dependence of s as $\exp(-i\omega t)$, the equation for the eigenfrequencies ω is

$$\det\left[(L - \omega) - \omega\sum_{\ell=1}^{N}\left(i\omega a^{(\ell)} - b^{(\ell)}\right)c^{(\ell)\dagger}\right] = 0 \ , \tag{7}$$

where † denotes hermitian adjoint, and N is the number of eigenfunctions $\underline{\xi}_\ell$ that are used. Here L is a diagonal square matrix which represents $(1/i)\mathcal{L}(\underline{r},\underline{v})$ with weight function $f_o(\varepsilon)$; $a^{(\ell)}$ and $b^{(\ell)}$ are column vector representations of $(MQ/\lambda_\ell)\underline{v}\cdot\underline{\xi}_\ell$ and $(MQ/\lambda_\ell)\underline{v}\cdot(\nabla\underline{\xi}_\ell)\cdot\underline{v}$, respectively, with weight function $f_o(\varepsilon)$. The column vector $c^{(\ell)}$ is the representation of $(\partial f_o/\partial\varepsilon)\underline{\xi}_\ell\cdot(\underline{E}^{(0)} + \frac{1}{c}\underline{v}\times\underline{B}^{(0)})$ with weight function unity. The weight functions are those required by the variational derivation.

The form of the matrix in Eq. (7), a diagonal matrix plus a sum of matrices of rank one, is of important practical significance. If ω does not equal one of the eigenvalues of L, which are all real, then it can be shown that Eq. (7) is identical to

$$[\det(L - \omega)][\det D] = 0 \ , \tag{8}$$

where D is an $\underline{N \times N}$ matrix whose elements are

$$D_{jk} = \delta_{jk} - c^{(j)\dagger}(L - \omega)^{-1}[i\omega^2 a^{(k)} - \omega b^{(k)}] \ . \tag{9}$$

The fact that L is diagonal, and the expectation that small values of N will be sufficient, render the determination of eigenfrequencies from Eq. (8) feasible, even though the dimension of the matrices in Eq. (7) is large - say 10,000 × 10,000.

Equilibria with Axial and Translational Symmetry

To find the eigenfunctions and eigenvalues of $(1/i)\mathcal{L}(\underline{r},\underline{v})$ it is valuable to use all symmetries of the equilibrium. With axial and translational symmetry, the appropriate variables are cylindrical coordinates θ and z, energy ϵ, the conserved canonical momenta p_θ and p_z, and a variable $\tau(r,\epsilon,p_\theta,p_z)$. The functions s and $\underline{\xi}$ can be taken proportional to $\exp[i(m\theta + kz)]$ and each pair of values of m and k considered separately. The variable $\tau(r,\epsilon,p_\theta,p_z)$ is proportional to the time required for an ion to move in equilibrium from a fixed point to a point (r,v_r) along a curve in the (r,v_r) phase plane corresponding to fixed ϵ,p_θ, and p_z. This time, along with the eigenfunctions and eigenvalues of $(1/i)\mathcal{L}(\underline{r},\underline{v})$, can be expressed exactly in terms of integrals that can be evaluated numerically. It is also possible to compute the MHD eigenfunctions $\underline{\xi}_\ell$. Therefore, the matrix elements in Eq. (7) can all be computed, and eigenfrequencies can be determined from Eq. (8).

This procedure is being applied to the sharp-boundary screw pinch as a first application.

This work was performed under the auspices of the United States Atomic Energy Commission.

References

(1) J. P. Freidberg, to be published in Physics of Fluids.

(2) H. Ralph Lewis, Phys. Fluids 15, 103 (1972).

Expansion of Toroidal Equilibrium with Finite Periodicity Length and $\ell = 0,1$ Fields in Leading Order

F.Herrnegger and J.Nührenberg

Max-Planck-Institut für Plasmaphysik, Euratom Association

Garching bei München, Germany

Abstract: The existence of an expandable toroidal magneto-hydrostatic equilibrium with finite rotational transform, but without Pfirsch-Schlüter correction is investigated. Under the specific scaling used, a solution accurate to second order (which includes the toroidal effects) exists only for a uniquely determined pressure profile.

A class of toroidal equilibria is investigated which is characterized as follows: β is of order one; the longitudinal current through each magnetic surface vanishes; the only expansion parameter used in the approximate solution is the quantity

$$\rho_{max}/R_o \sim \epsilon \tag{1}$$

where ρ_{max} is the radius of the discharge tube and R_o the radius of curvature of the magnetic axis, which is constant in lowest order; the periodicity length L_p and the torsion in lowest order $1/T_o$ of the magnetic axis obey the relations

$$2\pi\ \rho_{max}/L_p \sim 1,\ \rho_{max}/T_o \sim 1 \tag{2}$$

and the zeroth order equilibrium is the straight θ-pinch with circular plasma cross section. Under these conditions the equilibria are of the $\ell = 1$ stellarator type, where the $\ell = 1$ corrugation is of first order. $\ell = 0$ (i.e. M & S) and $\ell = 2,3,\ldots$ currugations may be added in first order. Further, the large toroidal radius is ordered as

$$\rho_{max}/R_T \sim \epsilon^2. \tag{3}$$

The equilibrium then has a rotational transform of order one, so that one has, in general, to expect the occurrence of the Pfirsch-Schlüter (PS) effect. Since this means that the current density parallel to the magnetic field is changed by a finite amount from the corresponding straight case (see for example Refs. 1,2), one can, in general, not expect an expandable equilibrium of the above type. On the other hand, it is well known from equilibrium calculations with the help of an expansion near the magnetic axis (see for example Refs. 2,3) that the PS-correction may be eliminated near

the magnetic axis by suitably choosing the configuration; the relevant condition is, for example in the simplest case of an M & S equilibrium (see Ref.2).

$$\oint \frac{ds}{R_o B_o^{3/2}} = 0, \qquad (4)$$

where B_o is the magnetic field on the magnetic axis and R_o its radius of curvature. Therefore, the expansion of an equilibrium characterized by Eq. (1) - (3) in the small parameter ϵ can only be successful if the relevant condition (which corresponds to Eq.(4) but is, of course, different in form for our case) is met. However, this is not sufficient and the calculation yields the additional result whether the PS-correction can be eliminated over the entire cross section.

We perform the calculation in Hamada coordinates. The equilibrium construction then reduces to obtaining the relationship of adequate geometrical coordinates with the Hamada coordinates. We use the geometrical coordinates ρ,φ,s of Ref. 4 (which are essentially Mercier's coordinates) and specify their relationship with the Hamada coordinates V,θ,ζ as follows:

$$\rho = \overset{0}{\rho} + \overset{1}{\rho}_{10} \cos\varphi + \overset{1}{\rho}_{01} \sin 2\pi ms/L + \overset{2}{\rho}_{00} + \overset{2}{\rho}_{20} \cos 2\varphi + \overset{2}{\rho}_{02} \cos 2\pi ms/L + \overset{2}{\rho}_{11} \sin(\varphi + 2\pi ms/L),$$

$$\varphi = 2\pi\theta + 2\pi m\zeta + \overset{1}{\varphi}_{10} \sin\varphi + \overset{1}{\varphi}_{01} \cos 2\pi ms/L + \overset{2}{\varphi}_{20} \sin 2\varphi + \overset{2}{\varphi}_{02} \sin 4\pi ms/L + \overset{2}{\varphi}_{11} \cos(\varphi + 2\pi ms/L) + \overset{2}{\tilde{\varphi}}_{11} \cos(\varphi - 2\pi ms/L),$$

$$s = L\zeta + \overset{1}{s}_{10} \sin\varphi + \overset{1}{s}_{01} \cos 2\pi ms/L + \overset{2}{s}_{20} \sin 2\varphi + \overset{2}{s}_{02} \sin 4\pi ms/L + \overset{2}{s}_{11} \cos(\varphi + 2\pi ms/L) + \overset{2}{S}_{11} \cos(\varphi - 2\pi ms/L), \qquad (5a) - (5c)$$

$$\frac{1}{R} = \overset{1}{\varkappa} + \overset{2}{\varkappa} \sin 2\pi ms/L + O(\epsilon^3), \qquad (6a) - (6b)$$

$$\frac{1}{T} = \overset{0}{\tau} + \overset{1}{\tau} \sin 2\pi ms/L + \overset{2}{\tau}_0 + \overset{2}{\tau}_2 \cos 4\pi ms/L.$$

Here, all quantities with superscript, which refers to the ϵ-order, are functions of V only; the subscripts are Fourier indices; L is the length of the magnetic axis and m the number of periods. The subscripts 10 represent the $\ell = 1$ corrugation, 01 the M & S corrugation of the straight circular θ pinch. 1/R and 1/T are curvature and torsion of the magnetic axis and it is easy to construct toroidally closed helical like curves with 1/R and 1/T of the above form. The first order expressions in Eq.(5) have been chosen such that the con-

dition corresponding to Eq.(4) can be satisfied. $\ell = 2$ and other corrugations have not been included because it can be shown that they have no influence on the existence of second order solutions. The second order terms in Eq. (5) are restricted to those which are necessary because of the second order inhomogeneities. Again, additional second order terms in Eq.(5) do not influence the existence of the second order solutions. The set of equations, which has to be solved, is given in Ref.2 (or, in slightly different coordinates, in Ref.4). The following first and second order equations are obtained:

$$(\overset{0}{\rho}\overset{1}{\rho}_{10})^{\cdot} + \frac{1}{2\pi L}\overset{1}{\varphi}_{10} = \frac{1}{2\pi L}\overset{1}{\varkappa}\overset{0}{\rho},$$

$$\overset{1}{s}_{10}(1 + \overset{0}{\rho}^2\overset{0}{\tau}^2) - \overset{0}{\tau}\overset{0}{\rho}^2\overset{1}{\varphi}_{10} = 2\overset{0}{\rho}\overset{1}{\varkappa}/\overset{0}{\tau},$$

$$2\overset{0}{\Phi}^{\cdot\cdot}(\overset{1}{s}_{10} - \overset{0}{\rho}\overset{1}{\varkappa}/\overset{0}{\tau}) + \overset{0}{\Phi}^{\cdot}[\overset{1}{s}^{\cdot}_{10} - 2\overset{0}{\rho}^{\cdot}\overset{1}{\varkappa}/\overset{0}{\tau} + \overset{0}{\rho}\overset{1}{\rho}_{10}\overset{0}{\tau}] = 0,$$

$$(\overset{0}{\rho}\overset{1}{\rho}_{01})^{\cdot} - \overset{0}{\tau}\overset{1}{s}_{01}/2\pi L = 0, \quad 2\overset{0}{\Phi}^{\cdot\cdot}\overset{1}{s}_{01} + \overset{0}{\Phi}^{\cdot}(\overset{1}{s}^{\cdot}_{01} - \overset{0}{\tau}\overset{0}{\rho}\overset{1}{\rho}_{01}) = 0,$$

$$\overset{0}{\tau}\overset{1}{s}_{01} - \overset{1}{\varphi}_{01} = \overset{1}{\tau}/\overset{0}{\tau}, \qquad \text{(7a) - (7f)}$$

$$(\overset{1}{\tau}/\overset{0}{\tau} - \overset{2}{\varkappa}/\overset{1}{\varkappa})\overset{1}{\varkappa}\overset{0}{\rho}/\overset{0}{\tau}^2 + \overset{1}{\rho}_{10}\overset{1}{\rho}_{01} - \overset{1}{s}_{10}\overset{1}{s}_{01} + (\overset{0}{\rho}\overset{1}{s}_{01} - \overset{1}{\rho}_{01}/\overset{0}{\tau})\overset{1}{\mathcal{H}}/\overset{0}{\tau} = 0, \qquad (8)$$

where we have, for brevity, omitted all second order equations except the integrability condition Eq.(8). ($\overset{0}{\Phi}$ is the zeroth order longitudinal flux; the dot indicates the derivative with respect to V). If toroidally closed curves with

$$\overset{2}{\varkappa}/\overset{1}{\varkappa} = \overset{1}{\tau}/\overset{0}{\tau} \qquad (9)$$

existed, Eq.(8) could be satisfied trivially by choosing $\overset{1}{\rho}_{01}$, $\overset{1}{s}_{01} = 0$.[1] However, toroidally closed curves satisfying Eq.(9) do not exist (Ref.5).[2] Therefore, the M & S corrugation is needed to satisfy the integrability condition. Evaluation of Eq.(8) near the magnetic axis yields

$$\frac{3}{2}\overset{0}{\tau}\overset{1}{s}_{01} + (\overset{2}{\varkappa}/\overset{1}{\varkappa} - \overset{1}{\tau}'/\overset{0}{\tau}) = 0 \qquad (10)$$

or, expressed in terms of the field on the magnetic axis

$$B_0 = \overset{0}{B}_0\left[1 - \frac{2}{3}(\overset{1}{\tau}/\overset{0}{\tau} - \overset{2}{\varkappa}/\overset{1}{\varkappa})\sin 2\pi\, ms/L\right], \qquad (11)$$

which coincides with the result from an expansion near the magnetic axis, as it was done in Ref.2. It turns out that the conditon Eq.(10) is not sufficient to satisfy Eq. (8) identically in V. This can only be achieved by determining the pressure profile appropriately. (This

unique profile is approximately linear in V and yields a plasma β of about 0.2). Therefore we conclude that equilibria of the type investigated here do not exist in the sense of an expansion that could be carried to arbitrary order. There exists, however, a unique "solution" of second order accuracy, which could, in the sense of Ref.6, be interpreted as a possibly favorable initial state.

Discussions with D.Lortz, M.Kaufmann and J.Neuhauser are gratefully acknowledged.

---

1) Due to a numerical error in Ref.4, the relation between $\overset{2}{\kappa}$ and $\overset{1}{\tau}$ was different so that it was concluded that the int egrability condition could be satisfied by choosing an appropriate toroidal curve.

2) This fact was only noted after the completion of Ref.2.

---

[1] Pfirsch,D., A.Schlüter, Max-Planck-Institut, Garching, Report No.MPI/PF/ 7/62 (1962)

[2] Nührenberg,J., Nuclear Fusion 12,No.3 (1972)

[3] Maschke,E., Plasma Physics 13 (1971) 9o5

[4] Nührenberg,J., Phys. Fluids 13 (197o) 2o82

[5] Strubecker,K., Differentialgeometrie I, p. 218 Sammlung Göschen Bd. 1113/111a (1964)

[6] Grad,H., Courant Institute, New York, Rep. No. MF-62 (197o)

A Class of Helically Symmetric MHD Equilibria[+]

D. Correa and D. Lortz

Max-Planck-Institut für Plasmaphysik, 8046 Garching bei München, Federal Republic of Germany

Abstract

Helically symmetric equilibria are discussed for the case that the equation is linear.

[+] "This work was performed under the terms of the agreement on association between the Max-Planck-Institut für Plasmaphysik and EURATOM".

Helically symmetric equilibria are conveniently described in terms of the vector field

$$\vec{w} = s\, q\, \nabla s \times \nabla u ,$$

where

$$u = \varphi + k z$$
$$q = (1 + k^2 s^2)^{-1}$$

and s, φ, z are cylindrical coordinates. Any helically symmetric equilibrium field can be written in the form

$$\vec{B} = \vec{w} \times \nabla F + f(F)\, \vec{w} , \quad p = p(F)$$

where $F(s,u)$ satisfies the equation

$$\mathcal{L} F + q^{-1} p' + f' f - 2 k q f = 0$$

$$\mathcal{L} = \frac{\partial^2}{\partial s^2} + q\left(\frac{1}{s} - k^2 s\right)\frac{\partial}{\partial s} + \frac{1}{s^2 q}\frac{\partial^2}{\partial u^2} .$$

Suppose that both p and f are linear

$$p = p_0 + p_1 F , \quad f = \alpha \frac{p_1}{k} + \gamma k F , \quad \gamma p_1 \neq 0$$

(The case $\gamma = 0$ has been discussed by Kadomtsev [1])

The function $\phi = p_1^{-1} k^2 F$ then satisfies

$$\left(\frac{\partial^2}{\partial \rho^2} + \frac{1-\rho^2}{1+\rho^2}\frac{1}{\rho}\frac{\partial}{\partial \rho} + \frac{1+\rho^2}{\rho^2}\frac{\partial^2}{\partial u^2}\right)\phi + \left(\gamma - \frac{2}{1+\rho^2}\right)(\alpha + \gamma\phi) + 1 + \rho^2 = 0$$

where $\rho = k s$. The periodic solutions of this equation can be written in the form.

$$\phi = -\frac{\alpha}{\gamma} - \frac{1}{\gamma^3}(\gamma + 2 + \gamma\rho^2) + \sum_{n=0}^{\infty}\left[C_n h_n^{(1)} + D_n h_n^{(2)}\right]\left[A_n \cos n u + B_n \sin n u\right]$$

$h_n^{(1,2)}$ are the two independent solutions of

$$\rho^2(1+\rho^2)h_n'' + \rho(1-\rho^2)h_n' + \left[(\gamma^2-n^2)\rho^2 + (\gamma^2-2n^2-2\gamma)\rho^2 - n^2\right]h_n = 0$$

If $\gamma^2 \neq n^2$ these solutions can be expressed by Bessel functions

$$h_n^{(1)} = 2^n n! \frac{(\gamma^2-n^2)^{-\frac{n}{2}}}{n-\gamma} \rho^{1+\gamma} \frac{d}{d\rho} \rho^{-\gamma} J_n\left(\sqrt{\gamma^2-n^2}\,\rho\right),$$

$$h_n^{(2)} = \frac{\pi}{2^n |n-1|!} \frac{(\gamma^2-n^2)^{\frac{n}{2}}}{n+\gamma} \rho^{1+\gamma} \frac{d}{d\rho} \rho^{-\gamma} N_n\left(\sqrt{\gamma^2-n^2}\,\rho\right).$$

The solutions for $\gamma^2 = n^2$ are obtained by taking the limes of $h_n^{(1,2)}$ as γ^2 approaches n^2, provided that $\gamma \neq -1$. For $\gamma = -1$ a special consideration is necessary.

We have:

$$\lim_{\gamma \to n} h_n^{(1)} = \rho^n \left(1 + \frac{n}{n+1}\rho^2\right),$$

$$\lim_{\gamma \to -n} h_n^{(1)} = \rho^n$$

$$\lim_{\gamma \to n} h_n^{(2)} = \rho^{-n}$$

$$\lim_{\gamma \to -n} h_n^{(2)} = \rho^{-n}\left(1 + \frac{n}{n-1}\rho^2\right), \quad n \neq 1$$

and

$$h_1^{(2)} = \frac{1}{\rho} - 2\rho \ln \rho, \quad \gamma = -1$$

For $\gamma > 0$ it can be shown that among these solutions there are some which have the following properties:

1) ϕ has a maximum at, say, $r = r_0$, $z = 0$ i.e. the cuts of the magnetic surfaces with the plane z = const are closed curves and the pressure decreases outward.

2) The current density on the magnetic axis vanishes, which implies that

$$\gamma \left[\alpha + \gamma \phi (r_0, 0) \right]^{\frac{1}{\gamma}-1} - r_0^2 = 0$$

3) Sufficient criteria derived in [2] can be satisfied in a finite neighbourhood of the magnetic axis.

These solutions represent stable configurations with a continuous pressure profile which are surrounded by vacuum.

References

1 Kadomtsev, B.B., JETP 10 (1960), 962

2 Lortz, D., Rebhan, E. and Spies, G., Nucl. Fusion 11 (1971), 583.

Specific Magnetic Inductance for Toroidal Systems

R.G.Bateman

Max-Planck-Institut für Plasmaphysik, Euratom Association

Garching bei München, Germany

Abstract: The magnetic inductance matrix, which depends upon geometry alone, has been generalized to toroidal systems with distributed current. This generalization can be made after the magnetic energy is minimized on each flux surface, holding the surface shapes and flux profiles fixed ($\Rightarrow \underset{\sim}{j}\cdot\nabla\psi=0$). It then follows that the flux between differentially close surfaces equals the total current within the surface times the specific inductance (the matrix relates longitudinal and azimuthal components). A special coordinate system appears naturally in the derivation and provides a useful alternative to Hamada coordinates. The coordinate system depends upon geometry alone, but, in it, the magnetic field lines are straight. The general formalism can be applied to the approximation of flux surface shapes for plasma systems with a given topology. The specific inductance can be explicitly calculated for systems with an ignorable coordinate.

For a vacuum magnetic field produced by an arrangement of surface currents, it is well known /1/ that the total currents are related to the total fluxes by a matrix which depends upon geometry alone (inductance matrix) and that the total magnetic energy can be factored into a product of total fluxes and the inductance matrix. Here we present an extension of this idea to systems with distributed currents. However, for the purposes of this extension, it is necessary to minimize the magnetic energy on each surface - i.e. while holding the shapes of the flux surfaces $V = V(x,y,z)$ fixed and holding the flux profiles $\psi_i(V)$ fixed ($i = 1,2$ for simply nested toroidal flux surfaces). The Euler equation for this minimization is $\underset{\sim}{j}\cdot\nabla V = 0$ where $\underset{\sim}{j} = \nabla \times \underset{\sim}{B}$. Note that $\nabla\cdot\underset{\sim}{B} = 0$ already implies $\underset{\sim}{B}\cdot\nabla V = 0$. Once this partial minimization is realized, it follows that /2/

$$I_i(V) = \Lambda_{ij}(V)\,\dot{\psi}_j(V) \qquad (1)$$

$$\int_{\min} d^3x\ \frac{1}{2}B^2 = \int dV\ \frac{1}{2}\,\dot{\psi}_i(V)\,\Lambda_{ij}(V)\,\dot{\psi}_j(V) \qquad (2)$$

where the symmetric, positive definite matrix $\Lambda_{ij}(V)$, which is called the specific susceptance (its reciprocal is the specific inductance), depends upon only the geometry of the flux surfaces and does not depend upon the total current profiles or flux profiles

$$I_i(V) = \oint_{C_i} d\underset{\sim}{\ell}\cdot\underset{\sim}{B} \qquad (3)$$

$$\psi_i(V) = \int_{S_i} d\underset{\sim}{s} \cdot \underset{\sim}{B} \qquad (4)$$

(see Fig.1 for the orientations of C_i and S_i). The proof of these results, as given in reference /2/, relies on a uniqueness theorem for the minimizing magnetic field (i.e. for the solution of $\underset{\sim}{j} \cdot \nabla V = o$ and $\underset{\sim}{B} \cdot \nabla V = o$). The existence of such a field is assumed.

A simple representation for Λ_{ij} can be established by using a special coordinate system (θ^1, θ^2, V) defined by

$$\oint_{C_i} d\ell \cdot \nabla\theta^j = \delta_{ij} \qquad (5)$$

$$\nabla V \cdot \nabla X \, (\nabla V \times \nabla\theta^j) = o \qquad (6)$$

Then, the specific susceptance matrix is

$$\Lambda_{ij}(V) = (-1)^j \oint_{C_i} d\ell \cdot \nabla V \times \nabla\theta^{j+1}. \qquad (7)$$

The special coordinate system determined by Eqs. (5) and (6) provides a useful alternative to Hamda coordinates. Our's is a coordinate system in which the magnetic field lines are straight but the system itself depends upon only the shape of the flux surfaces (Hamada coordinates are functionals of the flux profiles $\psi_i(V)$). Our coordinate system can be used out of equilibrium (it is independent of the presure profile). Even in equilibrium ($\underset{\sim}{j} \times \underset{\sim}{B} = \nabla P$) our coordinates reduce to Hamada coordinates only if $\nabla V \cdot \nabla \times \underset{\sim}{j} = o$ /3/.

For an example of the application of this formalism, suppose we confine our interest to a given class of flux surface shapes with only one free parameter a(V) for each surface. The function a(V) might, for example, be the relative outward shift of toroidal surfaces or the amplitude of a helical distortion. It can be shown that Λ is a functional of both a(V) and $\dot{a}(V)$

$$\Lambda_{ij} = \Lambda_{ij}\,(V\,;\, a(V),\, \dot{a}(V)). \qquad (8)$$

A plasma "equilibrium", constrained to this given subclass of surface shapes, must satisfy both

$$\dot{P}(V) + \psi_i(V)\, \dot{I}_i(V) = o \qquad (9)$$

$$\dot{\psi}_i \Lambda_{ij a} \dot{\psi}_j - (\dot{\psi}_i \Lambda_{ij\dot{a}} \dot{\psi}_j)^{\cdot} = o \qquad (10)$$

together with the side conditions that

$$\dot{\psi}_i \Lambda_{ija} \dot{\psi}_j \delta a = o \quad \text{at } V = o$$

and $\dot{a}(V)$ must be continuous wherever the current density is finite. The stability of a plasma with respect to incompresible perturbations involving only changes in a(V) is determined by the positiveness of

$$\delta^2\Phi = \int dV \left\{ [\dot{\psi}_i \Lambda_{ijaa} \dot{\psi}_j - 2(\dot{\psi}_i \Lambda_{ijaa} \dot{\psi}_j)^{\cdot}] (\delta a)^2 + \dot{\psi}_i \Lambda_{ijaa} \dot{\psi}_j (\delta \dot{a})^2 \right\}.$$

Acknowledgments:

This formalism was suggested by Harold Grad and developed at the NYU Courant Inst.

References:

1) A.A.Blank, K.O.Friedrichs, and H.Grad
Theory of Maxwell's Equations without Displacement Current NYO - 6486 - V (1957).

2) G.Bateman, Energy Principle with Specific Inductance, NYO - 1480 - 182 (1971); to appear in Nuclear Fusion.

3) G.Spies, private communication.

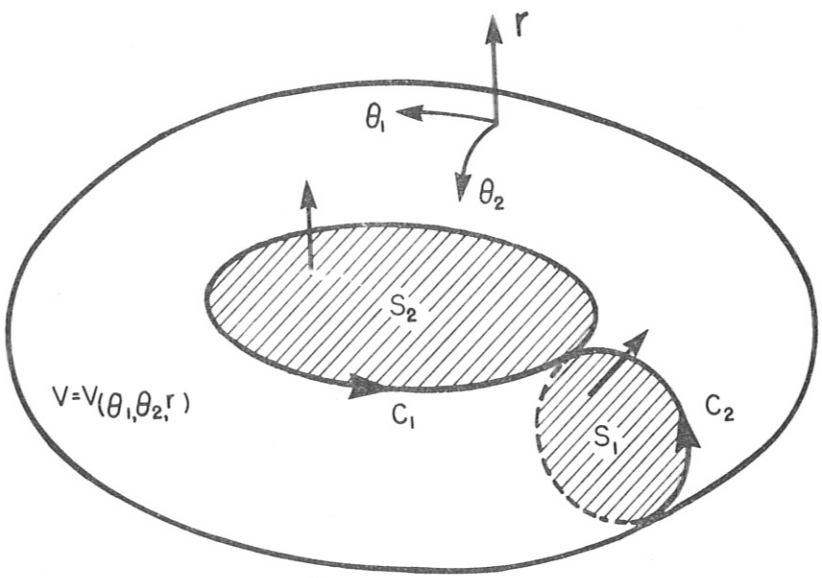

On the Spectrum of Ideal MHD

J.Tataronis and W.Grossmann

Max-Planck-Institut für Plasmapyhsik, Euratom Association,
Garching bei München, Germany

Abstract: "A major task of mathematics today is to harmonize the continuous and the discrete, to include them in one comprehensive mathematics, and to eliminate obscurity from both." E.T. Bell, "Men of Mathematics".

In this and the following paper /B6/ we are going to deal with the spectrum of eigenmodes of the linearized equations of motion of ideal MHD. By ideal we mean that the resistivity and viscosity of the fluid are zero, and that the pressure is a scalar. The eigenvalue problem to be considered can be written in the familiar form,

$$-\rho\,\omega^2 \underset{\sim}{v} = \underset{\sim}{F}\,(\underset{\sim}{v})\,, \text{ plus B.C.} \qquad (1)$$

where the frequency ω arises from the assumption that the perturbed variables have a time dependence of $e^{i\omega t}$, $\rho(\underset{\sim}{r})$ is the equilibrium mass density of the fluid, $\underset{\sim}{v}(\underset{\sim}{r}, \omega)$ is the perturbation of the fluid velocity and $\underset{\sim}{F}$ is a complicated differential operator representing the force acting on a differential fluid element and is dependent only on the position vector $\underset{\sim}{r}$. The exact form of $\underset{\sim}{F}$ can be found in most standard texts on MHD, for example in Ref. /17. Usually, the solutions of eq. (1) which satisfy the boundary conditions can exist only for certain values of ω. These values of ω, the eigenvalues, along with the corresponding $\underset{\sim}{v}$'s, the eigenfunctions, constitute the spectrum that we are seeking. As will be shown, there are two kinds of eigenfunctions in ideal MHD; one is a perfectly analytic function of $\underset{\sim}{r}$ and is square integrable. The second kind of eigenfunction is singular at isolated values of $\underset{\sim}{r}$ in the fluid, and the singularities are of such a nature that they are not square integrable. The consequence of this distinction are many fold. For example, due to the fact that this normalization is possible, the eigenvalues corresponding to the eigenfunctions of the first kind form a discrete set. However, eigenfunctions of the second kind have eigenvalues which can take on any value in some range and hence form a continuum. We thus say that eigenfunctions of the first kind belong to the discrete spectrum and those of the second kind belong to the continuous spectrum. Another consequence of being square integrable is that the eigenfunctions obey a variational principle. When normalization is not possible, then no variational principle can be set up.

The purpose of the present paper is to show the existence of the two kinds of spectra in ideal MHD and to describe the resulting plasma behaviour that each spectrum leads to. In the following paper /B6/ we shall examine the consequence of driving the continuous spectrum with an external source at a specified frequency. The latter problem has important applications in regard to the excitation of MHD waves in bounded plasmas.

The role of the continuous spectrum and its application in plasma physics has also been considered by Grad, Marsh and Weitzner /2/. In their work, as in ours, the possible relationships between mathematical pathology and physical significance are explored.

We shall show here that two types of spectra are possible by showing that they exist in two particular cases, namely in the planar sheet pinch and the cylindrical screw pinch. The results will show that the sheet pinch in the incompressible limit has only a continuous spectrum,

while the screw pinch has in general a continuous and a discrete spectrum.

The sheet pinch is characterized by an equilibrium magnetic field configuration whose cartesian x,y,z components are the following:

$$\underset{\sim}{B} = [0,\ B_y(x),\ B_z(x)] \tag{2}$$

The three equilibrium parameters $\underset{\sim}{B}$, ρ and the pressure p depend only on x. In addition we assume that perfectly conducting walls are located at $x = \pm a$ where we have the boundary conditions

$$v_x(x = \pm a) = 0 \tag{3}$$

Equation (1), which defines the eigenfunctions we are seeking, can now be seperated into components and combined to yield the following differential equation for $v_x(x)$:

$$\frac{d}{dx}\left[q(x,\omega)\ \frac{dv_x}{dx} \right] - k^2 q(x,\omega)\, v_x = 0, \tag{4}$$

$$q(x,\omega) = \rho(x)\,\omega^2 - f^2(x)/\mu_0$$

where a Fourier transform has been made in the y and z directions in the form $\exp[-i(k_y y + k_y z)]$. In addition we have set k^2 equal to $k_y^2 + k_z^2$ and f(x) equal to $\underset{\sim}{k}\cdot\underset{\sim}{B}(x) \equiv k_y B_y(x) + k_z B_z(x)$. μ_0 is the permeability of free space, and the assumption of incompressibility has been made. The components $v_y(x)$ and $v_z(x)$ are expressible in terms of $v_x(x)$. Thus the eigenvalue problem in eq. (1) reduces to eqs. (3) and (4) for the case of the sheet pinch.
Solutions of eq. (4) which satisfy the boundary conditions of eq. (3) do exist but are of a nature which would be unexpected within the classical formulation of MHD: the eigenfunctions are singular in space and the singularities are such that they are not square integrable. The singularities stem from the zeros of the factor $q(x,\omega)$ and can be shown to be logarithmic in form. Proof that the eigenfunctions of the sheet pinch must be singular and form a complete set would require much more space than is allowed in this paper. However, a strong indication that this is indeed the case can be obtained from Barston in reference /3/ where he solves for the natural oscillations of a non-uniform cold plasma slab, free of any applied magnetic field, and bounded by two perfectly conducting plates. It turns out that the fluctuating potential, φ, due to the plasma oscillations is described by the following eigenvalue problem:

$$\frac{d}{dx}\left[(\omega^2 - \omega_p^2(x))\ \frac{d\varphi}{dx} \right] - k^2 (\omega^2 - \omega_p^2(x))\,\varphi = 0 \tag{5}$$

$$\varphi(x = \pm a) = 0$$

where $\omega_p(x)$ is the electron plasma frequency at the point x, and ω and k are defined as before. The similarity between the oscillations of the sheet pinch as described here and the oscillations of a cold non-uniform plasma slab is apparent when eq. (5) is compared with eqs. (3) and (4). The oscillations of the sheet pinch are the oscillations of the lines of force of the magnetic field, i.e., the Alfven waves. The frequency of oscillation is given by $\omega_A(x) = \underset{\sim}{k}\cdot\underset{\sim}{B}(x)/(\mu_0\rho(x))^{1/2}$, and it is seen that at least one solution of eq. (4) is singular at

the point x where $\omega = \omega_A(x)$ just as one solution to eq. (5) is singular where $\omega = \omega_p(x)$. Because of the very close analogy between the two problems (note that the analogy is exact if ρ is independent of x), we can use Barston's work to deduce the following conclusions: the eigenmodes of the sheet pinch are singular and exist only if $q(\omega,x)$ vanishes somewhere within the boundaries of the plasma. Moreover, the spectrum of the modes is continuous in the sense that every real value of ω within a given range is allowed. This range is specified by the minimum and maximum values of $\omega_A(x)$ in the plasma. By letting v_x^{ω} be the singular eigenmode at the frequency ω, then the response of the plasma to given initial conditions can be expressed as an integral over the continuous spectrum:

$$v_x(x,t) = \int d\omega A(\omega) v_x^{\omega}(\omega,x) e^{i\omega t} \tag{6}$$

where the integration is carried out over the continuous spectrum and the coefficient $A(\omega)$ is determined by the initial conditions. As $t \to \infty$, one finds that $v_x(x,t)$ approaches the form

$$v_x(x,t) \propto \frac{e^{i\omega_A(x)t}}{t} \tag{7}$$

where the decay is due to phase mixing of the modes in the continuous spectrum.

One can arrive at this same result by using a Laplace transformation in time to solve the linearized equations of motion as an initial value problem. The nature of the spectrum of the plasma modes is then determined by the type of singularities in the complex ω plane which the Green's function of the equations of motion has. In this method the velocity perturbation $v_x(x,t)$ of the sheet pinch is represented by the Laplace integral as follows:

$$v_x(x,t) = \int_C \frac{d\omega}{2\pi} v_x(x,\omega) e^{i\omega t} \tag{8}$$

where

$$v_x(x,\omega) = \int_{-a}^{a} G(x,x';\ \omega) g(x',\omega) dx' \tag{9}$$

and the Green's function $G(x,x';\ \omega)$ satisfies the following differential equation:

$$\frac{d}{dx}\left[q(x,\omega)\frac{dG}{dx}\right] - k^2 q(x,\omega) G = \delta(x-x') \tag{10}$$

with $G(x = \pm a, x';\ \omega) = 0$. In eq. (8) C is the Laplace contour in the lower half complex ω plane, and $g(x',\omega)$ in eq. (9) contains the initial conditions and the forcing functions. Let $\psi_1(x,\omega)$ and $\psi_2(x,\omega)$ be two solutions of the homogeneous form of eq. (10) with $\psi_1(a,\omega) = 0$ and $\psi_2(-a,\omega) = 0$, then the solution of eq. (10) can be written as follows:

$$G(x,x';\ \omega) = \frac{\psi_1(x_>,\omega)\psi_2(x_<,\omega)}{J(\psi_1,\psi_2)} \tag{11}$$

where $J(\psi_1, \psi_2) = q(x,\omega)(\psi_1'\psi_2 - \psi_2'\psi_1)$ and $x_{>(<)}$ is the greater (lesser) of x and x'. It can be shown that J is independent of x and x'. What is of interest here is the asymptotic form of eq. (8) as $t \to \infty$, and this is determined by the singularities of $G(x,x';\omega)$ in the complex ω plane. The singularites are of two types: those of ψ_1 and ψ_2 and those of J. From eq. (10) it is clear that singularities of ψ_1 and ψ_2 are determined by the zeros of $q(x,\omega)$. When q is zero somewhere with the boundaries of the plasma then G behaves as $\log [\omega^2 - \omega_A^2(x)]$ near that point, i.e., the singularity is a branch point which represents the continuous spectrum of the sheet pinch. If we now perform the integration in eq. (8) along the branch cut and let $t \to \infty$, we recover the decaying solution in eq. (7). Another source of singularities of G comes from the zeros of J which would represent the discrete spectrum. It can be shown that if k is real then J does not vanish. Hence the sheet pinch has only a continuous spectrum. However, there are other plasma configurations which have both a continuous and a discrete spectrum. One is the cylindrical screw pinch. The analysis of this configuration proceeds exactly as above with the radial component $v_r(r,t)$ of the perturbation velocity replacing $v_x(x,t)$. The equations are almost identical in form with the sheet pinch with the exception that the Green's function satisfies a differential equation of the type:

$$\frac{d}{dr}\left[p(r,\omega)\,\frac{d(rG)}{dr}\right] - k^2 h(r,\omega)(rG) = \delta(r-r'). \qquad (12)$$

Because $p(r,\omega)$ is not identical with $h(r,\omega)$, one finds a discrete set of modes. These modes are unstable and are described by Newcomb. Again there is a continuous spectrum due to the zeros of $p(r,\omega)$.

Thus it is seen that the Laplace transform technique is a powerfull tool since it reveals naturally the continuous and discrete spectra. It is pointed out that Sedláček /4/ used the Laplace transform method to solve Barston's problem.

References

/1/ Schmidt,G., "Physics of High Temperature Plasmas", Academic Press, New York, 1966, pg. 120

/2/ Grad,H., Marsh,J., Weitzner,H., Abstract of Sherwood Theoretical Meeting, March 22-23, 1971, Courant Institute of Mathematical Sciences, New York University, Report, NYO-3077-185, MF-65

/3/ Barston,E.M., Annals of Physics 29, 282-303, 1964

/4/ Sedlacek,Z., J.Plasma Physics 5, 239, 1971

The Excitation of Waves and Resonances in High-Beta Plasmas

W.Grossmann and J.Tataronis

Max-Planck-Institut für Plasmaphysik, Euratom Association,
Garching bei München, Germany

Abstract: The problem of the excitation of waves and resonances in non-uniform high beta MHD plasmas is treated and it is shown that qualitatively different results are obtained than from the theory of uniform plasmas.

The problem of the excitation of the natural modes of any physical system can be reduced to the problem of the coupling of a source to the system. Strong coupling implies strong mode excitation. Hence the problem must proceed in two steps: First, the determination of the spectrum of modes of the system and second the determination of the conditions which lead to strong mode-source coupling. In this paper we are concerned with the excitation of MHD waves and resonances in high-beta non-uniform cylindrical plasmas. It is very important to emphasize the non-uniformity of the plasma because incorrect results are obtained if one simply applies theory derived from either sharp boundary or infinitely homogeneous plasmas to situations where, for example, the density and mangetic fiels depend continuously on some coordinate. The principle new effect which comes about from the non-uniformity of the plasma can best be seen by examining the response of the plasma, $\Phi(\underline{r},t)$, to some external source, $s(\underline{r},t)$, whether this source be initial conditions or a driving function at some specified frequency ω_o. By employing a Laplace transformation in time, $\Phi(\underline{r},t)$ can be put in the following form:

$$\Phi(\underline{r},t) = \int_c \frac{d\omega}{2\pi} G(\omega,\underline{r})\ s_t(\omega)\, e^{i\omega t} \qquad (1)$$

where $G(\omega,\underline{r})$ is a Green's function of the linearized equations of motion of the plasma and the source $s(\underline{r},t)$ has been written $s_r(\underline{r})\cdot s_t(t)$ where the spatial part $s_r(\underline{r})$ is in $G(\omega,r)$. $s_t(\omega)$ is the Laplace transform of the temporal part $s_t(t)$. The integration is carried out along the contour c in the lower half complex ω plane below all the singularities of the integrand. The natural modes, or waves, the excitation of which we are examining in this paper, are represented in equ. (1) as singularities of $G(\omega,\underline{r})$ in the complex ω plane. The nature of the singularities determines the temporal behaviour of the modes.

We first consider an infinite uniform plasma and in particular one in which the spatial variation of $\Phi(\underline{r},t)$ has the form: $\exp(-i\underline{k}\cdot\underline{r})$. In this case the Green's function is given by

$$G(\omega,\underline{r}) = \frac{Ae^{-i\underline{k}\cdot\underline{r}}}{D(\omega,k)} \qquad (2)$$

where A is a constant and $D(\omega,k)$ is the familiar dispersion function of the infinite uniform plasma found, for example, in reference /1/. The zeros of D give the normal modes of the plasma and lead to simple poles in $G(\omega,r)$. We can thus use the theory of residues to evaluate the integral in equ. (1) and we find

$$\Phi(\underline{r},t) = i\sum_j \frac{As_t(\omega_j)}{D_\omega(\omega_j,k)}\, e^{i(\omega_j t-\underline{k}\cdot\underline{r})} \qquad (3)$$

where the summation extends over the zeros of $D(\omega,k)$ for the given $\underline{k}$ value and D_ω has been written for $\partial D/\partial\omega$. In addition we should include in equ. (3) the contributions from any other type of singularity of $G(\omega,\underline{r})$ plus the contribution from the pole of $s_t(\omega)$ if the plasma is

driven at some frequency. However, in the manner in which the problem has been formulated, with only one wave number $\underline{k}$ present, G has only poles. Thus waves are excited which can grow, persist or decay depending on whether the imaginary part of ω_j is negative, zero, or positive respectively.

Let us now consider a plasma which is non-uniform in a certain direction. Again the response of the plasma to a source is given by equ. (1), but the Green's function no longer has the simple form given in equ. (2). Its exact form depends on the nature of the system, but, in general terms we can say that the singularity of $G(\omega,\underline{r})$ now takes the form of a branch point in the complex ω plane and that the sum over discrete frequencies shown in equ. (3) is replaced by an integration along the branch cut emanating from the branch point, i.e.

$$\Phi(\underline{r},t) = \int_{\substack{\text{branch}\\ \text{cut}}} \frac{d\omega}{2\pi} G(\omega,\underline{r})\, s_t(\omega)\; e^{i\omega t} \tag{4}$$

The details regarding the origin of the branch cut are given in B5 of this conference. In order to show the implications of the branch cut regarding the excitation of waves, it is best to consider specific examples. Although the above arguments apply to any cylindrically symmetric diffuse MHD plasma, we limit ourselves to examining the case of the simple theta-pinch. We assume that the theta-pinch equilibrium is independent of z and θ and is strongly non-uniform with smooth radial density, pressure and magnetic field profiles.

We identify in equ. (4) $\Phi(\underline{r},t)$ with $v_r(r,t)$, the radial component of the plasma perturbation velocity. Then, following the procedure given in B5, $G(\omega,r)$ is given by

$$G(\omega,r) = \int_0^R \tilde{G}(r,r';\omega)\; s_{\underline{r}}(r')\,dr'$$

where R is the radius of the theta-pinch and $\tilde{G}$ is determined by the following equation:

$$\left[\frac{\left(\omega^2\rho - \frac{k^2B^2}{\mu_o}\right)\left(\omega^2\rho\left(\gamma P+\frac{B^2}{\mu_o}\right) - \gamma\frac{Pk^2B^2}{\mu_o}\right)\frac{1}{r}\,(r\tilde{G})'}{\omega^4\rho - \omega^2\rho\left(\frac{m^2+k^2r^2}{r^2}\right)\left(\gamma P+\frac{B^2}{\mu_o}\right) + \left(\frac{m^2+k^2r^2}{r^2}\right)\gamma\frac{Pk^2B^2}{\mu_o}} \right]' +$$

$$\left(\omega^2\rho - \frac{k^2B^2}{\mu_o}\right)\frac{\tilde{G}}{r} = \delta(r-r'). \tag{5}$$

The right hand side of equ. (5) is a delta function placed at the radial position r'. Equation (5) is derived from the linearized MHD equations of motion in the manner described in B5. The quantities ρ, P, and B are the equilibrium density, pressure and magnetic field profiles and m and k are the fourier transform variables for the θ and z direction respectively. The parameter γ is the ratio of specific heats. The differential operator of equation (5) posesses both a continuous and a discrete spectrum and consequently it is possible to find examples of waves with time dependence as given by (3) as well as the non-exponential time behaviour as presented in B5.

As an example of a discrete mode which is excited by any arbitrary perturbation of the equilibrium, i.e. the source term in (1) s_t is a constant, we examine the m=0, k=0 compressional wave or sometimes called the natural frequency of the plasma. In this case the singularities of

the Green's function are simple poles and lead to purely oscillatory time behaviour. For this mode one can solve numerically the homogeneous form of equation (5) for given experimental profiles and obtain the natural eigenfrequency ω and the eigenfunction. We have investigated several different profiles and have derived for two dimensional compression, γ=2, the equivalent sharp boundary model result that the natural frequency is independent of beta and the plasma profile. This frequency is:

$$\omega^2 = \frac{8B_o^2}{\mu_o \rho_o a^2} \tag{6}$$

where B_o is the magnetic field strength outside the plasma of density ρ_o and a is the plasma radius. These oscillations, observed in every theta-pinch experiment, are observed to be damped in time due to time varying equilibrium properties. End loss from a theta-pinch is one source of the non-constant equilibrium.

We now examine another wave which leads to non-sinusoidal time behaviour. This wave is the longitudinal Alfven wave. In the uniform plasma case, this wave is uncoupled from the remainder of the dispersion relationship. For the non-uniform theta-pinch under the approximation of incompressibility, $\gamma \to \infty$, we obtain an equivalent uncoupled description of the Alfven wave whose Green's function is found from:

$$\left[\frac{r(\rho\omega^2 - \frac{k^2B^2}{\mu_o})(r\tilde{G})'}{m^2 + k^2r^2}\right]' - (\rho\omega^2 - \frac{k^2B^2}{\mu_o})\frac{\tilde{G}}{r} = \delta(r-r'). \tag{7}$$

As shown in B5, the above operator for real k has only a continuous spectrum. The calculation of the Green's function is in practical situations extremely difficult because of the very complicated homogeneous form of (7) when arbitrary density and magnetic fields are chosen. In order to obtain a feeling for the nature of response, we approximate the density and magnetic fields as simply as possible. Assuming constant density and a magnetic field which varies linearly with r, it can be shown that the singularity in the corresponding Green's function is logarithmic in nature and has the following form:

$$G \sim \ell n\ (\omega^2 - \frac{k^2B^2}{\mu_o\rho_o} r^2). \tag{8}$$

As shown in B5, when a plasma is subjected to an initial perturbation or impulse the singularities of the Green's function as given by (8) lead to a response which decays in time as 1/t. This phenomenon is caused by phase mixing since the perturbation excites a spectrum of Alfven waves all with different wave speeds. It should be recalled that in a uniform plasma a single Alfven wave is excited which propagates without damping. If, however, the plasma is subjected to a source with a driving frequency ω_o, then the product of $G(\omega,\underline{r})$ and $s_t(\omega)$ in equ. (4) for our test model has the following form for the dominant singularities:

$$\frac{\ell n\ (\omega^2 - \omega_A^2)}{\omega - \omega_o} \tag{9}$$

where we have written $\bar{\omega}_A$ for $k^2B_o^2r^2/\mu_o\rho_o$ and represents the local Alfven frequency. The singularities of (9) lead to the following results: If the driving frequency does not lie inside the Plasma spectrum; that is $\bar{\omega}_A^2(\min) \leq \omega_o^2 \leq \bar{\omega}_A^2(\max)$, then the only waves which will be excited will be an oscillation in the plasma at the driving frequency plus, of course, Alfven waves which due to the above arguments of phase mixing will decay away. If, however, the driving frequency ω_o is equal to a local value of Alfven frequency $\omega_A(r)$ for $o < r < R$, then parametric amplification of an Alfven wave with the time dependency given by

$$v_r \sim e^{i\omega_A t} \ln \omega_A t \qquad (10)$$

will occur at that value of r in the plasma. Equ. (10) is obtained by setting ω_o equal to ω_A in equ. (9) and integrating around the branch cut in the complex ω plane for $t \to \infty$. If the driving signal is too broad in frequency then a spectrum of the Alfven waves will be excited, all with different propagation speeds and hence will agian, through phase mixing, decay. The driving signal must then be very sharp and lie within the acceptable spectrum of the plasma.

Actually there is another mechanism responsible for phase mixing and this concerns the exciting of a definite k mode. If the driving signal excites not one k, but a spectrum of k's, then again phase mixing occurs and, as one moves away from the source, the signal is observed to decay in space. This phenomenon can be just as important as the phase mixing in time which was treated above.

Finally, we mention that a number of experimental investigations have observed damping of Alfven waves. The phenomenon which we have discussed is present in every inhomogeneous plasma and can be expected to play a role in the observation of damped wave propagation in stable plasmas. Another damping mechanism, mentioned earlier, is due to non-constant equilibrium properties in time. The determining factor which ultimately should decide which mechanism plays the stronger role is the ratio of the time scale of the changing equilibrium to the Alfven wave time. If this ratio is large then one should expect, based on uniform plasma results, a number of Alfven transits before such effects of the time varying equilibrium seriously effect the waves.

References

/1/ Friedrichs,K.O., Los Alamos Sci. Lab. Report, LAMS-2105 (1954)

MHD STABILITY STUDIES OF NUMERICALLY OBTAINED TOROIDAL EQUILIBRIA

D. A. Baker and L. W. Mann

University of California, Los Alamos Scientific Laboratory, Los Alamos, New Mexico U.S.A.

ABSTRACT

This work pertains to axisymmetric toroidal MHD equilibria and their stability. Of particular interest are high β equilibria with hollow pressure profiles as observed experimentally in the Los Alamos toroidal z-pinch. This study includes toroidal curvature effects in the determination of MHD stable toroidal z-pinch configurations. Diffuse profile toroidal equilibria free from limitations on aspect ratio, were obtained numerically. These solutions are analyzed for MHD stability by means of a double Fourier expansion of δW in the poloidal and toroidal variables and finite differencing the remaining variable. The resulting large, quadratic form is then tested for positive definiteness corresponding to stability.

I. INTRODUCTION

This work is an extension of previous equilibrium and stability studies of axisymmetric toroidal equilibria having poloidal fields only. In the former case the minimization of δW leads to an eigenvalue problem requiring integration of an ordinary differential equation along the field lines. The MHD stability analysis was performed for the Los Alamos toroidal quadrupole experiment for diffuse profiles and irregular boundaries by solving both the equilibrium equation and the corresponding stability eigenvalue equation numerically.[1] The large measure of success of that work in both predicting stability as well as its utility in interpreting the experimental results has motivated us to attempt a numerical study for mixed-field toroidal equilibria exemplified by the Los Alamos toroidal z-pinch. [2] The Euler-Lagrange equations arising from a minimization of δW in the mixed toroidal and poloidal field case are coupled partial differential equations which normally contain troublesome singularities. Rather than solve these equations we chose instead to minimize a discretized δW numerically. The numerical approach offers a method of studying realistic diffuse profile toroidal equilibria free from restrictions on boundary shapes and aspect ratios.

II. EQUILIBRIUM SOLUTIONS

Equilibrium Equation - We desire solutions of the ideal MHD static equilibrium equations*

$$\vec{J} \times \vec{B} = \nabla p \tag{1}$$

$$\nabla \times \vec{B} = \mu \vec{J} \tag{2}$$

$$\nabla \cdot \vec{B} = 0 \ . \tag{3}$$

for configurations having azimuthal symmetry with boundaries with otherwise arbitrary shape. To exploit this symmetry we introduce a cylindrical coordinate system (r,φ,z) with the z axis oriented along the major symmetry axis so that all quantities are φ independent. For convenience we decompose the magnetic field $\vec{B}$ and current density $\vec{J}$ into poloidal $\vec{B}_p, \vec{J}_p$ and toroidal B_φ, J_φ parts. The divergence-free condition on $\vec{J}$ and $\vec{B}$ is satisfied by introducing poloidal stream functions ψ and $\bar{I}$ such that

$$\vec{B}_p = \nabla \times (\hat{\varphi}\, \psi/r) \equiv (1/r)\, \nabla\psi \times \hat{\varphi} \tag{4}$$

$$\vec{J}_p = \nabla \times (\hat{\varphi}\, \bar{I}/r) \equiv (1/r)\, \nabla I \times \hat{\varphi} \ . \tag{5}$$

where $\hat{\varphi}$ denotes the φ coordinate unit vector. With appropriate choices of the values assigned to $\psi(r,z)$ and $\bar{I}(r,z)$ on the boundaries these functions represent $(2\pi)^{-1}$ times the poloidal magnetic and current fluxes linking the circular contour r = constant z = constant. It then follows from equations (1) and (2) that toroidal field and current densities are related to these functions as follows

$$B_\varphi = \mu \bar{I}/r \tag{6}$$

$$J_\varphi = r[p' + (\mu/r^2)\, \bar{I}\bar{I}'] \tag{7}$$

where primes denote derivatives with respect to ψ. When expression (7) for J_φ and B_r and B_z obtained from Eq. (4) is substituted into the φ component of Eq. (2) the equilibrium equation governing ψ is obtained [3,4]

$$r \frac{\partial}{\partial r}\left(\frac{1}{r}\frac{\partial \psi}{\partial r}\right) + \frac{\partial^2 \psi}{\partial z^2} + \mu(r^2 p' + \mu \bar{I}\bar{I}') = 0 \ . \tag{8}$$

Equation (8) along with a specification of $p(\psi)$, $\bar{I}(\psi)$ and the boundary values of ψ poses a boundary value problem. For pulsed fields produced inside perfectly conducting walls the condition that the normal component of $\vec{B}$ vanish at the walls corresponds to the boundary condition that ψ is constant. Once ψ is obtained all other equilibrium quantities of interest can be computed from the foregoing equations.

Method of Solution - Equation (8) is an elliptic differential equation with nonlinear source terms. Exact analytic solutions are obtainable only for very special source functions p and $\bar{I}$ and for simple boundaries. We have been successful in obtaining numerical solutions by successive overrelaxation of an elementary difference equation corresponding to Eq. (8) for toroidal multipoles, z-pinches and Tokamaks.[5,6] Numerical solutions of Eq. (8) have been reported for Astron and Tokamak geometries by other authors.[7,8] The procedure is not entirely straightforward, however. There is no unique choice for the source functions; a continuum of these functions exist corresponding to equilibria having different pressure and magnetic field profiles. We have either guessed or used source functions taken from linear one-dimensional equilibrium solutions. Often solutions for several such trial and error functions are obtained before an equilibrium with the desired properties is found. Moreover, for a given choice of source functions and boundary conditions solutions of Eq. (8) need not be unique. In cases where such bifurcated solutions exist special differencing tech-

*We use rationalized MKSA units with vacuum permeability denoted by μ.

niques may be required to obtain convergence to the desired solution.[7] In addition, care must be exercised in the choice of starting values of the ψ function loaded on the finite difference mesh before the relaxation iterations are begun. The nonlinearity of the problem leads to nonconvergence for certain choices of starting values. We have obtained convergence for the forementioned cases for rather crude starting guesses to the form of the solution.

III. STABILITY ANALYSIS

General - Our primary aim was to find stable toroidal equilibria and a scheme was needed for checking stability of any given two-dimensional numerical solution once it is obtained. We have first concentrated on a numerical analysis using a discrete form for δW of the energy principle. In this regard we obtained valuable ideas and suggestions from B. R. Suydam who had previously done a considerable amount of studying on such an approach. An analogous one-dimensional numerical approach has proven useful in obtaining MHD stable profiles for linear z-pinch geometry.[2]

Discrete Formulation of δW - The derivation of the final quadratic form for δW is lengthy and tedious. It will suffice here to outline the steps involved leaving the details to a longer paper to be published later. The starting point is the general integral representing the contribution to energy change associated with a small perturbation $\vec{\xi}(r)$ from the equilibrium configuration.[9]

$$\delta W = \tfrac{1}{2}\int \frac{Q^2}{\mu} - \vec{J}\cdot(\vec{Q}\times\vec{\xi}) + \gamma p(\nabla\cdot\vec{\xi})^2 + (\nabla\cdot\vec{\xi})(\vec{\xi}\cdot\nabla p)\,d\tau \tag{9}$$

$$Q = \nabla\times(\vec{\xi}\times\vec{B})$$

where all operators and variables are equilibrium quantities except $\vec{\xi}$. We introduce a right handed coordinate system (x_1, x_2, x_3) which is natural to the equilibrium field. The coordinate x_1 labels the poloidal flux surfaces, x_2 is the azmuthal angle φ and x_3 measures position along the poloidal flux lines and is chosen so that the coordinate surfaces are mutually orthogonal. The associated line element is $ds^2 = \Sigma\, h_i^2 dx_i^2$ with metric coefficients h_i. A typical coordinate system of this type is (ψ,φ,χ), a system commonly used at Princeton.[9] Because of the frequent appearance of the combination $\xi_2 B_3 - \xi_3 B_2$ it is convenient to work with the perturbation variables ξ_1, ξ_2, ξ_3 instead of ξ_1, ξ_2, ξ_3, where $\xi_3 = h_1(\xi_2 B_3 - \xi_3 B_2)$.

Since the equilibrium is axisymmetric one can Fourier analyze and integrate over the φ variable

$$\vec{\xi}(\vec{r}) = \sum_{k=-\infty}^{+\infty} \vec{\xi}(x_1 x_3)e^{ik\varphi} \tag{10}$$

so the δW is of the form

$$\delta W = \sum_{k=-\infty}^{+\infty} \iint \delta W_k(\xi_1, \bar{\xi}_3)\,dx_1\,dx_3 \tag{11}$$

Since these k modes are uncoupled they can be studied by examining each δW_k individually. Minimization of δW in Eq. (9) with respect to displacements along the field lines yields[9]

$$\vec{B}\cdot\nabla[\gamma p(\nabla\cdot\vec{\xi})] = 0 \tag{12}$$

This equation expressed in generalized coordinates, Fourier transformed and integrated over x_3 yields

$$\left[\nabla\cdot\vec{\xi}\right]_{x_3} = \left[\nabla\cdot\vec{\xi}\right]_0 \exp\left[-\frac{ikB_2}{k_1 B_3}\int_0^{x_3}\frac{h_1 h_3}{h_2}\,dx_3\right] \tag{13}$$

Since the metric coefficients are inherently positive this expression shows that periodicity of $\nabla\cdot\vec{\xi}$ for an integration path extending completely around a poloidal flux surface is satisfied by either $\nabla\cdot\vec{\xi}$, k, or B_2 vanishing. The closed field line case with no toroidal field, B_3, is treated by our earlier work.[1] The k = 0 case is special. It is doubtful, however, that our previously discussed iteration process will converge to an equilibrium which is unstable to toroidally symmetric perturbations. We treat here the divergenceless perturbations i.e. $k \neq 0$ and $B_2 \neq 0$. The condition $\nabla\cdot\vec{\xi} = 0$ allows one to eliminate $\bar{\xi}_2$ from δW_k and also eliminates the pressure terms in Eq. (9). At this point δW_k is a quadratic form in the variables ξ_1, $\bar{\xi}_3$ and their first derivatives ($\partial\bar{\xi}_3/\partial x_1$ does not appear). In matrix notation W_k is given by the real part of the integral over x_1 and x_3 of $E C E^{\dagger}$ ($\dagger$ denotes the hermitian conjugate) where

$$E = (\xi_1, \bar{\xi}_3, \partial\xi_1/\partial x_1, \partial\xi_1/\partial x_3, \partial\bar{\xi}_3/\partial x_3)$$

and C is a 5 × 5 symmetric matrix containing elements c_{ij} which are functions of the equilibrium magnetic field components, the metric coefficients and their derivatives. In the general case all but four of the c_{ij}'s are nonzero giving eleven independent functions.

For systems where the c_{ij}'s vary smoothly with x_3 one can expect them to be well represented with a reasonable number of terms of a Fourier series. With this expectation in mind we normalize x_3 so that it increases by 2π once the short way around the flux surface and expand the c_{ij}, ξ_1 and $\bar{\xi}_3$ in truncated series (2M + 1 terms)

$$c_{ij} = \sum_{m=-M}^{M} F_{ij}e^{imx_3},\quad \xi_1(x_1,x_3) = \sum_{m=-M}^{+M} \xi_1^m(x_1)e^{imx_3}$$

with an analogous expansion for $\bar{\xi}_3$. When these expressions are inserted into δW_k and the integration over x_3 carried out these m modes are coupled. The terms δW_k and δW_{-k} are then combined pairwise. The $\bar{\xi}_3^m$ variables then appear algebraically and the minimization of δW_k with respect to $\bar{\xi}_3$ can be done analytically. A successive completion of the squares of the $\bar{\xi}_3$ variables lends itself to a recursive algorithm conveniently done on the computer. When this minimization is completed the energy integral is in the form

$$\delta W_k = \mathrm{Re}\left\{\int UKU^{\dagger}dx_1\right\}$$

where K is a (4M + 2) × (4M + 2) matrix whose elements are given in terms of the Fourier transforms equilibrium quantities along each poloidal flux line and

$$U = \left(\xi_1^{-M},\ \xi_1^{-M+1}\cdots\xi_1^{M},\ \frac{\partial\xi_1^{-M}}{\partial x_1},\ \frac{\partial\xi_1^{-M+1}}{\partial x_1}\cdots\frac{\partial\xi_1^{M}}{\partial x_1}\right).$$

The elements of K are real and symmetric so that only real ξ_1 need be considered. As a final step the integration over x_1 is done by dividing the integration interval into N-1 intervals with end points $x_1^1, x_1^2, \ldots x_1^N$ separated by Δx_1. The integration is then replaced by a sum with derivatives in the integrand replaced by the finite difference expression

$$\frac{d\xi^m}{dx_1}\Big|_{n+\frac{1}{2}} = \left(\xi^m_{n+1} - \xi^m_n\right)/\Delta x_1$$

where the subscript n now indicates the evaluation of ξ_1^m at x_1^n.

The final expression for the energy is quadratic of the form

$$\delta W_k = XWX \qquad (14)$$

where

$$X = \left(\xi_1^{-M}, \xi_1^{-M+1} \ldots \xi_1^{M}, \xi_2^{-M}, \xi_2^{-M+1} \ldots \xi_2^{M}, \right.$$

$$\left. \ldots\ldots \xi_N^{-M}, \xi_N^{-M+1} \ldots \xi_N^{M}\right)$$

is a row matrix of N(2M + 1) variables and W is a symmetric N(2M + 1) × N(2M + 1) band matrix of width 4(2M + 1).

Stability of the system then depends upon whether $\delta W_k < 0$ for any positive k. If Eq. (14) is a positive definite quadratic form for each k the system is stable within the resolution of the calculation.

Computer Program - The foregoing procedure has been implemented into a computer program for the CDC 7600 which performs the following steps:

(1) Solve Eq. (8) for the equilibrium on the 2-D mesh.

(2) Fit a 2-D interpolating function to the mesh.

(3) Compute N poloidal flux lines.

(4) Compute the c_{ij} quantities at intervals along these lines.

(5) Fourier transform the c_{ij}.

(6) Compute the elements of the K matrix.

(7) Compute the elements of the final W matrix.

(8) Tests W_k to see if it corresponds to a positive definite quadratic form.

The first four steps above are vital and must be done with considerable care if the c_{ij} and hence the W matrix elements are to have suitable precision. The c_{ij} elements involve field components and the curvatures of field lines and require that accurate first and second derivatives be obtained from the mesh. Step (5) is greatly speeded up by using Discrete Fast Fourier Transforms.[10] We have made use of subroutines which have been optimized for CDC computers by R. C. Singleton, B. R. Hunt, and L. E. Rudsinski.

The last step (8) can be done with any routine capable of computing the lowest coefficient of the diagonalized matrix. If the latter coefficient is positive or negative the system is stable or unstable respectively. We have used several routines for this task including Lagrange's reduction[11] which consists of a successive completion of squares and corresponds to a nonorthogonal linear transformation. If orthogonal transformations are used the problem corresponds to checking the sign of the lowest eigenvalue of W.

IV. APPLICATION

As a first use of the method we attacked the problem of finding a MHD stable toroidal z-pinch configuration which is directly applicable to the Los Alamos ZT-1 experiment. We imposed the following requirements on the equilibrium: (1) hollow pressure profile, (2) vacuum field region outside the pinch with a small amount of reversed toroidal field, and (3) aspect ratio and field configurations having general characteristics similar to ZT-1. The result of this study is the toroidal equilibrium having the profiles shown in Fig. 1. This profile was found by first working at large aspect ratios since stable profiles are known to exist in cylindrical geometry.[2,12] After a suitable stable cylindrical configuration was found the aspect ratio was then reduced to that of ZT-1 (7 to 1) and the toroidal equilibrium computed and checked for stability. The equilibrium of Fig. 1 was tested for stability for k values with corresponding toroidal wave lengths extending from 1 mm to the machine circumference (240 cm) with 17 coupled poloidal m modes and 24 integration intervals and found to be stable for this numerical resolution. In a numerical approach such as this one, there always is the possibility of predicting instability if a finer resolution is used (i.e. larger equilibrium mesh, inclusion of higher k and m modes and smaller integration intervals). This is particularly true if extremely localized unstable modes exist. The large amounts of computer time required for fine resolution calculations on scales much smaller than the typical gyro radii for practical applications is hard to justify in view of the inadequacy of the ideal MHD model for such small scales.

V. CONCLUSION AND FUTURE IMPROVEMENTS

The work done to date demonstrates that a numerical approach is indeed practical in achieving a closer correlation between experiment and MHD theory by allowing analyses of toroidal equilibria to be done which have realistic profiles. The "yes" or "no" answer to stability afforded by the method used here is adequate if one is only interested in finding stable configurations as we have done for ZT-1. When one wishes to check experimental distributions which often have a nasty habit of not being totally MHD stable it would be advantageous to compute the growth rates and form of the unstable modes. Further modifications of the present scheme with this goal in mind making use of the Rayleigh quotient[9] are planned.

VI. ACKNOWLEDGMENTS

Many people have assisted in the foregoing studies. We especially wish to acknowledge the important contributions made by B. R. Suydam. Discussions of some of the fine points of MHD theory held with J. P. Freidberg and J. L. Johnson have been valuable. Particularly important supporting subroutines and advice in their use in the computer program have been furnished by H. R. Lewis, B. L. Buzbee, B. R. Hunt, and T. L. Jordan. The assistance of R. W. Mitchell and many members of the Los

Alamos computer division is gratefully acknowledged. The encouragement, advice and suggestions supplied by J. L. Phillips and members of his toroidal z-pinch group have been vital in making the toroidal z-pinch calculations relevant to the ZT-1 experiment.

This work was performed under the auspices of the U.S. Atomic Energy Commission.

VII. REFERENCES

[1] D. A. Baker and L. W. Mann, Bull. Amer. Phys. Soc. Vol. 14, 1051 (1969).

[2] D. A. Baker et al., Plasma Phys. Cont. Fusion (Proc. Madison, Wis. Conf.), IAEA, Vienna Vol. 1, 203 (1971).

[3] H. Grad and H. Rubin, Proc. 2nd Int. Conf. on Atomic Energy Vol. 31, 190 (1958).

[4] V. D. Shavfranov, Reviews of Plasma Physics Vol. 2, 113 (Plenum Pub. Corp., N. Y., 1966).

[5] D. A. Baker, M.D.J. MacRoberts, and L. W. Mann, Bull. Am. Phys. Soc. Vol. 13, 1526 (1968).

[6] D. A. Baker and L. W. Mann, Bull. Am. Phys. Soc. Vol. 15, 1448 (1970).

[7] B. Marder and H. Weitzner, Plasma Physics Vol. 12, 435 (1970).

[8] R. A. Dory, Bull. Am. Phys. Soc. Vol. 14, 1016 (1969).

[9] I. B. Bernstein et al., Proc. R. Soc. A244, 17 (1958).

[10] J. W. Cooley and J. W. Tukey, Math. of Computation Vol. 19, pp. 297 (1965).

[11] E. T. Browne, Theory of Determinants and Matrices 107 (Univ. N.C. Press, 1958).

[12] D. C. Robinson, Plasma Physics Vol. 13, 439 (1971).

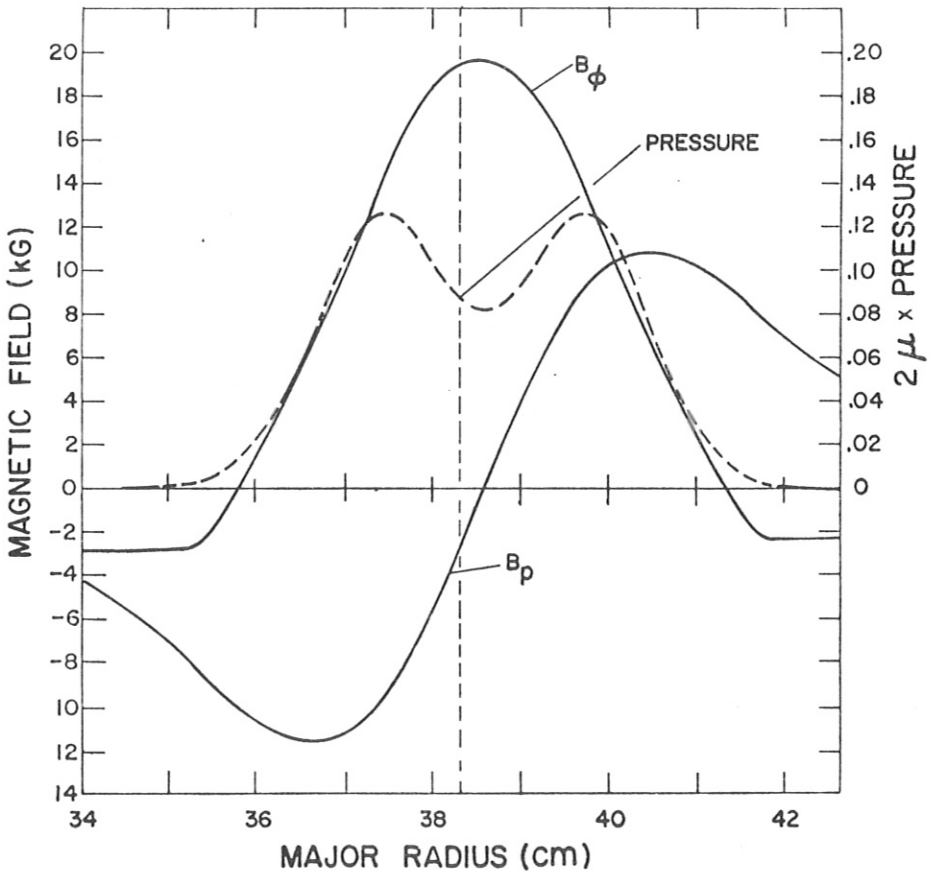

Fig. 1. Distributions of plasma pressure, toroidal and poloidal magnetic fields (B_ϕ,B_p) along a major radius of a numerically determined MHD stable toroidal z-pinch equilibrium.

Stability of Two-Dimensional Magnetohydrodynamic Equilibria

by

J. P. Freidberg and B. M. Marder

University of California, Los Alamos Scientific Laboratory

Los Alamos, New Mexico

ABSTRACT

A numerical procedure is presented for computing the stability of high β, diffuse two-dimensional magnetohydrodynamic equilibria. The method is tested on the problem of the bumpy θ pinch with arbitrary size bumpiness.

A great deal of insight pertaining to gross plasma stability has developed from the study of sharp boundary plasma models. As experiments become more sophisticated the need arises for diffuse profile theories in order to be able to make quantitative as well as qualitative comparisons.

In this paper we present a numerical procedure for performing the stability calculation based on the variational form of magnetohydrodynamics. We first Fourier-transform the perturbation with respect to the ignorable coordinate of the equilibrium. The remaining part of the perturbation is expanded as double series of complete admissible functions of the equilibrium coordinates. The minimization is then performed over the expansion coefficients.

We have tested the double expansion procedure on the problem of the bumpy θ pinch with arbitrary size bumpiness. For this problem the procedure proved to be quite satisfactory, being easy to code, giving good accuracy and requiring relatively few functions for convergence.

We consider the equilibrium and stability of a high β, diffuse θ pinch with superimposed $\ell = 0$ fields. The equilibrium is characterized by the field quantities $B_z(r,z)$ and $B_r(r,z)$. In the analysis that follows we shall consider the $\ell = 0$ fields to be of arbitrary size so that the equilibrium is truly two-dimensional. We shall, however, make use of the usual "θ pinch approximation" which assumes weak "z" dependence for both equilibrium and stability.

The appropriate ordering for the equilibrium problem is

$$B_z(r,z) \sim 1 \qquad B_r(r,z) \sim \epsilon \qquad \frac{\partial}{\partial r} \sim 1 \qquad \frac{\partial}{\partial z} \sim \epsilon$$

where ϵ measures the "z" dependence. In this ordering, the equation for magnetohydrodynamic equilibrium reduces to

$$\frac{1}{r}\frac{\partial}{\partial r}\frac{1}{r}\frac{\partial \psi}{\partial r} = -\mu_o \frac{dp(\psi)}{d\psi} \qquad \psi(0,z) = 0 \qquad \frac{1}{r}\frac{\partial \psi}{\partial r}(\infty,z) = B_c(z) \qquad (1)$$

$B_e(z)$ is the externally applied magnetic field far from the plasma. For this calculation we choose $B_e(z) = B_o(1 + \delta_o \cos hz)$, where B_o is the average value of applied magnetic field, $2\pi/h$ is the period of the $\ell = 0$ field and δ_o is the bulge strength. The function $p(\psi)$ is chosen to give experimentally observed bell-shaped pressure profiles; $p(\psi) = p_o \exp[-4\psi/B_o a_o^2]$ where p_o is the pressure on axis and a_o is the scale length for the plasma radius. Equation (1) can be solved analytically.

We treat perturbations of the form $\underline{\xi}_\perp = \exp[-i\omega t + i\theta]\hat{\underline{\xi}}_\perp(r,z)$ with $\hat{\underline{\xi}}_\perp(r,z + 2\pi/h) = \hat{\underline{\xi}}_\perp(r,z)$ and introduce a scalar function $\xi(r,z)$ using $\nabla\cdot\underline{\xi}_\perp = 0$.

$$\hat{\xi}_r(r,z) = \xi(r,z) \qquad \hat{\xi}_\theta(r,z) = i\frac{\partial}{\partial r} r\xi(r,z) \tag{2}$$

We obtain, in the usual manner, an energy principle which states that the eigenfunctions, ξ_n, minimize the quotient

$$\omega^2 = \frac{\delta W(\xi,\xi)}{K(\xi,\xi)} \tag{3}$$

with

$$\delta W = \tfrac{1}{2}\int\left[(\underline{B}\cdot\nabla\xi)^2 + (\underline{B}\cdot\nabla\frac{\partial}{\partial r} r\xi)^2 + r\underline{B}\cdot\nabla B_r\left(\frac{\partial\xi}{\partial r}\right)^2\right]\underline{dr} \quad K = \tfrac{1}{2}\int\rho\left[\xi^2 + \left(\frac{\partial}{\partial r} r\xi\right)^2\right]\underline{dr}$$

The essence of the numerical method is that the function $\xi(r,z)$ is expanded in a truncated double Fourier series and the quotient (3) minimized over this class of functions. The actual minimization procedure is performed with respect to the coefficients of the double series. Since the true eigenfunctions can be represented by a Fourier series, this method can in principle achieve arbitrary accuracy by including more terms. In practice, physical insight can guide the choice of expansion functions, and as a result, relatively few are actually needed for good convergence.

For the bumpy θ pinch, the eigenfunctions behave as r^{m-1} for small radius and are periodic in z. Thus, an appropriate m = 1 expansion is

$$\xi(r,z) = \sum_{\ell,n} C_{\ell n} J_o\left(\sigma_n \frac{r}{a(z)}\right) e^{i\ell hz} \tag{4}$$

By defining σ_n so that $J_o(\sigma_n b_o/a_o) = 0$ we insure that $\xi(r,z)$ vanishes on the approximate flux surface given by $r/a(z) = b_o/a_o$. The $C_{\ell n}$'s are complex coefficients which are to be determined. When Eq. (4) is substituted into Eq. (3) we obtain

$$\omega^2 = \min_{C_{ij}} \frac{\sum_{\ell npq} C_{\ell n} W_{\ell npq} C^*_{pq}}{\sum_{\ell npq} C_{\ell n} D_{\ell npq} C^*_{pq}} \tag{5}$$

where $W_{\ell npq}$ and $D_{\ell npq}$ are numerically computed matrix elements depending only on the equilibrium and the Fourier expansion functions.

Equation (5) is more conveniently written by expressing $C_{\ell n}$ as a one-dimensional vector, $\underline{x}$, of length (L × N), the number of cosines times the number of Bessel functions retained. We then obtain

$$\omega^2 = \min \frac{\underline{x}^T W \underline{x}}{\underline{x}^T D \underline{x}} \tag{6}$$

with W and D being (L × N)×(L × N) symmetric matrices. Since D is positive definite Eq. (6) can be put into standard form by defining $\underline{x} = D^{-\frac{1}{2}} \underline{y}$. This yields

$$\omega^2 = \min \frac{\underline{y}^T D^{-\frac{1}{2}} W D^{-\frac{1}{2}} \underline{y}}{\underline{y}^T \underline{y}} = \min \frac{\underline{y}^T S \underline{y}}{\|\underline{y}\|^2}$$

To complete the minimization it is necessary to find the eigenvalues, ω_n^2, and eigenvectors $\underline{y}_n$ of the symmetric matrix $S = D^{-\frac{1}{2}} W D^{-\frac{1}{2}}$.

A reliable test of the accuracy of this method is afforded by simply increasing the number of Fourier functions in the expansion. Of course, the (r,z) grid must also be sufficiently fine to resolve the higher harmonics. In the bumpy pinch problem 6 Bessel functions and 5 cosines on a 55 × 36 grid were sufficient for convergence. The matrix S is then 30 × 30. The entire calculation, equilibrium and stability, consumes about 35 seconds of CDC-7600 time and requires no extensive memory.

This method of using a Fourier expansion in a Rayleigh-Ritz type minimization has many desirable features. If the expansion functions are carefully chosen very few are required to give a good approximation to the true minimizing function. Boundary conditions are easily incorporated into the expansion functions. The method requires little computing time and is straightforward to program. Finally, simple tests can be performed to check the accuracy of the procedure.

The growth rates and eigenfunctions for the m = 1, k = 0 mode of a bumpy θ pinch were computed for a large range of equilibrium parameters. The results were interpreted with respect to two basic aims.

First, as a test of the numerical procedure, the results were compared with existing small δ_o analytic theory in the appropriate limits. Our second aim was to examine the effects of arbitrary δ_o on the growth rates. A recent calculation by Weitzner treats the stability of the bumpy pinch also in the small δ_o limit for diffuse profiles. The profiles chosen by Weitzner were Gaussian. The growth rates were tabulated by Weitzner by numerically solving a coupled set of ordinary differential equations.

To test our numerical procedure, we set $b_o/a_o = 2.5$, $\delta_o = .01$ and computed the growth rates as a function of β. For this small a δ_o we would expect good quantitative as well as qualitative agreement with Weitzner's results. Our results agree with Weitzner's theory to four figures over the whole range of β in the appropriate small δ_o limit. Illustrated in Fig. 1 are the eigenfunctions, $\xi(r,z)$, for the first three unstable modes for δ_o = .2, β = .5, and $b_o/a_o = 2.5$. We see that the plasma displacement is smooth, and behaves in the expected manner with the fastest mode having no nodes, second fastest one node, etc.

We have presented a numerical method for computing the growth rates and eigenfunctions for an arbitrary two-dimensional, diffuse, high β, magnetohydrodynamic equilibrium. As a test of the procedure we treated the problem of the bumpy θ pinch with arbitrary size bumpiness. Our results are in excellent agreement with the existing diffuse theory of Weitzner in the limit of small bumpiness.

The numerical procedure turns out to (1) be easy to code, (2) require only moderate storage and (3) run quickly.

ACKNOWLEDGEMENT

This work was performed under the auspices of the U. S. Atomic Energy Commission.

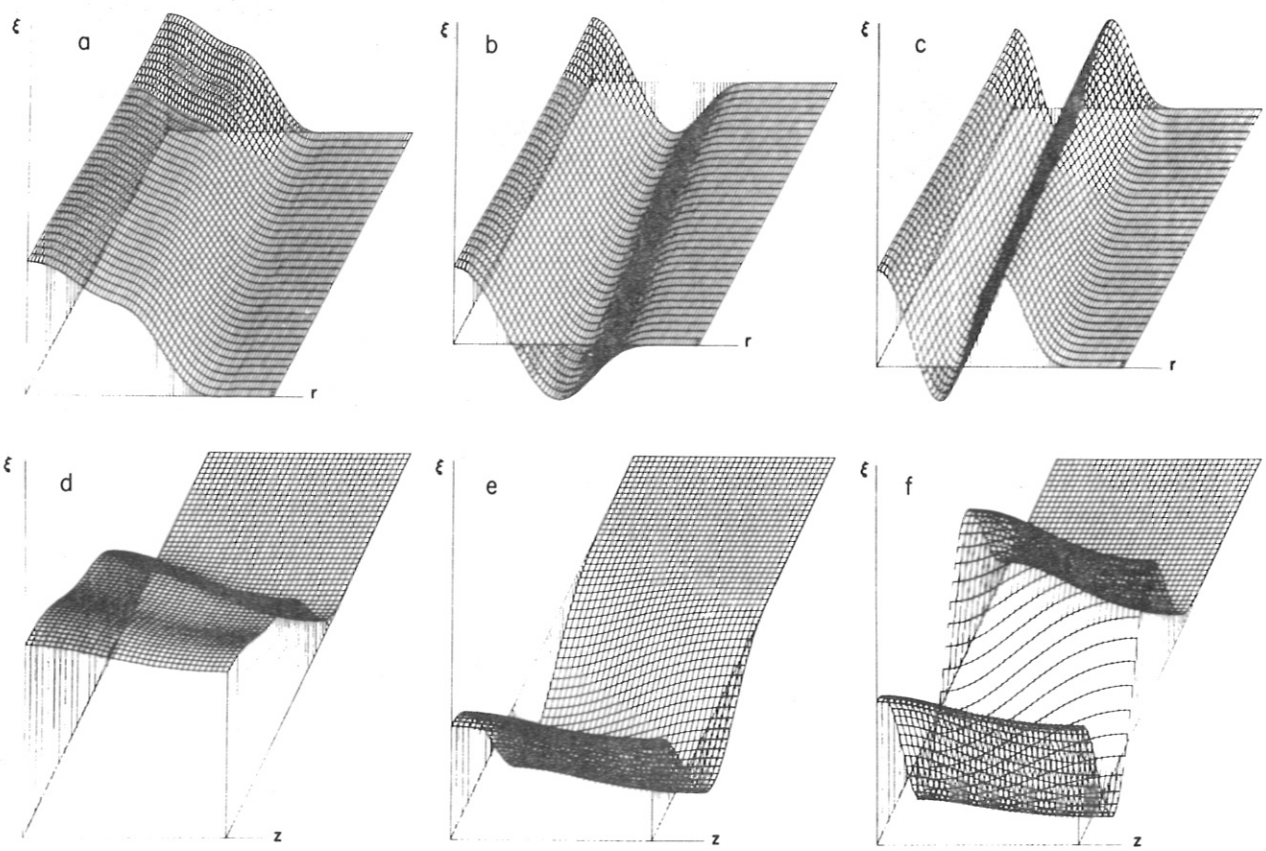

STABILITY OF A FINITE β, $\ell = 2$ STELLERATOR

by

J. P. Freidberg

University of California, Los Alamos Scientific Laboratory

Los Alamos, New Mexico

ABSTRACT

The stability of an infinitely long, high β, $\ell = 2$ stellerator is investigated. The calculation is carried out by using the new Scyllac expansion in the sharp boundary ideal magnetohydrodynamic model. It is found that for any given size $\ell = 2$ field and mode number m, an infinite but discrete set of wavenumbers k exist for which the plasma is unstable to all β; that is the critical β equals zero. These modes can be described as long wavelength interchanges. Thus, with regard to sharp boundary stability, neither $\ell = 0$ nor $\ell = 2$ offer any particular advantage over the other as a sideband field required to produce toroidal equilibrium in the $\ell = 1$ Scyllac configuration.

The stability of an infinitely long, high β, $\ell = 2$ stellerator is investigated using the ideal magnetohydrodynamic sharp boundary model. Our motivation for studying this problem is to determine whether the $\ell = 2$ configuration would have favorable stability properties in a parameter range of interest to the Scyllac program.

There is preliminary evidence that such desirable stability properties should exist. To understand this we first briefly review some relevant Scyllac theory and low β stellerator theory. The difference between each of these theories is associated with the relative size of three dimensionless parameters which appear and are used as expansion parameters. These

are β = plasma pressure/magnetic pressure, ϵ = plasma radius $\times$ helical pitch number and δ = helical plasma distortion/plasma radius. Current ideas on Scyllac can be traced back to the stability results of the "old" Scyllac expansion in which it is assumed that $\beta \sim 1$ and $\delta \ll \epsilon < 1$. The corresponding dispersion relation for m = 1, k = 0 modes is given by

$$\frac{\omega^2}{v_a^2/a^2} = -(\ell - 1)\,\epsilon^2\delta^2\,\frac{\beta(2 - \beta)}{2}$$

where v_a is the Alfven speed. From this result it follows that the system is m = 1 unstable for any ℓ except $\ell = 1$. On this basis the Scyllac experiment was designed as an $\ell = 1$ system. Recent calculations pertaining to Scyllac have been concerned with calculating higher order $\ell = 1$ terms in the m = 1, k = 0 dispersion relation since the leading order term vanishes. In particular the $\epsilon^4\delta^2$ correction has been found for the old Scyllac expansion. In addition a "new" Scyllac expansion has been devised where $\beta \sim 1$ and $\epsilon \ll \delta < 1$. The leading order term again vanishes for $\ell = 1$ and the $\epsilon^2\delta^4$ correction has been calculated.

Thus most of the effort on Scyllac has been concerned with $\ell = 1$, since all other ℓ values are m = 1 unstable. In a paper by Grad and Weitzner a more optimistic result concerning higher ℓ numbers is pointed out. (This result is closely associated with the earlier critical β calculations of Johnson, et al.). Using low β stellerator theory which assumes $\beta \sim \delta^2 \ll \epsilon < 1$ they find an m = 1, k = 0 dispersion relation given by

$$\frac{\omega^2}{v_a^2/a^2} = -(\ell - 1)\,\epsilon^2\delta^2[\beta - 2(\ell - 1)\delta^2]$$

Thus for any $\beta \leq \beta_{crit} = 2(\ell - 1)\delta^2$ the system is stable to this mode. It is also pointed out that with sufficiently large helical fields (i.e. large δ)

substantial critical β's ~ 5 could be obtained. Admittedly these values are somewhat artificial since the expansion is being used outside its range of validity. Nonetheless it is suggestive that such a scaling may persist even at finite β and finite δ. To answer this question correctly, we see, by an examination of the existing theories, that what is required is a calculation $\ell = 2$ stability using the new Scyllac expansion and including the $\epsilon^2\delta^4$ correction. It is this problem that we address ourselves to in this paper. By calculating the growth rates numerically we are able to do the above calculation for both β and δ arbitrary and $\epsilon \ll 1$, keeping only the leading order term in ϵ^2.

The results of this calculation are as follows: for $m = 1$, $k = 0$, a critical β is found as would be predicted from low β stellerator theory. For finite β,δ the value of β_{crit} is somewhat lower than predicted by the low β theory in the regime of experimental interest. In fact the highest value of β_{crit} for any strength $\ell = 2$ field is about .12. This is somewhat discouraging from the Scyllac point of view because of the high β requirements of shock heating. However, the stability picture is actually much worse. The reason for this is that as in low β stellerators, the worst modes are not $k = 0$ modes, but interchange modes in which the perturbation remains in phase with the rotational transform of the magnetic field. We show here that if the wavenumber k of the perturbation satisfies

$$\frac{k}{h} = (2p + m)\left(1 - \frac{L}{2\pi}\right) - m \qquad |p| = 0,1,2\ldots$$

then the critical β is reduced to zero. Here h is the helical pitch number, m the mode number and $L/2\pi$ the rotational transform. Thus if one allows long but not infinite wavelength $m = 1$ modes, wavenumbers k exist which are

unstable for all β. Clearly this configuration does not, as it stands, possess any of the favorable stability properties anticipated earlier.

At first glance these results might appear to contradict early low β stellerator results which predict stability to <u>all</u> k modes. A more careful examination indicates that no such contradiction exists. The reason for this is associated with the fact that the early stellerator theory contains terms which are very high order in the Scyllac expansions and are hence, not included. Of course many of the finite β effects of the Scyllac expansion are not found in the stellerator expansion. The point is that these higher order effects in stellerators can be stabilizing, thereby increasing the critical β away from zero. Two such effects are shear, which would correspond to an $\epsilon^4\delta^2$ term in the $\ell = 2$ dispersion relation and possible favorable curvature arising because of the toroidal geometry. Each of these leads to a small critical β; for instance shear results in a $\beta_{crit} \sim \epsilon^2$. These effects are important for stellerators which are intended to operate at very small β. However, they do not appear particularly important for Scyllac where high critical β's are required in order that shock heating be effective.

This work was performed under the auspices of the U. S. Atomic Energy Commission.

B 10 Toroidal High Beta Equilibrium.

H.WEITZNER. Courant Inst. Math.Sci.,N.Y.U.-

Most toroidal high beta equilibrium studies have been based on the piecewise constant pressure, sharp boundary model. Here, equilibrium is obtained by formal expansion for the case of a continuous pressure profile in ideal magnetohydrodynamics. The small parameter on which the expansion is based is the approximate helical wave number times plasma radius;hence the equilibrium is assumed to vary slowly the long way around the torus. With the assumption that there be no net current flowing the long way around the torus on any flux surface, or with any other constraint on this current, the equilibrium is essentially uniquely determined for any value of beta. Numerical work indicates that the expansion breaks down at low beta and that the distortions of the flux surfaces from cylinders are not small. Numerical results of the approximate equilibrium equations are given and the pressure profiles appear to be quite reasonable. Preliminary comparisons with the Scyllac experiment indicate that the distributed pressure equilibrium condition is a closer approximation to the experiment than the sharp boundary model. Some comments on the stability of such configurations will be included.

No paper has been submitted.